UNIVERSITÄT HOHENHEIM

Institute of Crop Science (340)

Department of Nutritional Crop Physiology (340h)

D-70599 Stuttgart-Hohenheim, Germany

Supervisor: Prof. Dr. Uwe Ludewig

SP P 1685
Ecosystem Nutrition

DISSERTATION

„SITE-DEPENDENT DIFFERENCES IN DNA METHYLATION AND THEIR IMPACT ON PLANT ESTABLISHMENT IN *POPULUS TRICHOCARPA*"

**Submitted to the faculty of Agricultural Science,
in fulfillment of the regulations to acquire the degree:
Doctor scientiarum agriculturae (Dr. sc. agr.)**

Presented by: Brigitte Schönberger

Stuttgart, 2016

This thesis was accepted as a doctoral thesis (Dissertation) in fulfilment of the regulations to acquire the doctoral degree "Doktor der Agrarwissenschaften - Doctor scientiarum agriculturae (Dr. sc. agr.)" by the Faculty of Agricultural Sciences at the University of Hohenheim on 26.10.2016.

Date of the oral examination: 15.11.2016

Examination Committee

Head of the oral examination: Prof. Dr. Jörn Bennewitz

Supervisor and Reviewer: Prof. Dr. Uwe Ludewig

Co-Reviewer: Prof. Dr. Artur Pfitzner

Additional examiner: PD. Dr. Stefan Scholten

"Think like a proton and stay positive."

Unknown

Table of contents

Index of figures

Index of tables

List of abbreviations

A	adenine
BS-Seq	bisulfite sequencing
C	cytosine
$CaCl_2$	calcium chloride
CAL	calcium acetate lactate
CpG	dinucleotide consisting of cytosine – phosphate – guanine
(c)DNA	(complementary) deoxyribonucleic acid
CMT3	chromomethylase 3
$CuSO_4$	copper(II) sulfate
DMR(s)	differentially methylated region(s)
DRM	domains rearranged methylase
FDR	false discovery rate
Fe(III)-Na-EDTA	ethylenediaminetetraacetic acid ferric sodium salt
G	guanine
Gb	giga base pair
H	represents the nucleotides: adenine, thymine or cytosine
H_3BO_3	boric acid
HCl	hydrochloric acid
HNO_3	nitric acid
K	potassium
KCl	potassium chloride
KH_2PO_4	potassium dihydrogen phosphate
^mC	methylated cytosine
MET1	methyltransferase 1
$MgSO_4$	magnesium sulfate
miRNA(s)/miR	microRNA(s)
$MnCl_2$	manganese(II) chloride
Na_2MoO_4	sodium molybdate

NBS-LRR	nucleotide-binding site leucine-rich repeat
NCBI	National Center for Biotechnology Information
NH_4NO_3	ammonium nitrate
NLA	*nitrogen limitation adaptation* gene
NW-FVA	Nordwestdeutsche Forstliche Versuchsanstalt
ORF	open reading frame
+/–P	adequate/deficient phosphorus treatment
P	phosphorus
P_i	phosphate
P_2O_5	phosphorus pentoxide
PHO2	putative ubiquitin-conjugating enzyme E2
PHR1	phosphate starvation response protein 1
PHT	phosphate transporter
*POPTR*_00XXsXXXXX/*Pt*XXsXXXXX	gene codex of *Populus trichocarpa*
PPFD	photosynthetic photon flux density
PPR	pentatricopeptide repeat
Ptc-miRXXXX(a-e)	microRNA codex of *Populus trichocarpa*
qPCR	quantitative real time polymerase chain reaction
r	Pearson's product-moment correlation coefficient
RdDM	RNA-directed DNA methylation
RNA	ribonucleic acid
SE	standard error
siRNA(s)	small interfering RNA(s)
SPL3	squamosa promoter binding Protein-Like 3
Tm	melting temperature
TSS	transcriptional starting site
VDLUFA	Verband Deutscher Landwirtschaftlicher Untersuchungs- und Forschungsanstalten
$ZnSO_4$	zinc sulfate

Abstract

Phosphate (P_i) limits total biomass production in natural tree ecosystems. Due to the low mobility of P_i in soil, higher plants, like trees, require special adaptations for phosphorus (P) acquisition. The genetic and physiological basis of this adaptation has been studied extensively. In addition, phosphorus starvation was recently suggested to affect epigenetic modifications in varying annual plant species. However, the impact of differential DNA methylation and microRNAs (miRNAs) on gene expression as well as site-dependent P-related physiology is largely unknown in perennials.

In this study *Populus trichocarpa* clones, established from stem cuttings from two different locations, were grown in hydroponic culture with different P levels. Morphological and physiological parameters as well as, using bisulfite sequencing, site-specific genome-wide methylomes were determined. Gene and miRNA expression of differentially methylated regions was quantified via qPCR. Site-dependent differences in plant establishment were encountered, together with site-specific differentially methylated chromosomal regions. Methylation differences were nucleotide context-specific and extensively regulated miRNAs and their target genes in an organ-specific way. Though no direct relation between differential methylation in coding regions and their corresponding gene expression was observed, a general site-dependent transcriptional repression by DNA methylation was detected. Nevertheless, differential DNA methylation and gene expression was not affected by P nutrition, although recent studies described P-starvation induced DNA methylation changes, suggesting species-specific epigenetic mechanisms. However, differentially methylated miRNAs, together with their target genes, showed P-dependent expression profiles, indicating miRNA expression changes as a P-related epigenetic

modification in poplar. Hence, it was shown that differences in DNA methylation or differentially methylated miRNAs might influence plant establishment and partially correlate with P acquisition, and thus be responsible for a site-dependent adaptation and growth performance, interesting for plant breeding, conservation biology and biodiversity studies of vegetatively propagated perennials.

Zusammenfassung

In natürlichen (Wald-)Ökosystemen gehört Phosphor (P) zu den wichtigsten Faktoren für die Gesamtbiomasseproduktion. Aufgrund der geringen Mobilität von anorganischem Phosphat (P_i) im Boden benötigen höhere Pflanzen, wie Pappeln, sogar auf nährstoffreichen Ackerböden eine mehr oder weniger ausgeprägte Anpassung der P-Aufnahme. Die genetische als auch physiologische Grundlage hierzu wurde in den letzten Jahren umfangreich erforscht. Neueste Studien zeigten auch in verschiedenen einjährigen Pflanzenarten starke durch P-Mangel hervorgerufene epigenetische Veränderungen. Jedoch ist kaum bekannt, inwiefern epigenetische Veränderungen, wie DNA Methylierungen und Gen-Inaktivierungen via microRNAs (miRNAs), in perennierenden Pflanzen zur P-Mangelanpassung gehören und ob diese eine schnellere Anpassung an Umwelt-bezogenen Stress als genetische Mutationen darstellen.

In diesem Forschungsprojekt wurde untersucht, ob genetisch identisches Pappelmaterial (*Populus trichocarpa* cv. Muhle Larson) von verschiedenen Standorten genomweite epigenetische Unterschiede in DNA Methylierung und in differentiell methylierten miRNA-Expressionen aufzeigte und ob diese Unterschiede für Standort-spezifische Anpassungen verantwortlich sein könnten. Hierzu wurde die zwar nicht-heimische, aber bereits vollständig sequenzierte Balsampappel (*Populus trichocarpa*) als Modellpflanze verwendet. Genetisch identisches Startmaterial (Schnitthölzer) von zwei verschiedenen Standorten (Kurzumtriebsplantagen) wurde zuerst hinsichtlich seines P-Gehalts charakterisiert und im Gewächshaus mit unterschiedlichen Phosphorangeboten angezogen. Des Weiteren wurden morphologische und physiologische Parameter erfasst und

Methylierungsunterschiede der DNA durch Bisulfit-Sequenzierung genomweit kartiert. Anschließende Expressionsanalysen wurden für differenziert methylierte Gene, miRNAs und deren Zielgene mittels qPCR durchgeführt. Im Fokus standen hierbei die auf P-Ernährung und Wachstumsleistung bezogenen Methylierungsunterschiede der DNA und miRNA. Signifikante Standort-spezifische Wachstumsunterschiede der Pflanzen gingen mit Standort-spezifischen differenziert methylierten chromosomalen Regionen einher. Die Methylierungsunterschiede zeigten zusätzlich eine Spezifität in verschiedenen Nukleotid-Kontexten und eine extensive Beeinflussung von miRNAs und deren Zielgenen in einem P-abhängigen und Organ-spezifischen Kontext. Allerdings wurde kein direkter Zusammenhang zwischen differentiell methylierten Genbereichen und den dazugehörigen Genexpressionsveränderungen festgestellt, auch wenn eine Standort-spezifische, allgemeine Repression der Transkription durch DNA Methylierung nachgewiesen werden konnte. Anders als in aktuellen Studien beschrieben, wurde kein direkter Einfluss des P-Ernährungszustandes auf die DNA Methylierungsmuster und Genexpression beobachtet, was auf Spezies-spezifische epigenetische Mechanismen hindeuten könnte: Eine Anpassung an P-Mangel könnte in Pappeln durch unterschiedliche Expression differentiell methylierter miRNAs und deren Zielgene ablaufen.

Die beobachteten epigenetischen Anpassungen erklären demnach das Standort-spezifische Wachstum der Bäume, was bei zukünftigen Züchtungs- und Biodiversitätsstudien von Pflanzen, die nicht über Samen vervielfältigt werden, berücksichtigt werden sollte.

1. Introduction

As sessile organisms, plants have to adapt much more efficient to rapid and long-term environmental changes than mammals. For instance, plants are not able to escape uncomfortable biotic or abiotic conditions like herbivore enemies, pathogen attacks, competing neighboring species, varying climates and differences in nutrient availabilities (Sterck *et al.*, 2007). Besides pathogen infections, mainly nutrient deficiencies lead to limitations of growth performance and plant establishment, requiring efficient and flexible alterations in adaptation strategies. Nowadays, these special adaptation mechanisms have been investigated intensively, primarily in annual plants, regarding different stress conditions, including nutrient deficiencies. Hence, the genetic and recently also the epigenetic basis of adaptation strategies has become a main focus in plant research due to advanced techniques, such as next generation sequencing.

1.1. Phosphorus nutrition

As an essential macronutrient, phosphorus (P), in addition to nitrogen, is primarily limiting for the total biomass production in trees and natural forest ecosystems (Wright *et al.*, 2011). This is related to the function of P in plants: It is a main component of key molecules, such as nucleic acids, phospholipids and adenosine triphosphate (Schachtman, 1998). Therefore, phosphorus is involved in regulatory metabolic pathways and key enzyme reactions, e.g. protein synthesis, cell division, development of new tissue and complex energy transformations in plants (Theodorou & Plaxton, 1993). As a result, common P deficiency symptoms are described as reduced or stunted shoot growth, a short, but dense root system and accumulation of anthocyanin

in leaves leading to abnormal dark-green till reddish-purple leaf coloration, which causes photo-inhibitory damage to chloroplasts (Vance *et al.*, 2003).

The main source of P for plants is inorganic phosphate (P_i) in the soil. Due to the poor availability and low mobility of P_i, higher plants like trees cope with altered P availabilities via changes in gene expression to adjust their uptake and induce P-saving metabolisms, such as the expression of high affinity P_i transporters (Loth-Pereda *et al.*, 2011), changes in root architecture (Sato & Miura, 2011), mycorrhiza formation (Björkman, 1970; Karandashov & Bucher, 2005), releasing exudates in the rhizosphere for P mobilization (Radersma & Grierson, 2004) and efficient internal P recycling (Ticconi & Abel, 2004). However, little is known whether further gene regulatory or epigenetic mechanisms, like DNA methylation or microRNAs (miRNAs), are involved in tree adaptation to a certain P status.

1.2. Epigenetics

Most commonly, the term epigenetics describes heritable adaptation in gene expression without any changes in nucleotide sequence (Wolffe, 1999). Besides histone modifications and RNA interference, DNA methylation is considered as an epigenetic mechanism leading to heritable differences in gene expression, mostly in an inhibitory manner (Figure 1).

To be more precisely, proper depositions of histones are required to control the transcriptional machinery (Cosgrove & Wolberger, 2005). Furthermore, small non-coding RNAs and the proteins generating or binding them are involved in stress-signaling and can subsequently induce transcriptional or post-transcriptional gene silencing (Castel & Martienssen, 2013). DNA methylation seems to have an impact on controlling gene expression, especially by methylation of transposable elements (Mirouze *et al.*, 2009).

Alongside already well-investigated mammalian epigenetics (Holliday, 2006; Lister *et al.*, 2009; Tomizawa *et al.*, 2011), recent studies in plants have also uncovered a major role of epigenetic adaptation in gene expression alteration due to environmental stress (Martienssen & Colot, 2001; Feng & Jacobsen, 2011).
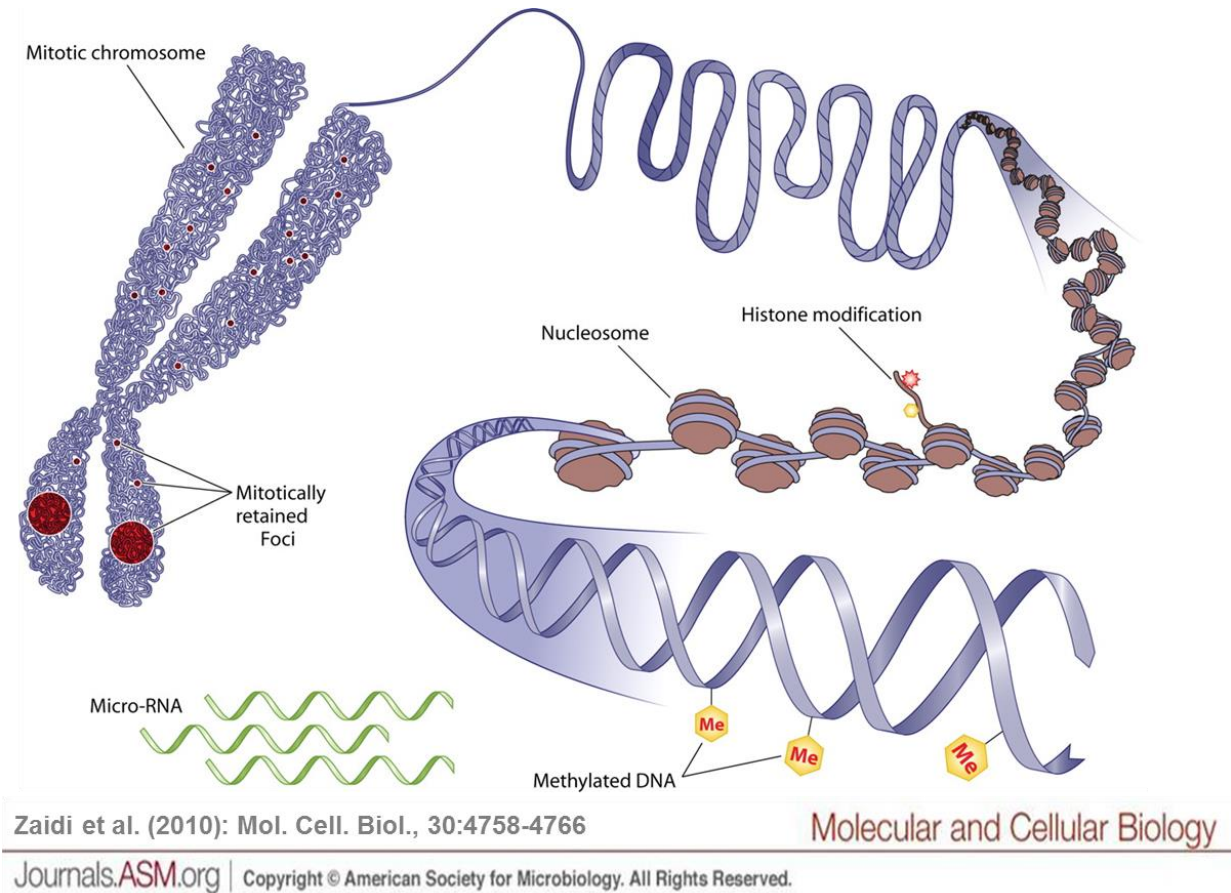
Figure 1: Epigenetic mechanisms by Zaidi *et al.*, 2010.
A general and detailed drawing of a mitotic chromosome with its mitotically retained foci and nucleosomes is shown. Here described and well-defined epigenetic mechanisms include: histone modification, DNA methylation and non-coding RNA-mediated (microRNA) alteration of gene expression (Zaidi *et al.*, 2010). Epigenetic mechanisms are described to be non-mutational changes in gene expression, leading to possibly inheritable adaptations towards environmental stress conditions.

For example, it has been shown that several abiotic and biotic stresses are associated with epigenetic re-programming in plants (Gutzat & Mittelsten Scheid, 2012). Especially, P availability seems to trigger epigenetic modifications, e.g. P_i starvation and recovery conditions induce methylation changes preferentially in transposable elements close to highly induced P-related genes in rice, but not in *Arabidopsis*, where

the P_i starvation response is described to be regulated by chromatin remodeling (Smith *et al.*, 2010), suggesting species-specific adaptation mechanisms (Secco *et al.*, 2015). Besides, in an annual plant like *Arabidopsis*, the methylation of cytosines in DNA is passed about four orders of magnitude faster to the next generation than single point mutations (around 1 base pair per generation). This potentially allows faster adaptation to environmental constraints than mutations (Schmitz *et al.*, 2011). However, the transgenerational inheritance of differential DNA methylation and its importance as "inherited memory", passing acquired properties to the next generations, are in most cases still in question (Heard & Martienssen, 2014).

1.3. DNA methylation and cytosine context

Cytosine methylation, an epigenetic modification leading to environmental adaptation via gene expression alteration, is mainly found in transposable elements (TEs), silent loci and repeated sequences. However, cytosine methylation might also be observed in coding regions (Cokus *et al.*, 2008; Lister *et al.*, 2008; Henderson *et al.*, 2010). Thereby, DNA methylation in promoter regions seems to silence genes, whereas DNA methylation in gene body sequences is positively correlated to gene expression in mammals (Yang *et al.*, 2014) as well as in different plant species like *Arabidopsis* (Aceituno *et al.*, 2008), rice (Secco *et al.*, 2015) and poplar (Liang *et al.*, 2014). Nevertheless, most of these correlations have been conducted on a whole methylome/transcriptome scale, leaving individual cases of gene expression alterations due to their DNA methylation relatively uninvestigated. In addition, recent studies have also questioned differential DNA methylation and actively regulating gene expression (Seymour *et al.*, 2014). Therefore, understanding of methylations in coding regions still remains unclear, primarily in plants.

Besides the chromosomal loci of methylation, another important aspect of differential DNA methylation is the cytosine (C) context, in which the methylation occurs: CpG (dinucleotide consisting of cytosine – phosphate – guanine), CHG or CHH (where H represents adenine [A], thymine [T] or cytosine [C] as a single letter abbreviation; Figure 2).

In plants, methylations are observed in both symmetrical (CpG and CHG) and asymmetrical (CHH) sequences (Finnegan *et al.*, 2000). CpG methylations are maintained via the methyltransferase 1 (MET1) and therefore more likely transmitted through cycles of DNA replication (Kankel *et al.*, 2003; Saze *et al.*, 2003). Thus, methylations of CpG are considered as inheritable or conserved methylations. By contrast, chromomethylase 3 (CMT3) and domains rearranged methylase 1 and 2 (DRM1/2) genes are responsible for so called "de novo" methylations appearing mainly in CHG and CHH contexts. These influence adaptive, short-term stress responses within one generation (Cao & Jacobsen, 2002a,b; Figure 2). Though, CHG methylations are also symmetrical sequences and could be inherited as well.

However, in clonal and vegetatively propagated poplar trees, "de novo" methylations might be of crucial importance due to a lack of genetic recombination via seed propagation to inherit adaptive traits.
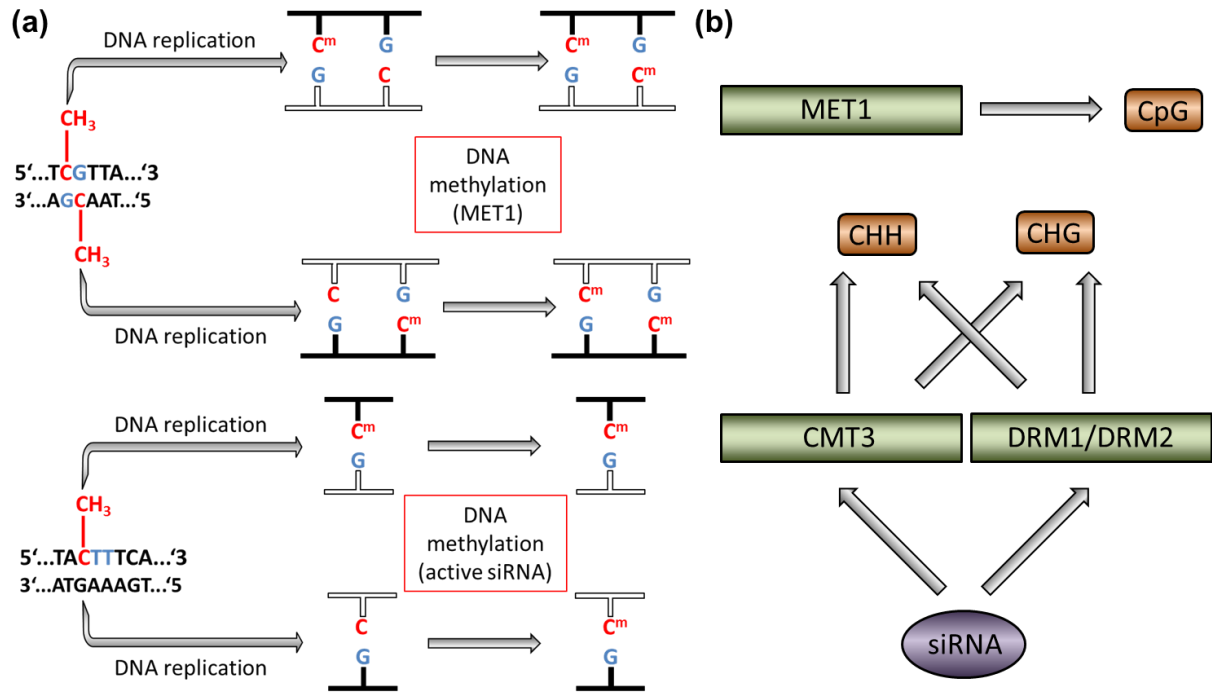
Figure 2: Maintenance of DNA methylation related to the cytosine context.
DNA replication of methylated cytosines (^mC) in symmetric context (here: CG/CpG) is shown in (a). First, both daughter strands are hemimethylated, which is recognized by specific methyltransferases (e.g.: methyltransferase 1/MET1) to maintain symmetric methylations. Besides, ^mC in asymmetric context (CHH, where H represents any other DNA nucleotide than guanine) requires a small interfering RNA (siRNA) signal to maintain methylation. DNA sequence is presented as single letter abbreviations: guanine as G, cytosine as C, adenine as A and thymine as T. Furthermore, the maintenance of DNA methylation in different contexts via specific methyltransferases is indicated in (b): MET1 is involved in the maintenance pathway of symmetric CpG methylation. In addition, CMT3 (chromomethylase 3) and DRM1/2 (domains rearranged methylase 1/2) are responsible for the maintenance of "de novo" methylations (CHH and CHG), which are directed by short interfering RNAs (siRNAs). Figure has been modified after Chan *et al.*, 2005.

1.4. RNA interference

Besides DNA methylation, miRNAs contain extra-chromosomal sequence-specific information and are also involved in epigenetic mechanisms. They are nuclear localized, small (~ 21-24 nucleotides), non-coding, single-stranded RNAs, which are hairpin-derived RNAs with imperfect complementarity to targets (Castel & Martienssen, 2013). A subset of these act as key regulators of gene expression,

mainly by transcriptional silencing, translational repression, post-transcriptional cleavage or degradation (Sunkar & Zhu, 2004; Figure 2).

For instance, in many plant species, such as poplar, miRNA targeted genes are involved in a mechanistic network of plant P signaling, e.g. the miR399-phosphate starvation response protein 1 (PHR1)-putative ubiquitin-conjugating enzyme E2 (PHO2) regulon (Fujii *et al.*, 2005; Bari *et al.*, 2006) and miR156-squamosa promoter binding protein-like 3 (SPL3)-phosphate transporter 1;5 (PHT1;5) pathways (Lei *et al.*, 2016). Furthermore, miR827 and its target the *nitrogen limitation adaptation* (*NLA*) gene are not only involved in adaptive responses to low-nitrogen conditions, but have also pivotal roles in regulating the P_i homeostasis in *Arabidopsis* (Kant *et al.*, 2011). The role of miRNAs in regulating plant adaptive responses to nutrient stresses was also detected in rice and *Arabidopsis* for sulfur stress: the expression of miR395, a sulfurylase-targeting miRNA, was increased upon sulfate starvation (Jones-Rhoades & Bartel, 2004).

On the other hand, small transcribed RNAs with perfect complementarity to targets that cause transcript degradation, also called small interfering RNAs (siRNAs) in other species, are correlated with and crucially determine chromosomal DNA methylation (Castel & Martienssen, 2013; Figure 2 and Figure 3). This phenomenon is called RNA-directed DNA methylation (RdDM) and describes the maintenance of "de novo" methylation of DNA with certain sequence identities by silenced RNA (Figure 2). Thereby, methylation might occur comparably at symmetric (CpG and CHG) and asymmetric cytosine contexts (CHH; Cao *et al.*, 2003).
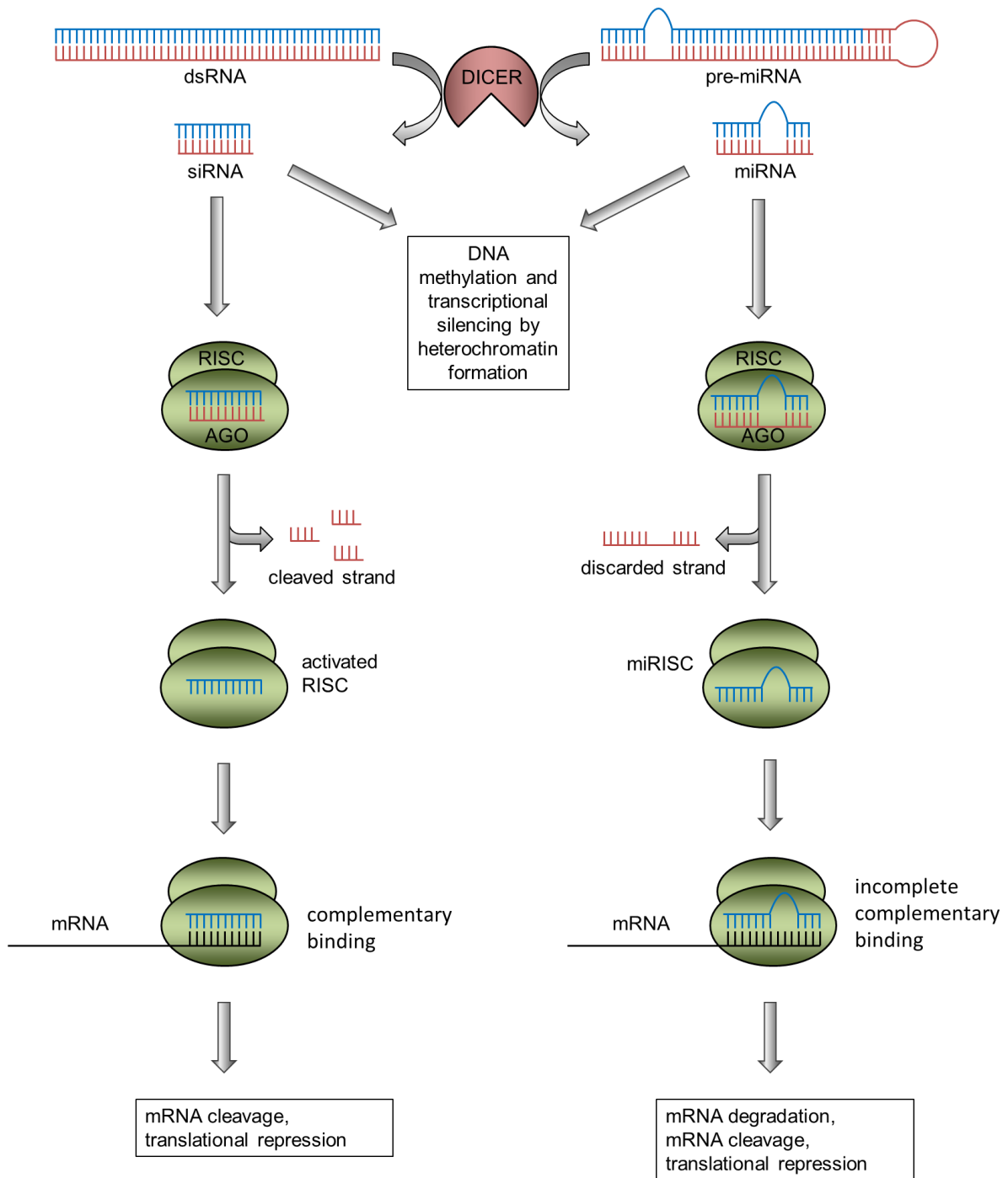
Figure 3: Difference between miRNA and siRNA in gene silencing mechanisms.
Transcribed double stranded RNA (dsRNA) or nucleus-derived premature microRNA (pre-miRNA) is processed by the Dicer enzyme into si- or miRNA. These small RNAs are loaded into the cytosolic RNA-induced silencing complex (RISC) with its essential catalytic component, the Argonaute protein (AGO). In the siRNA-RISC, AGO cleaves the passenger strand of siRNA. Afterwards, siRNA-RISC is binding to a complementary target mRNA, inducing mRNA cleavage and translational repression. In miRISC, the passenger strand is discarded. Subsequently, miRISC is guided to possible target mRNAs. Via incomplete complementary binding, mRNA degradation, cleavage and translational repression are induced. Additionally, DNA methylation and transcriptional silencing by heterochromatin formation are mediated by si- or miRNAs. Figure has been modified after Lam *et al.*, 2015.

1.5. Interaction DNA methylation and miRNA

Hence, epigenetic mechanisms, such as DNA methylation and gene silencing by miRNAs, seem to have crucial functions in regulating gene expression in response to abiotic and biotic stresses. Though, only a few recent studies have investigated a possible interaction between DNA methylation and miRNAs in plants.

Ci *et al.*, 2015 described that DNA methylation potentially regulated the expression of miRNAs and their target genes under temperature stress. In addition, methylation and miRNAs expression in bisexual flower development correlated negatively (Song *et al.*, 2015). Slowly, knowledge about this mutual adjustment is increasing, but so far it still remains unclear.

1.6. Epigenetics in perennial plants

Nevertheless, most of these researches focus on annual herbaceous plants, leaving perennials and vegetatively propagated plants relatively uninvestigated. In perennial, vegetatively propagated plants, such as black cottonwood (*Populus trichocarpa*), DNA methylation and miRNAs may likely have different or additional roles than in annual plants. For example, it has been shown that the oil content of vegetatively propagated oil palms is regulated by the abundance of DNA methylation (Ong-Abdullah *et al.*, 2015). Furthermore, the analysis of clonal white poplar populations indicates a quite limited genetic biodiversity, but detects a variable epigenetic status, where environmental conditions are strongly linked to DNA methylation (Guarino *et al.*, 2015). Additionally, the methylome resolution of *Populus trichocarpa* has revealed an association between drought stress and DNA methylation (Liang *et al.*, 2014).

Thus, seasonal and eco-site adaptation may potentially allow (reversible) adaptation to environmental constraints and "memorize" environmental conditions over winter.

For instance, genetically uniform material grown on two different sites with contrasting conditions might lead to phenotype alterations. These adaptive alterations might still be observed in vegetatively propagated plants, like poplar, under common environmental and experimental conditions (Figure 4). A "memory" for the previous environmental growth conditions may be an advantage, so that the plant is readily adapted to its environment, even before external soil-derived or climatic stimuli influence the growth.
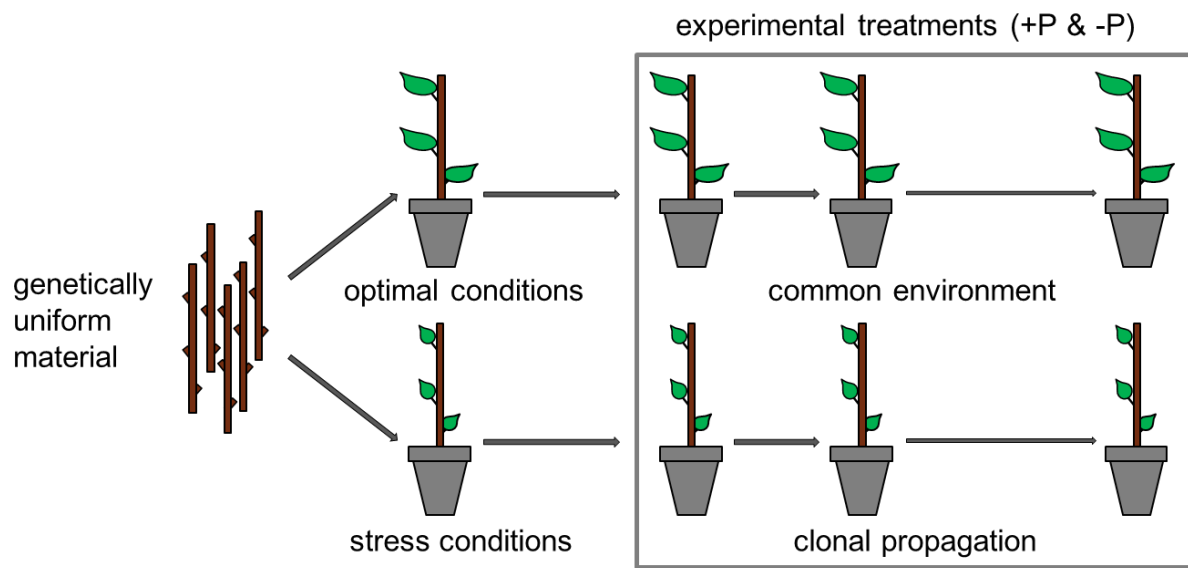
Figure 4: Schematic phenotypical adaptation of vegetatively propagated perennials.
Genetically uniform material (cuttings) is grown under optimal and stress conditions. Subsequently, vegetative propagation in common environmental and experimental conditions are performed, whereas +P describes optimal and –P deficient phosphorus supply.

1.7. Objective of this research project

In this research project, I concentrated on DNA methylation and its impact on miRNAs (but no other chromatin modifications, such as histone modifications or histone variant exchanges, which also may be inherited) and defined differential DNA methylation as an "epigenetic" mechanism, irrespective of its proof of inheritance due to clonal propagation.

Hence, it was analyzed whether genetically identical, clonal starting material (cuttings) from *Populus trichocarpa* (cv. Muhle Larson), which was grown on two different locations in northern Germany, showed "memory" with respect to their host site via differential DNA methylation in coding regions, including differentially methylated miRNAs, leading to corresponding gene expression changes which might be responsible for differences in plant establishment and growth performance. Thereby, due to already well described correlations between P availability and epigenetic modifications (Smith *et al.*, 2010; Secco *et al.*, 2015), the P nutrition background of these trees was a major focus (Figure 5).

More explicitly, it was hypothesized that:

> ➢ Clonal *Populus trichocarpa* material grown at different sites with
>   contrasting P availability shows differences in yield and phenotype
> ➢ The genome of these clonal trees grown at different sites reveals
>   site-specific epigenetic modifications (context-dependent
>   methylations in CpG, CHG and CHH)
> ➢ DNA methylation differences in coding regions and
>   miRNAs are related to their expression and thereby
>   to previous host site adaptations
> ➢ Species-specific epigenetic mechanisms are responsible for the
>   P starvation adaptation and/or P acquisition strategies
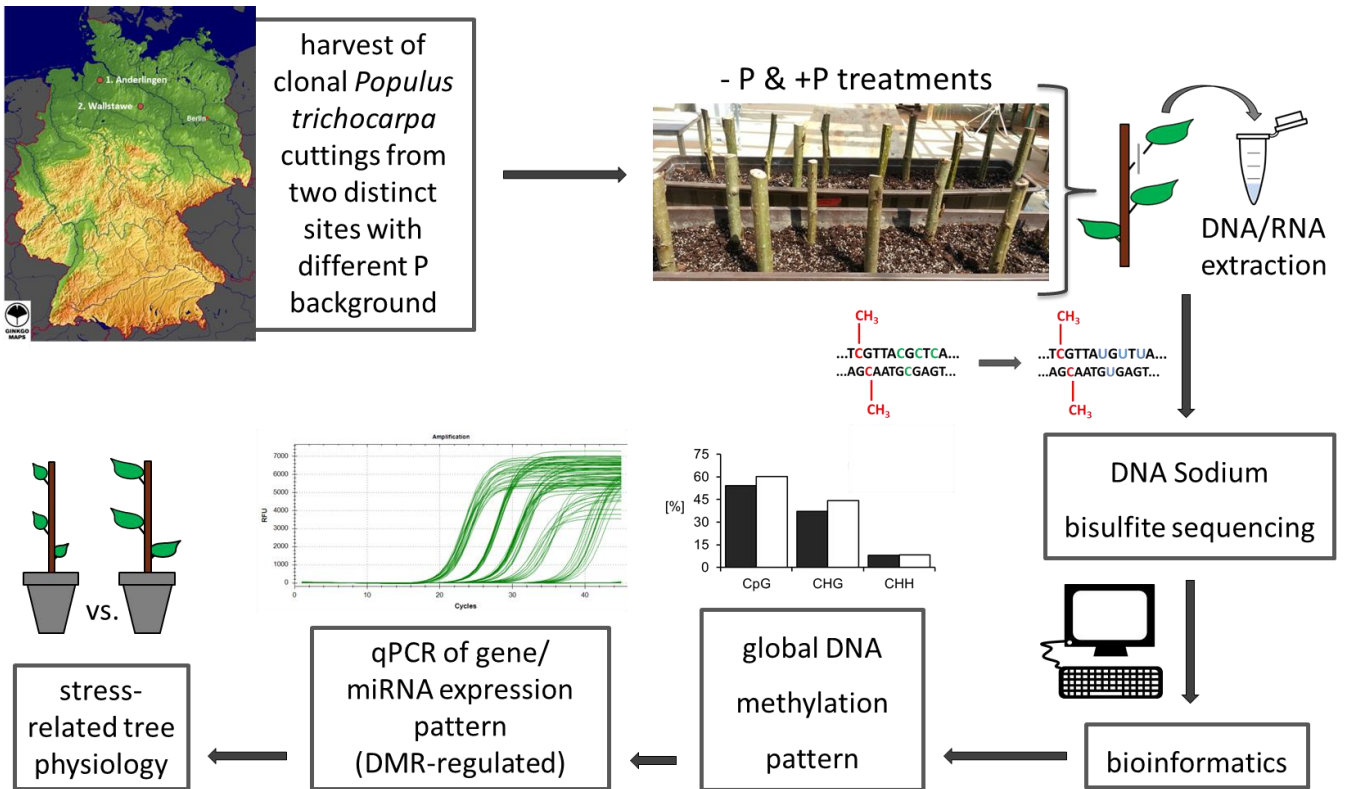
Figure 5: Schematic experimental design.

Clonal *Populus trichocarpa* cuttings (cv. Muhle Larson) are harvested from two distinct sites in northern Germany (Anderlingen vs. Wallstawe) with different phosphorus (P) supply. Subsequently, these cuttings are grown under optimal (+P) and deficient (-P) phosphorus nutrition. From these plantlets DNA extraction for DNA Sodium bisulfite sequencing and RNA extraction for quantitative real time polymerase chain reaction (qPCR) analysis is performed. Sequenced reads are processed via bioinformatic tools to detect the global DNA methylation pattern. Thereby, differentially methylated regions (DMRs) are identified in coding regions and microRNA (miRNA) sequences. Finally, DMR-regulated genes and miRNAs as well as their target expression are analyzed via qPCR to explain the stress-related tree physiology.

By understanding site-specific and species-specific adaptations not only in their genetic, but also in their epigenetic aspects, the knowledge of epigenetic mechanisms and molecular interactions might be expanded. In addition, novel adaptive, environmental and nutritional "memory" traits in trees depending on their ecosystems might be identified and analyzed, which may be useful in plant breeding, conservation biology and plant biodiversity studies, preferentially in perennial vegetatively propagated plants.

2. Material

2.1. Growth experiment

Hydroponic cultures were performed on modified Hoagland medium.

Table 1: Modified Hoagland medium and its corresponding salt concentrations.

¼ Hoagland	concentration [µM]
NH_4NO_3	1000
$MgSO_4$	500
$CaCl_2$	1000
$MnCl_2$	9
$ZnSO_4$	0.765
$CuSO_4$	0.32
H_3BO_3	46
Na_2MoO_4	0.016
Fe(III)-Na-EDTA	50
P optimum (+P) treatment	**concentration [µm]**
KH_2PO_4	1000
P deficiency (-P) treatment	**concentration [µm]**
KH_2PO_4	10
KCl	990

Additional used material for growth experiments were:

Populus trichocarpa (cv. Muhle Larson) cuttings and soil samples from different short rotation forestry sites in Germany	provided by the "Nordwestdeutsche Forstliche Versuchsanstalt" (NW-FVA; Janßen *et al.*, 2012)
paraffin wax	Merck

2.2. Kits

Table 2: Used kits, their corresponding application and supplier.

kit	application	supplier
DNeasy Plant Mini Kit	DNA extraction from plant tissues	Qiagen
EpiTect Bisulfite Kit	DNA bisulfite conversion	Qiagen
innuPREP RNA Kit	RNA extraction	analytikjena
innuPREP Micro RNA Kit	miRNA extraction	analytikjena
KAPA SYBR FAST qPCR Kit (2x) Universal	performance of qPCR	peqlab
Methyl-Seq Kit	library preparation for BS-Seq	EpiGnome
miRNA 1st-Strand cDNA Synthesis Kit	cDNA synthesis of miRNAs	Agilent
QuantiTect Reverse Transcription Kit	cDNA synthesis	Qiagen
Small RNA Analysis Kit	quantification of small non-coding RNA	Agilent

2.3. Bioinformatic tools

Table 3: Used bioinformatic tools, their corresponding application and reference.

bioinformatic tool	application	reference
bsseq	visualization and analysis of bisulfite sequencing data	Hansen *et al.*, 2012, Bioconductor
Bismark	mapping of BS-Seq data to references and performing methylation calls	Krueger & Andrews, 2011, Babraham bioinformatics
DMRcaller	analysis of chromosomal methylation distribution	Bioconductor
Ensembl Plants	providing access to plant genomes and its database	www.plants.ensembl.org
FastQC	quality control for high throughput sequence data	Babraham bioinformatics
miRBase	searchable plant database of published miRNA sequences and annotation	Kozomara & Griffiths-Jones, 2014

bioinformatic tool	application	reference
NCBI	providing access to genome information and annotation	www.ncbi.nlm.nih.gov/
SeqMonk	visualization and tracking of mapped sequence data	Babraham bioinformatics
Trimmomatic	flexible read trimming tool for high throughput sequence data	Bolger *et al.*, 2014
PopGenIE	resource for integrative exploring of the *Populus* genome	Sjödin *et al.*, 2009
psRNAtarget	prediction of small RNA targets by plants	Dai & Zhao, 2011

2.4. Real-time quantitative PCR (qPCR) primer sets

Primers used in qPCR were created by Primer-BLAST (Ye *et al.*, 2012) with an estimated primer melting temperature (Tm) of approximately 60 °C.

Table 4: Information about used primes sets.

primer set	forward primer (5' -> 3')	reverse primer (5' -> 3')
DMR[1] **transcript**		
*POPTR*_0001s01660	CTGATGACCGGATCCCTACC	GCCTTGATGTGCCTCTACGA
*POPTR*_0002s03260	CTGGTCTGTTCCCTGGATTCT	CACAACCCTGCACAAAGCAA
*POPTR*_0005s01450	TAGTGGATGAGGGACACCGT	GCATACCTGCACGTCCTAGA
*POPTR*_0006s20500	TCCCTGGAGATCCCCTTGAT	TCTTCACTCATTCCCTTGCGA
*POPTR*_0008s20220	TCTAATCAGGTTGGAGCAACAGA	TCTAATCAGGTTGGAGCAACAGA
*POPTR*_0010s11680	TGAGAAGGCTGCACTGGATG	AGCCTCCTCACCTCTGTCAT

---

[1] DMR = differentially methylated region

primer set	forward primer (5' -> 3')	reverse primer (5' -> 3')
*POPTR*_0012s04860	GGAAGGGGCAGATCACGAAT	GCGACTAAACACGGATAGCCT
*POPTR*_0014s01810	GCGTGACCTCCTTCCAACTC	TGTTCACCAATGGCTGTGGAT
*POPTR*_0014s18950	CGGCGGAATATGTTGGTAGG	TGTTGGTAAACCTCCCTCTCA
*POPTR*_0017s02120	GGGATAATAACAGCGCTCTGGA	TCCCTGTGGAAGGCATTTCT
*POPTR*_0017s14590	TGGTTCCTGCAATGGCCTAC	ATCAAGTACTCTAGCAGCTATTCCC
*POPTR*_0018s14780	GCTCTTTCTCACTCGGTCCTT	AGCGTTTGGCCATTCTCCTT
endoribonuclease Dicer		
*POPTR*_0018s30840	TCGCTCTGGGAAGGTCAATC	AACTGCGGACTGTCTTAGGC
*POPTR*_0002s182401	GGATAGACCGTACGAAGCAC	AGAATCGCACAACCAACCAG
miRNA target		
*POPTR*_0006s04360	ACGCAAGGGTTTTGGTCACT	TCCCTTATCACCCCAGCAGTA
*POPTR*_0006s9220	CATTGGACTTCTCGCCACCA	AATAATCCAGGCCACAAGCTAC
*POPTR*_0013s14900	AACTTGAAGGCTGTGCCGTA	ACGCCAGAATAGCTGAACCA
*POPTR*_0004s02320	TGTTGTTCTTCGAAGCAAGGT	CCAATTACTCCTGCCTTTAGGA
DMR[1] miRNA		
Ptc-miR827	TTTTCGTTGATGGTCATCTAA	universal reverse primer (Agilent's miRNA 1st-Strand cDNA Synthesis Kit)
Ptc-miR1446a-e	TTCTGAACTCTCTCCCTCAA	
Ptc-miR481ab	GCTTAAGCTGTTAAGTGAGGTCCT	
Ptc-miR481cd	AGGACCTCACCTAACAGCTTAAGC	
Ptc-miR6432	CCATCTTTTTCTCTAGAGCCG	
reference		
*POPTR*_EF1α	GGCAAGGAGAAGGTTCACAT	CAATCACACGCTTGTCAATA
*POPTR*_RP	ATGTTGTGACCGCTGATTGTT	AAACCGCTCCTCGAACCTA
*POPTR*_18S	TCAACTTTCGATGGTAGGATAGAG	CCGTGTCAGGATTGGGTAATTT

---

[1] DMR = differentially methylated region

2.5. Instrumental equipment

Table 5: Used instruments, their corresponding application and supplier.

instrument	application	supplier
2100 Bioanalyzer	quantification of total and short, non-coding RNA	Agilent, Waldbronn, Germany
CFX96 instrument	qPCR performance	Bio-Rad, Munich, Germany
HiSeq 2000	high throughput bisulfite sequencing	Illumina, provided by GATC Biotech AG, Constance, Germany
NanoDrop ND-1000 spectrophotometer	quality and concentration measurement of DNA, RNA and miRNA	Thermo Scientific, Brunswick, Germany
spectrophotometer U-3300	measurement of phosphorus concentration	Hitachi, Schwäbisch Gmünd, Germany
Whinrizo	measurement of morphological parameters	Regent Instrument Inc., Canada

3. Methods

3.1. Growth conditions

In spring 2013, 2014 and 2015, cuttings of *Populus trichocarpa* (cv. Muhle Larson) were harvested from different short rotation forestry sites in Germany (Anderlingen, Wallstawe, Stölzingen and Lehmbach; Janßen *et al.*, 2012). The cuttings, which were 20 cm long and had a diameter of approximately 1 cm (Figure 6a), were stored in a cold room (4 °C) until planting. A surface disinfection was performed using 70 % ethanol (Taghavi *et al.*, 2005) and exposed cutting ends were sealed with paraffin wax to avoid fungal infections by high moisture (Figure 6b).
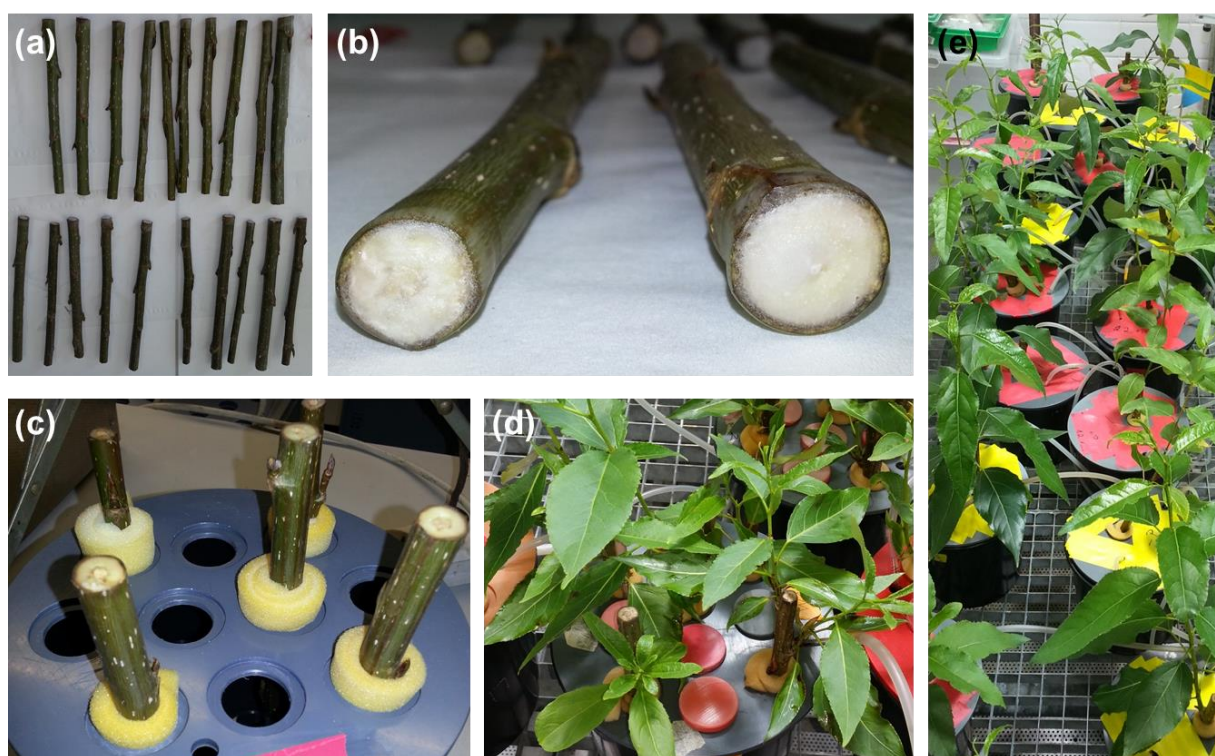
Figure 6: Planting of clonal *Populus trichocarpa* cuttings in hydroponic culture.
Cuttings (a) of clonal Populus *trichocarpa* (cv. Muhle Larson) derived from two different short rotation forestry sites were sealed with paraffin wax (b) and transferred to tap water filled pots (c). After root development in tap water (d), rooted cuttings were transferred to hydroponic culture (e) using modified ¼ Hoagland solution – with optimal (e - yellow pots) and deficient phosphorus supply (e – red pots).

Afterwards ten cuttings per chosen sites (Anderlingen and Wallstawe) were placed with bottom ends in tap water (Figure 6c) for two weeks to stimulate root development (Figure 6d). Rooted cuttings were planted in 2.8-l pots filled with modified ¼ Hoagland solution (Table 1) in controlled climate chambers (Lewis *et al.*, 2010): Air temperature was maintained at 22 : 18 °C (light, 16h : dark, 8h) with a photosynthetic photon flux density (PPFD) of approximately 100 – 150 µmol m^{-2} s^{-1}. Air humidity was kept constant at a level of 55 % (Figure 6e).

To generate subsequently P deficiency, plantlets were divided into two groups, which were subjected to the following nutrient supplies: adequate phosphorus (+P) treatment (modified ¼ Hoagland solution was changed once per week) and deficient phosphorus (-P) treatment (modified ¼ Hoagland solution was changed every week, whereas P_i was supplied as 0.01 M potassium dihydrogen phosphate [KH_2PO_4] supplemented with potassium chloride [KCl] to ensure all plants receive the same potassium [K] amount; see 2.1).

3.2. Nutrient, lignin and soil analysis

In addition to the measurement of the P concentration of material from at least three harvested or cutting-derived plants per chosen sites (Anderlingen and Wallstawe), soil samples taken from 30 cm depth (B horizon) were used to determine P concentration (calcium acetate lactate [CAL] extract; VDLUFA, 1997a), pH (calcium chloride [$CaCl_2$] suspension) and soil texture or rather soil particle size (sieving and filtering) to perform soil classification (VDLUFA, 2000). In the growth experiment, leaves, stems and roots of the two chosen sites (Anderlingen and Wallstawe) and treatments (+P & -P) were harvested after plantlets reached a height of 50 cm for P analysis and morphological comparisons via WinRHIZO (Regent Instrument Inc., Canada).

For P analysis, separated plant material (leaves and wood) from the short rotation forestry sites was dried at 60 °C, ground and ashed at 500 °C for 4 hours. Afterwards, the samples were two times treated with 3.4 M nitric acid (HNO_3) and heated till total evaporation occurred. Subsequently, 4 M hydrochloric acid (HCl) was added to each sample, which were ten times diluted and shortly boiled with hot deionized water. Finally, P concentrations were measured by spectrophotometer U-3300 (Hitachi, Schwäbisch Gmünd, Germany) after sample coloration via vanadate-molybdate reagent.

Furthermore, for lignin analysis, wooden cuttings were dried at 60 °C, grounded and subsequently lignin proportion was quantified via the acid detergent lignin method (VDLUFA, 2012).

3.3. Whole genome bisulfite sequencing

Two replicates (five plantlets per replicate) from each chosen site (Anderlingen and Wallstawe) were used to determine their methylome. DNA was extracted from young leaves using Qiagen's DNeasy Plant Mini Kit according to manufacturer's protocol. Subsequently, DNA concentration and quality was measured by NanoDrop ND-1000 spectrophotometer (Thermo Scientific, Brunswick, Germany). To generate the methylation pattern of clonal *Populus trichocarpa* leaf material derived from cuttings of two different short rotation forestry sites (Anderlingen and Wallstawe), the library preparation was performed using EpiGnome's Methyl-Seq Kit (Figure 7a; Khanna *et al.*, 2013). However, instead of the recommended sodium bisulfite conversion kits, Qiagen's EpiTect Bisulfite Kit was used, according to the standard protocol.

Ultra-high throughput paired-end (100 bp) bisulfite sequencing (BS-Seq; Figure 7b) was applied by using Illumina's HiSeq 2000 platform following the manufacturer's instructions and library spiking of 20 % PhiX as internal standard.
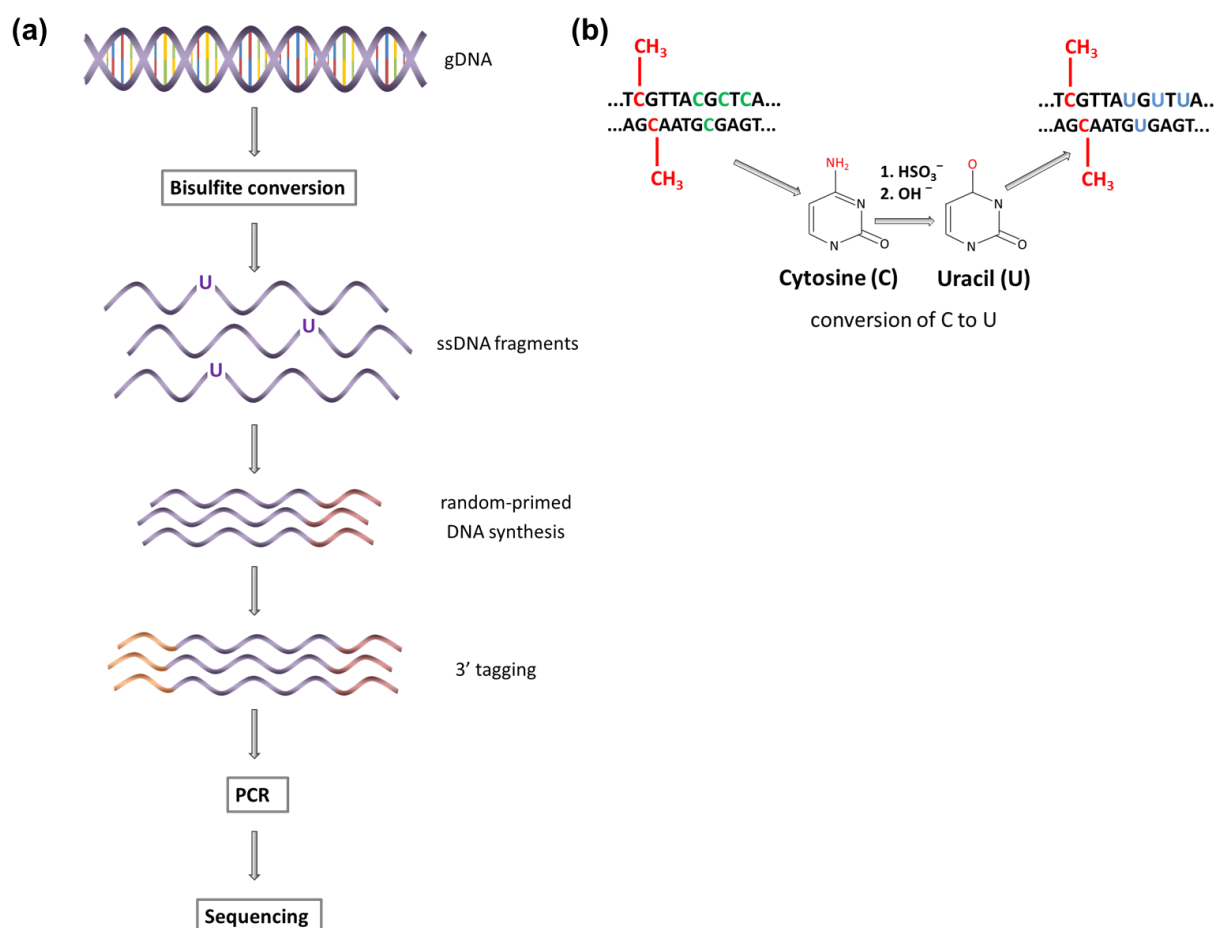
Figure 7: Outline of bisulfite sequencing library preparation.
Genomic DNA (gDNA) is treated with sodium bisulfite, leading to single stranded DNA fragments (ssDNA), where unmethylated cytosines (C) are converted to uracil (U). Subsequently, random-primed DNA synthesis and adapter 3'end-tagging is performed. Via polymerase chain reaction (PCR) all Us are converted to thymines (T). This PCR-amplified sodium bisulfite treated and converted DNA is ready for sequencing (a). By treating DNA sequences with sodium bisulfite, all cytosines (C) which are unmethylated (green) are converted to uracil (U; blue) by hydrolytic deamination. 5'-meythlcytosine residues (red) are unaffected by this treatment (b). Nucleotide sequence is represented as C (cytosine), G (guanine), T (thymine), U (uracil) and A (adenine). Figure has been modified after Khanna *et al.*, 2013.

The sequencing proceedings were performed by GATC Biotech AG, Constance, Germany. Finally, raw data were processed according to EpiGnome's Methyl-Seq Bioinformatics User Guide. The working pipeline of sequencing and its evaluation procedure is given in Figure 8.

Figure 8: Outline of sequencing procedure and bioinformatic evaluation.
Isolated DNA is sodium bisulfite treated and thereby converted. For bisulfite sequencing, library preparation is performed to obtain the sequenced reads. Subsequently, raw reads are trimmed to extract all clean reads, which are used for alignment to a reference genome. Afterwards, every single methylation call is identified, genome widely tracked and visualized. Finally, different samples are compared to determine and analyze differentially methylated regions (DMRs).

3.4. Bioinformatics and mapping of BS-Seq reads

Poor quality reads and residual adapter sequences were filtered by Trimmomatic (Bolger *et al.*, 2014). Additionally, quality of the filtered reads was analyzed using the FastQC tool (Babraham Bioinformatics). In order to align the BS-Seq reads to reference sequences, the *Populus trichocarpa* genome (v2.0) provided by the National Center for Biotechnology Information (NCBI; Tuskan *et al.*, 2006) was prepared, converted and subsequently implemented for aligning BS-Seq reads and identifying methylation calls using the Bismark tool (Krueger & Andrews, 2011). Methylation calls and further analyses were genome-widely tracked and visualized by the SeqMonk software (Babraham bioinformatics).

Besides, bisulfite conversion efficiency was calculated from unmethylated chloroplast sequence as a negative control following the formula:

$$p = 1 - \frac{(\# \text{ methylated cytosines})}{(\# \text{ of cytosines})}$$

(Becker *et al.*, 2011; Liang *et al.*, 2014).

The conversion efficiency rates amounted 99.17 % (Anderlingen) and 99.11 % (Wallstawe). These values were used to measure the false discovery rate (FDR) according to the correction algorithm by Lister *et al.*, 2009.

Methylation distribution over every single chromosome was detected by Bioconductor's package DMRcaller. Furthermore, methylation levels around annotated transcriptional starting sites were identified by the free software R for statistical computing. In addition, BS-Seq-derived differentially methylated regions (DMRs) were determined by the BSmooth algorithm and minimum absolute t-statistics using Bioconductor's package bsseq, whereas methylation calls with a minimum coverage of three reads per sample were included in further analysis (Hansen *et al.*, 2012). Thereby, the mean difference across the DMR in methylation between Anderlingen and Wallstawe of at least 0.1 and a quantile-based cutoff of 0.025 and 0.0975 was chosen.

The top 200 DMR events of every context (CpG, CHG and CHH – where H represents A, T or C; single letter abbreviation) were analyzed, compared and visualized in detail to select annotated genes affected by differentially methylated states via MapMan (Thimm *et al.*, 2004), NCBI, PopGenIE (Sjödin *et al.*, 2009) and SeqMonk (Babraham Bioinformatics). To include DMRs in promoter sequences 2000 bp before the open reading frame (ORF) of genes were considered in further analyses as well.

3.5. Mature miRNA analysis

DMRs were analyzed using miRBase (Kozomara & Griffiths-Jones, 2014) to find mapped differentially methylated miRNA genes of *Populus trichocarpa*. Therefore, miRNAs from leaves and roots (+P & -P) were isolated via analytikjena's innuPREP Micro RNA Kit following the standard protocol. Subsequently, miRNA concentration and quality was measured by NanoDrop ND-1000 spectrophotometer (Thermo Scientific, Brunswick, Germany). The expression of the identified differentially methylated miRNAs was quantified via qPCR (see following subsection 3.6) by addition of a poly-A-tail and a universal adapter following the instructions of Agilent's miRNA 1st-Strand cDNA Synthesis Kit.

Forward primers were designed using the miRNA sequences of miRBase (Kozomara & Griffiths-Jones, 2014), whereas the universal reverse primer, annealing to the 5' end added universal adapter, was provided by the kit (Table 4). Total short, non-coding RNA quantification was performed using the Agilent 2100 Bioanalyzer (Waldbronn, Germany) and Agilent's Small RNA Analysis Kit according to the standard protocol.

3.6. Transcription analysis

Gene selection for transcription analysis was performed by including only DMRs which occur in gene and predicted promoter sequences in each context due to high probability of changes in gene expression related to DNA methylation. Additionally, target genes of differentially methylated miRNAs were identified via psRNAtarget tool with an maximum expectation value to score the complementarity between small RNA and their target transcripts of 2.0 (Zhang, 2005; Dai & Zhao, 2011).

Furthermore, related transcripts, like Dicer homologs, were detected via Ensembl Plants' BioMart. Therefore, RNA was extracted using analytikjena's innuPREP RNA Kit according to manufacturer's instructions. Subsequently, RNA concentration and

quality was measured by NanoDrop ND-1000 spectrophotometer (Thermo Scientific, Brunswick, Germany). Afterwards, 1 µg of total RNA was reverse transcribed to cDNA via the QuantiTect Reverse Transcription Kit. PCR reactions were performed using peqlab's KAPA SYBR FAST (2X) Master Mix Universal qPCR Kit. Primers used in qPCR for gene or miRNA candidates were created by Primer-BLAST (Ye *et al.*, 2012) with an estimated primer melting temperature (Tm) of approximately 60 °C (Table 4), whereas primers for reference genes were chosen according to Xu *et al.*, 2011. Real-time qPCR was carried out using a two-step protocol in the Bio-Rad CFX96 instrument, Munich, Germany (Figure 9).

Gene expression studies were obtained in leaves and roots of both treatments (+P & -P) harvested after plantlets reached a height of 50 cm. Target genes and differentially methylated genes were annotated and classified via MapMan (Thimm *et al.*, 2004), Ensembl Plants, NCBI and PopGenIE (Sjödin *et al.*, 2009).
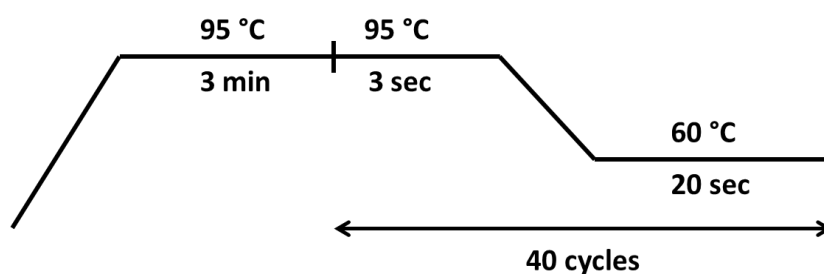
Figure 9: Two-step qPCR protocol of the KAPA SYBR FAST qPCR Kit.
Enzyme (KAPA SYBR FAST DNA Polymerase) activation requires 3 min of 95 °C, subsequently optimal denaturation of targets is carried out for 3 sec at 95 °C (first step). Annealing and data acquisition requires 20 sec of 60 °C (according to the annealing temperature of the used primer sets; second step). 40 cycles of the first and second step are performed for reliable qPCR results.

4. Results

4.1. Poplar establishment and P nutrition at different rotation forestry sites

Cuttings and leaf samples of poplar clones (*Populus trichocarpa* cv. Muhle Larsen) were obtained from four short rotation forestry sites in Germany (Anderlingen, Wallstawe, Stölzingen and Lehmbach; Janßen *et al.*, 2012) to investigate their P background in wood and leaves (Figure 10).

Obviously, plant material derived from Anderlingen showed in both measurements not always significant, but always the lowest phosphorus concentration, whereas the other short rotation forestry sites revealed more or less the same P levels (Figure 10b-c), leading to a deeper focus on cuttings derived from Anderlingen and Wallstawe due to their different P history and geographical proximity.

In the two chosen sites, phosphorus concentrations in leaves (Figure 11a), wood (Figure 11b) and soil (Figure 11c) were measured to analyze their P background history. In addition, according to VDLUFA, 2000, soil texture analysis classified the soils from the two distinct sites as sandy (Anderlingen) and as loamy sandy (Wallstawe), indicating similar soil features in soil aeration, but an improved water and nutrient holding capacity in Wallstawe due to a slightly higher proportion of silt and clay (Figure 11d).
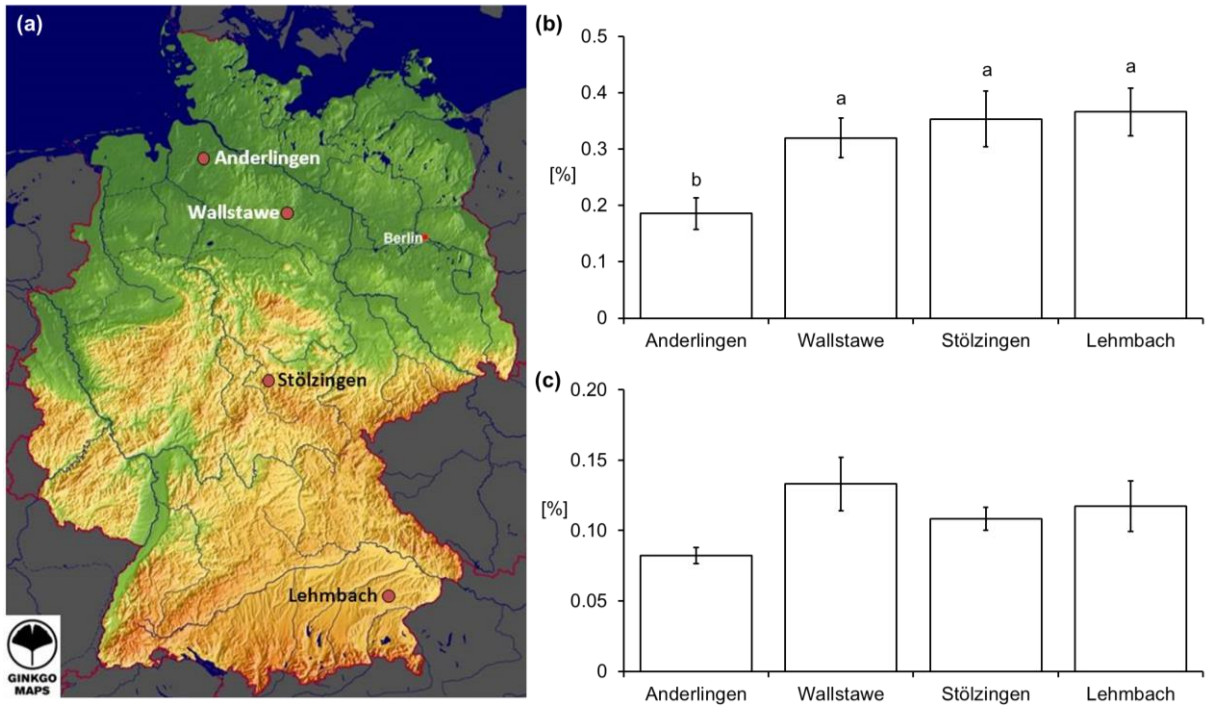
Figure 10: Phosphorus background of clonal *Populus trichocarpa* material derived from different short rotation forestry sites in Germany.

Four short rotation forestry sites in Germany (and its capitol Berlin) are shown in (a), where the same *Populus trichocarpa* (cv. Muhle Larson) clones are grown. Phosphorus (P) background has been determined by measuring the acid extractable P concentration (y-axis) of leaves (b) and wood (c) harvested from the four different sites (x-axis). Data are presented as the mean $\pm$ standard error (SE), $p \leq$ 0.05 and 95 % confidence intervals and were obtained from 3 independent measurements (b,c).

Although, P concentrations between both sites were not always significantly different, plant material directly derived from Anderlingen always showed lower P concentrations in all measurements than the plant material directly derived from Wallstawe (Figure 11). Furthermore, by categorizing the soil P concentration into the classification of agricultural used fertilizing management by the VDLUFA, 1997b, Anderlingen's soil was considered to have a low (B) and Wallstawe's soil to have a sufficient (C) P availability (Table 6). Therefore, Anderlingen was considered as low P_i and Wallstawe as high P_i site.
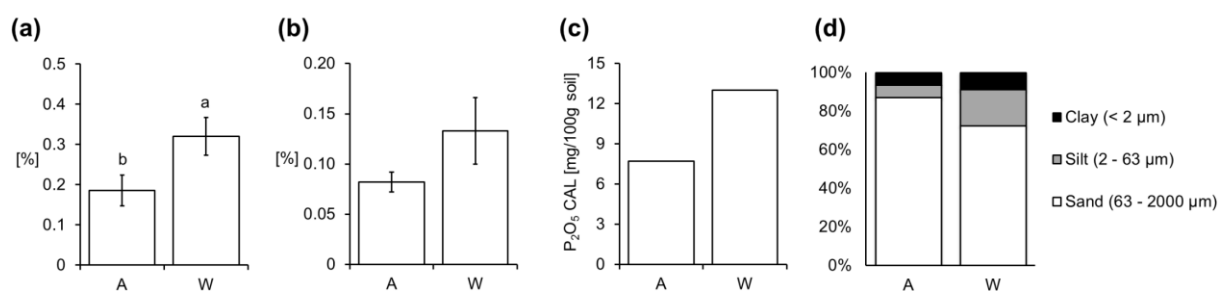
Figure 11: Phosphorus nutrition facts of two different sites.

Acid extractable phosphorus (P) concentrations (y-axis) are given for leaf (a) and wood (b) material from clonal *Populus trichocarpa* (cv. Muhle Larson) harvested from two short rotation forestry sites (A = Anderlingen vs. W = Wallstawe; x-axis). P concentration (P_2O_5 in mg/100 g soil, extracted via calcium acetate lactate [CAL] method) in the soil of the two different sites (c) and their soil texture analysis by sieving and filtering (d) are additionally illustrated. Data are presented as the mean ± standard error (SE), $p \leq 0.05$ and 95 % confidence intervals and were obtained from 3 independent measurements (a,b).

Table 6: Classification of agricultural used fertilizing management by VDLUFA, 1997b.

classification	A	B	C	D	E
mg P_2O_5/100 g soil	≤ 5.0	6 – 9	10 – 20	21 – 34	≥ 35
P availability	very low	low	sufficient	high	very high

Additionally, the pH in 30 cm soil depth (B horizon) was determined as 5.9 in Anderlingen and 5.0 in Wallstawe (Table 7). Both values indicated lightly acid soils, where P_i could be partially absorbed and fixed by aluminum.

Table 7: Soil pH of two short rotation forestry sites (in 30 cm depth).

site	Anderlingen	Wallstawe
pH	5.9	5.0
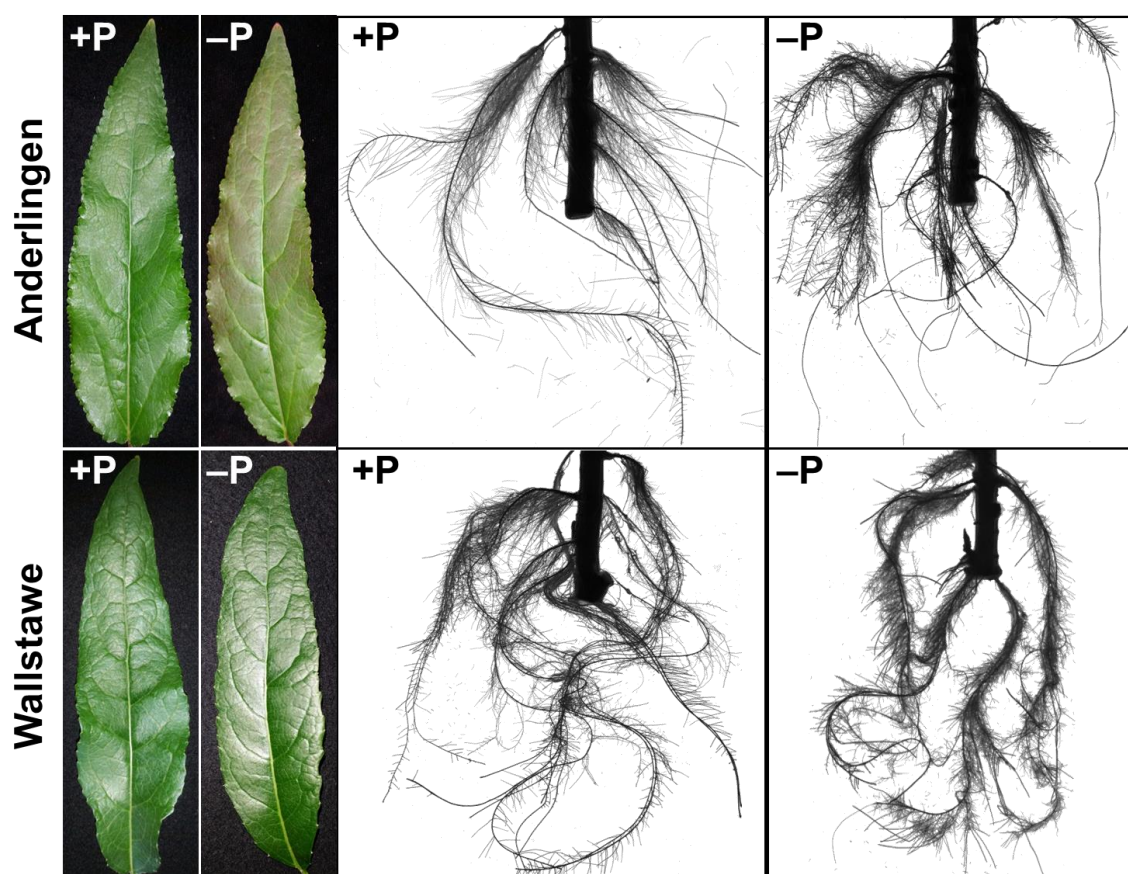
Figure 12: Site-dependent morphological adaptations of *Populus trichocarpa* clones under different phosphorus nutrition levels.

Leaf and root morphology from clonal *Populus trichocarpa* (cv. Muhle Larson) derived from cuttings of two different short rotation forestry sites (Anderlingen vs. Wallstawe) under adequate (+P) and deficient (-P) phosphorus supply are illustrated.

Stem cuttings derived from these sites had slightly different P stored in the stem (Figure 11b), with cuttings from the low P_i site (Anderlingen) establishing worse than those from the high P_i site under a common environment in the growth chamber and adequate (+P) and deficient (-P) phosphorus supply (Figure 12). Interestingly, typical P deficiency symptoms (e.g. anthocyanin accumulation in leaves, short dense root system, stunted growth, etc.) were strongly visible in the low P_i site, but not in the high P_i site (Figure 12), even though plants were grown under the same environmental conditions (see 2.1).

(a)

(b)
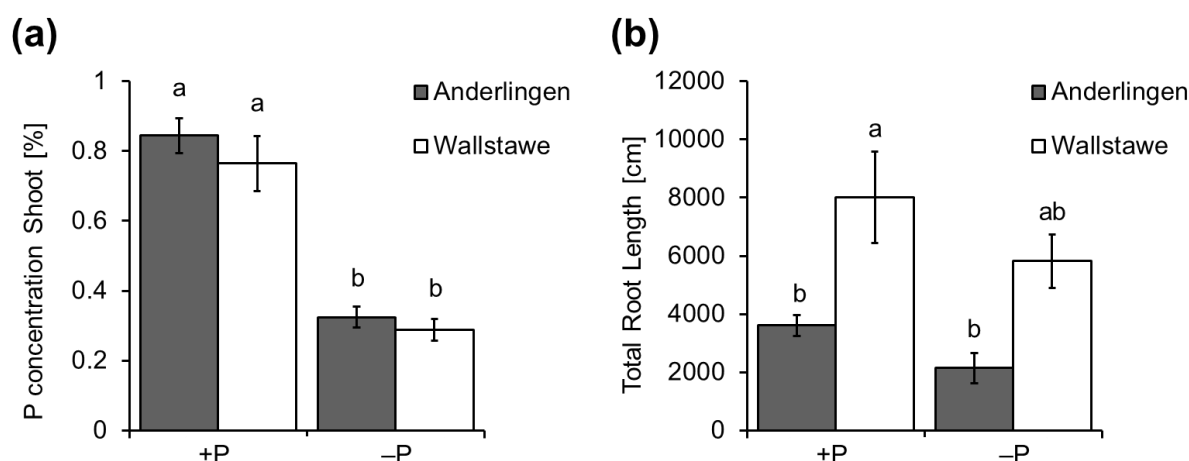
Figure 13: Site-dependent physiological parameters of *Populus trichocarpa* clones under different phosphorus nutrition levels.

Acid extractable phosphorus (P) concentration in shoots (a) and total root length (b) from clonal *Populus trichocarpa* (cv. Muhle Larson) derived from cuttings of two different short rotation forestry sites (Anderlingen vs. Wallstawe) under adequate (+P) and deficient (-P) phosphorus supply. Data are presented as the mean ± SE, p ≤ 0.05 and 95 % confidence intervals and were obtained from 3 independent experiments.

However, P concentration in the shoot did not depend on the history of the cuttings and was similarly high when cultivated on high or low P_i with an expected significant difference of P concentration between –P and +P treatment (Figure 13a). Though, root architectural traits and the growth performance, determined by the (shoot and root) biomass production, differed significantly, depending on whether cuttings were derived from Anderlingen or Wallstawe, suggesting a site-dependent, but not necessarily a P-dependent "memory" effect in plant establishment (Figure 13b and Figure 14).

(a)

(b)

(c)
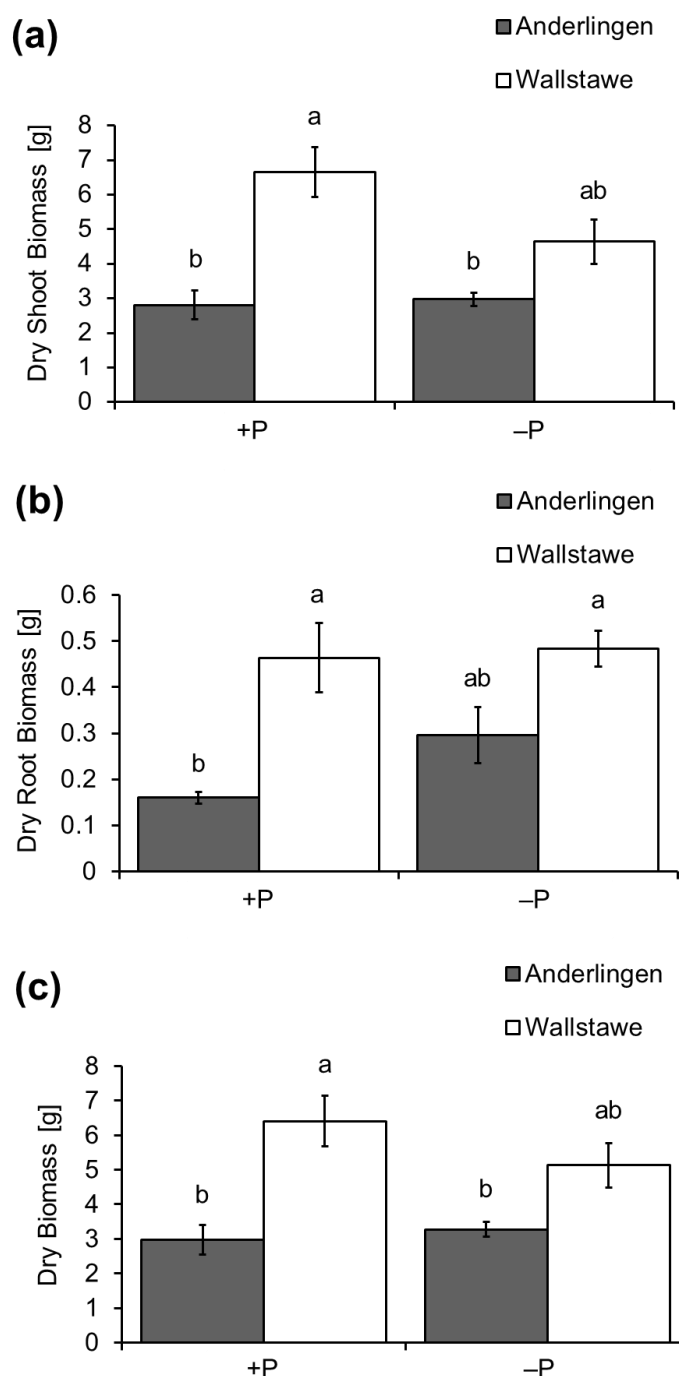
Figure 14: Site-dependent growth performance of *Populus trichocarpa* clones under different phosphorus nutrition levels.

Dry shoot (a), dry root (b) and total dry biomass (c) from clonal *Populus trichocarpa* (cv. Muhle Larson) derived from cuttings of two different short rotation forestry sites (Anderlingen vs. Wallstawe) under adequate (+P) and deficient (-P) phosphorus supply are shown. Data are presented as the mean ± SE, $p \leq 0.05$ and 95 % confidence intervals and were obtained from 3 independent experiments.

4.2. Site-dependent methylome and context-specific methylation differences

The whole genome DNA methylation pattern was derived from bisulfite sequencing of leaf material originating from cuttings of the low P_i (Anderlingen) and high P_i site (Wallstawe) using the Illumina Hiseq 2000 platform. Hence, two sets of raw sequence data were obtained with an output of 16.48 giga base pair (Gb) in material derived from Anderlingen and 16.27 Gb in material derived from Wallstawe (Table 8).

The *Populus trichocarpa* genome (v2.0), the first sequenced tree genome, served as a reference for mapping (Tuskan *et al.*, 2006). After applying several filter criteria (e.g. excluding poor quality reads or adapter sequence contaminations), it was possible to uniquely align 57 % (Anderlingen) and 52 % (Wallstawe) of the reads for further analysis (Figure 15). In bisulfite sequencing, high proportions of multiple alignments (~ 20 %) were observed due to the loss of nucleotide variation by the bisulfite-mediated cytosine to thymine conversion (Figure 7). Additionally, the estimated whole genome coverage of these data was 17.27 and 15.58 (Table 8).

Table 8: Two bisulfite sequencing data sets of clonal *Populus trichocarpa* (cv. Muhle Larsen) derived from two short rotation forestry sites (Anderlingen vs. Wallstawe).

sample	Anderlingen	Wallstawe
raw reads (Gb)	16.48	16.27
clean reads (Gb)	14.71	14.55
unique aligned reads (%)	57	52
unique aligned reads (Gb)	8.38	7.57
average coverage	17.27	15.58
conversion efficiency rate (%)	99.17	99.11
conversion error rate (%)	0.83	0.89

Besides, the conversion efficiency rates were determined by the unmethylated chloroplast sequence and amounted 99.17 % (Anderlingen) and 99.11 % (Wallstawe), respectively (Table 8). However, high quality data were obtained with minor global differences between the sites and identified a level of methylation of around 20 % (Figure 15). A slightly higher but not significantly different amount of methylated cytosines (^{m}Cs) in the whole genome was uncovered in plants derived from the high P_i site Wallstawe (20 % vs. 17 %).
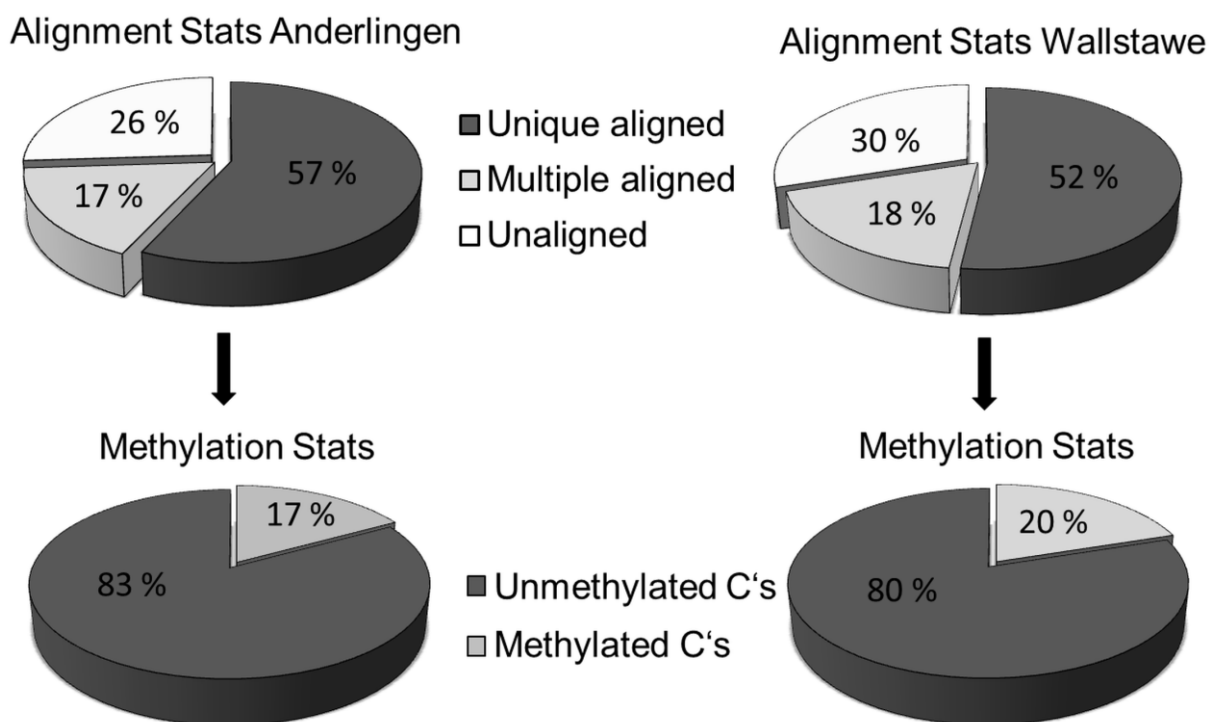
Figure 15: Alignment and methylation statistics of whole genome bisulfite sequencing of clonal *Populus trichocarpa* **leaf material.**

Alignment statistics and absolute percentage of methylated cytosines in the whole genome are given for bisulfite sequenced leaf material from clonal *Populus trichocarpa* (cv. Muhle Larson) cuttings derived from two different short rotation forestry sites (Anderlingen vs. Wallstawe).

In addition, it was analyzed, if the clean sequenced and aligned reads were covering the whole *Populus trichocarpa* genome (v2.0), which served as a reference. Therefore, reads used in further analysis were visualized by the SeqMonk software (Figure 16). Both samples derived from the two distinct sites (Anderlingen and Wallstawe) showed a similar pattern of genome coverage in different chromosomal loci. More explicitly, certain chromosomal areas showed low or no coverage in both sequencing samples (white spots in Figure 16), indicating repetitive regions in the genome, which were difficult to align uniquely. However, the whole reference genome was more or less similarly covered by the sequenced plant material derived from Anderlingen or Wallstawe, allowing further analyses and comparisons.
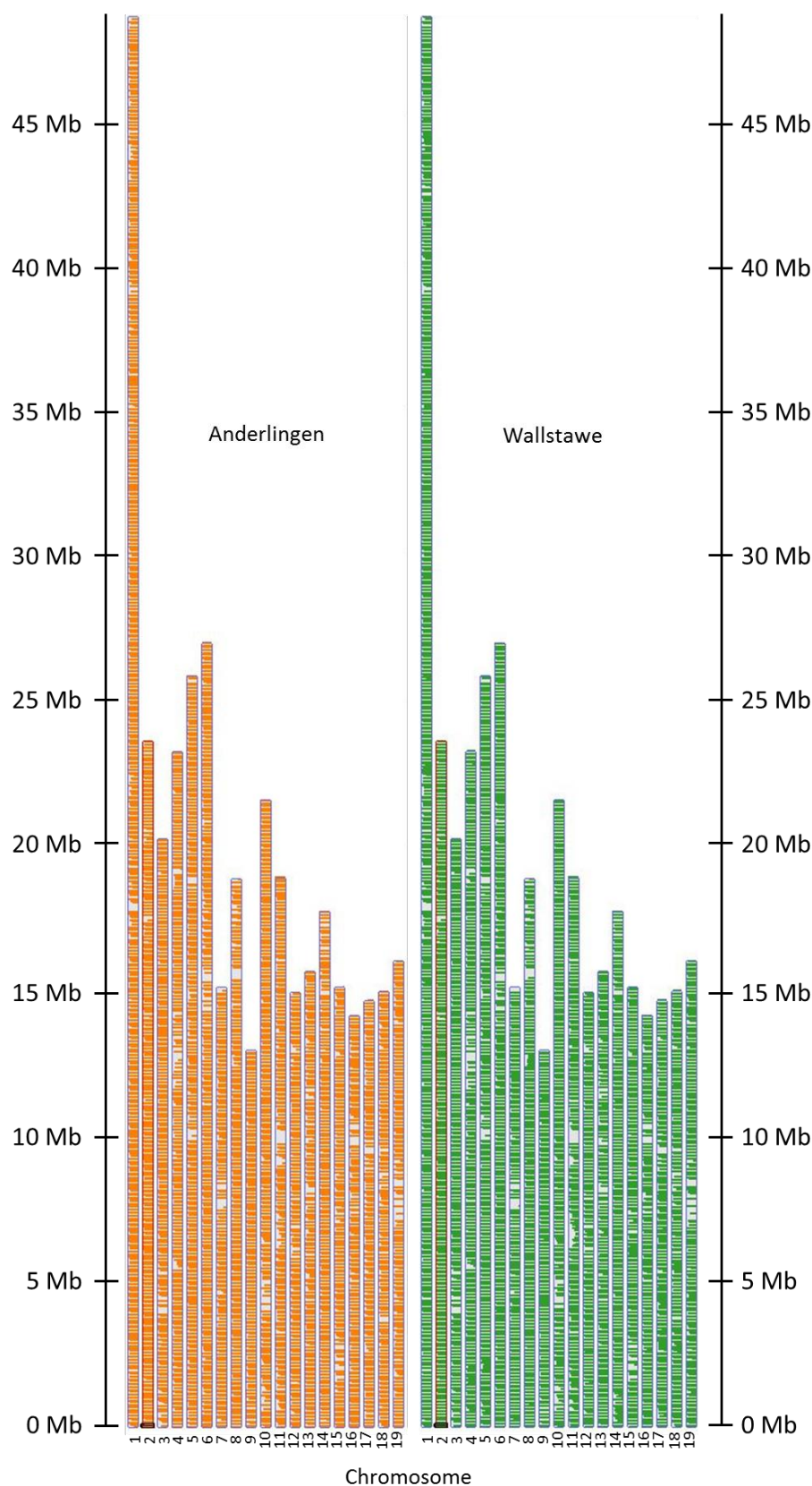
Figure 16: Sequencing coverage of the *Populus trichocarpa* genome.
The x-axis indicates the 19 chromosomes of *Populus trichocarpa*. The y-axis represents the number of mega base pairs (Mb). Clonal *Populus trichocarpa* leaf samples derived from two different sites were sequenced. Thereby, the coloration indicates, if and how deep the whole genome was covered by sequencing (orange = samples from Anderlingen; green = samples from Wallstawe; white spots = missing coverage). Figure has been modified and generated by the SeqMonk software.

Subsequently, distributions of relative and absolute cytosine methylation levels were detected by the Bismark application (Krueger & Andrews, 2011) and showed a higher proportion in symmetric ^{m}CpG and ^{m}CHG than in asymmetric ^{m}CHH levels (Figure 17 and Figure 18). Though, the absolute proportion of ^{m}Cs differed the most in the asymmetric "de novo" CHH methylations (32 % vs. 27.6 %; Figure 18).
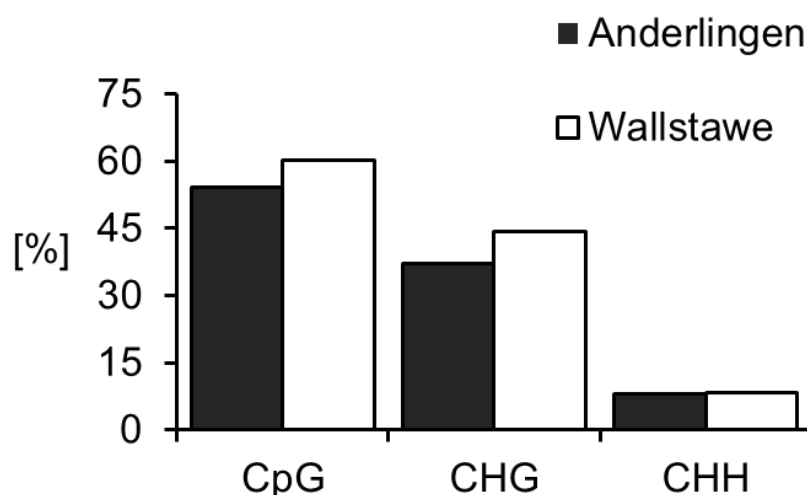
Figure 17: Methylation context statistics.

Relative percentage (y-axis) of every methylated cytosine context (CpG, CHG and CHH – where H represents the nucleotides A, T or C; x-axis) from clonal *Populus trichocarpa* (cv. Muhle Larson) leaves derived from two distinct short rotation forestry sites (Anderlingen vs. Wallstawe).
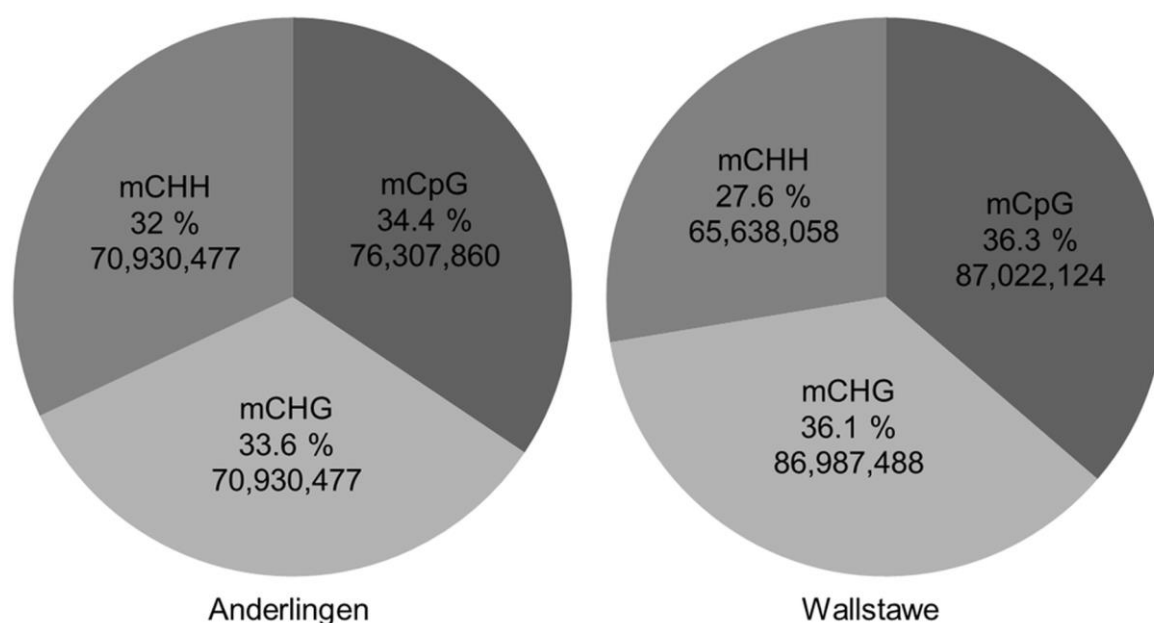
Figure 18: Absolute ^{m}C level of the *Populus trichocarpa* DNA methylome.
The absolute percentage and absolute number of methylated cytosines (^{m}C) in every context (CpG, CHG and CHH – where H represents the nucleotides A, T or C; single letter abbreviation) identified in clonal *Populus trichocarpa* (cv. Muhle Larson) leaf material derived from two different short rotation forestry sites (Anderlingen vs. Wallstawe).

To assess the risk of bias in the analyzed sequencing reads, the methylation calls for every read (length of 90 bp) in one sequenced library sample were plotted. Thereby, an equal distribution of cytosines and methylated cytosines in every context over all reads was observed, predicting a low risk of statistical bias (Figure 19).

Though, the highest relative proportion of methylation was once again observed in the symmetric CpG context, followed by the methylation rate of "de novo" cytosine contexts (CHG and CHH). In addition, relative proportions of total cytosine calls in an average read were obtained in the following order CHH, CpG and CHG context, confirming the statistical probability of finding each cytosine context event in DNA sequences.
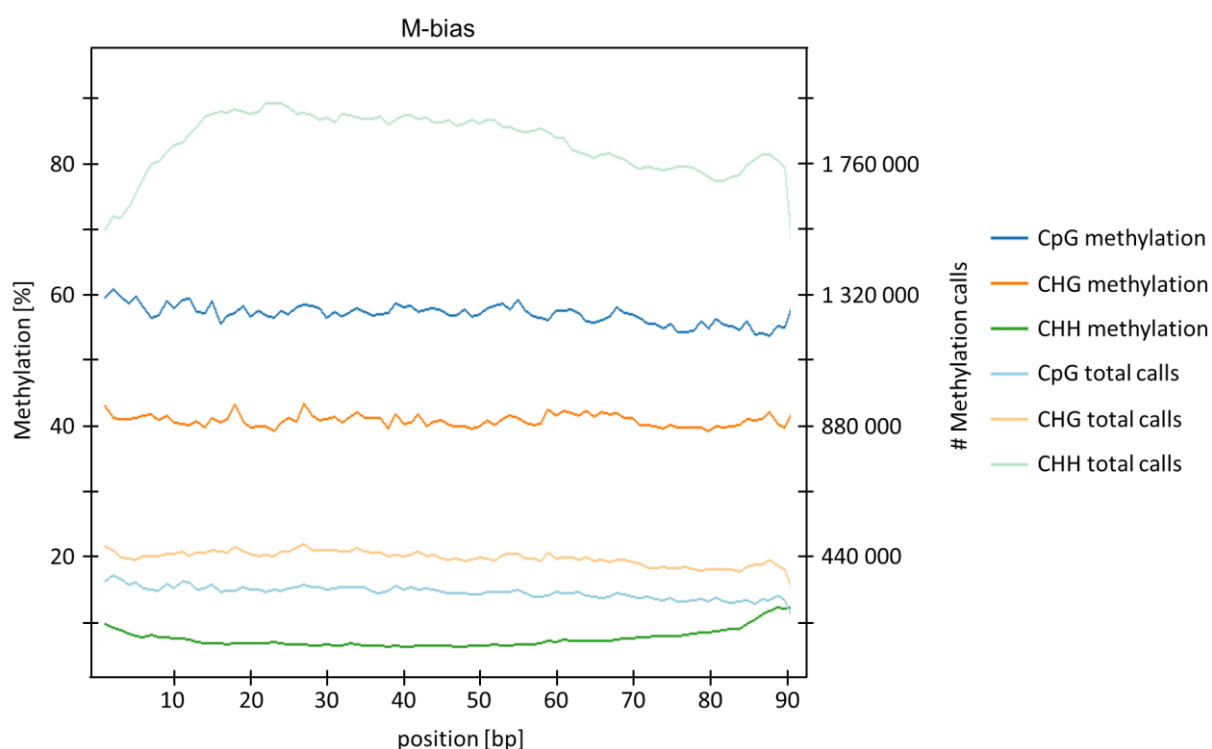
Figure 19: Sequencing M-bias statistics.
The y-axis shows the methylation percentage (left) and total number (right) of cytosines (C) in different contexts (CpG, CHG and CHH – where H represents the nucleotides A, T or C; single letter abbreviation). The x-axis represents the average read in one bisulfite sequenced library sample (100 bp and paired end sequencing), thereby the analyzed read length is 90 base pairs (bp) due to a contamination cutoff of the first and last 5 bp. Distribution of CpG (blue), CHG (orange) and CHH (green) methylation in total CpG (light blue), CHG (yellow) and CHH (light green) calls indicates possible sequencing bias and bioinformatic analysis bias.
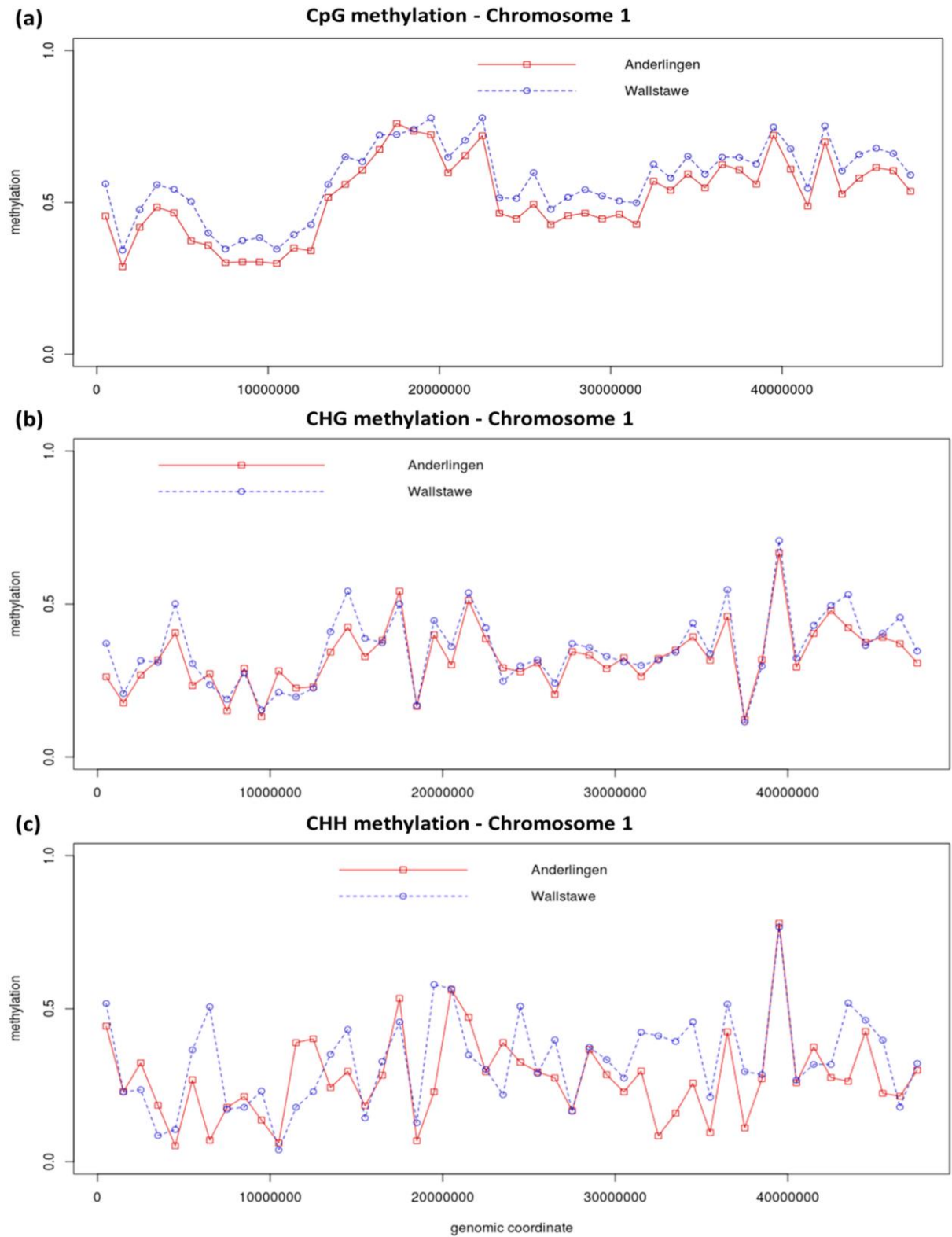
Figure 20: Chromosomal methylation distribution in clonal *Populus trichocarpa*.
The y-axis represents the methylation abundance of every cytosine context (CpG (a), CHG (b) and CHH (c) – where H represents the nucleotides A, T or C; single letter abbreviation) over chromosome 1 of clonal *Populus trichocarpa* (cv. Muhle Larson) leaf material derived from two different short rotation forestry sites (Anderlingen vs. Wallstawe). Genomic coordinates are illustrated in base pairs (x-axis).

Furthermore, chromosomal methylation distribution indicated high ^{m}CpG densities in the assumed centromeric non-coding heterochromatin (Figure 20a). Though, ^{m}CHG and ^{m}CHH showed no trend in chromosomal accumulation (Figure 20b,c).

Surprisingly, chromosomal CHH methylation distribution uncovered more variability between the plant material derived from Anderlingen or Wallstawe (Figure 20c): Chromosomal areas were detected, where sometimes Anderlingen or Wallstawe plants showed higher CHH methylation abundances. Besides, in the CpG and CHG context a clear trend of higher methylation levels in Wallstawe plants was observed (Figure 20a,b). All these observations confirmed a site-specific epigenetic adaptation, mainly by variable "de novo" and different conserved methylation patterns in clonal plants.

In addition, detection of methylation levels around transcriptional starting sites (TSS) showed relatively low methylation abundances directly at the TSS and in neighboring upstream sequences, independent from the cytosine context (Figure 21). Although, higher CpG methylation in promoter regions (2 kb upstream; Figure 21a) and higher CHG methylation in gene body regions (2 kb downstream; Figure 21b) were preferentially observed in plants derived from Wallstawe, confirming previous results (Figure 17, Figure 18 and Figure 20). Again, CHH methylation around TSS indicated no pattern of abundance due to the host site of the plants (Figure 20c).

However, with the overall higher methylation in seedlings from the P-rich site Wallstawe, differential methylation was often due to higher methylation in the high P-site Wallstawe, but the reverse pattern was also found, especially in the ^{m}CHH context (Figure 20c and Figure 21c).

(a) **(b)** **(c)**
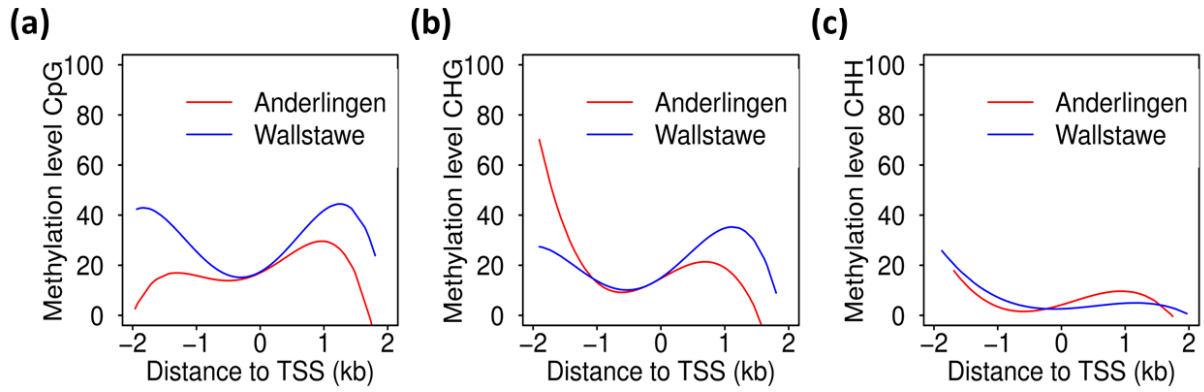
Figure 21: Methylation distribution around transcriptional starting sites (TSS) in clonal *Populus trichocarpa.*

Percentage of methylation levels (y-axis) around TSS of every cytosine context (CpG (a), CHG (b) and CHH (c) – where H represents the nucleotides A, T or C; single letter abbreviation) in clonal *Populus trichocarpa* (cv. Muhle Larson) leaf material derived from two different short rotation forestry sites (Anderlingen vs. Wallstawe). Distance to TSS is given in kilo base pairs (kb), whereas the promoter region is defined as -2 kb upstream and the gene body region as 2 kb downstream sequences (x-axis).

After determination of the unbiased methylation status in the two data sets derived from the high P_i and low P_i site, the top 200 differentially methylated regions (DMRs) in every context (CpG, CHG and CHH; in total 600 DMRs) were identified, using previously described criteria (see 3.4.; Hansen *et al.*, 2012). Two examples of chromosomal DMRs are given in Figure 22.
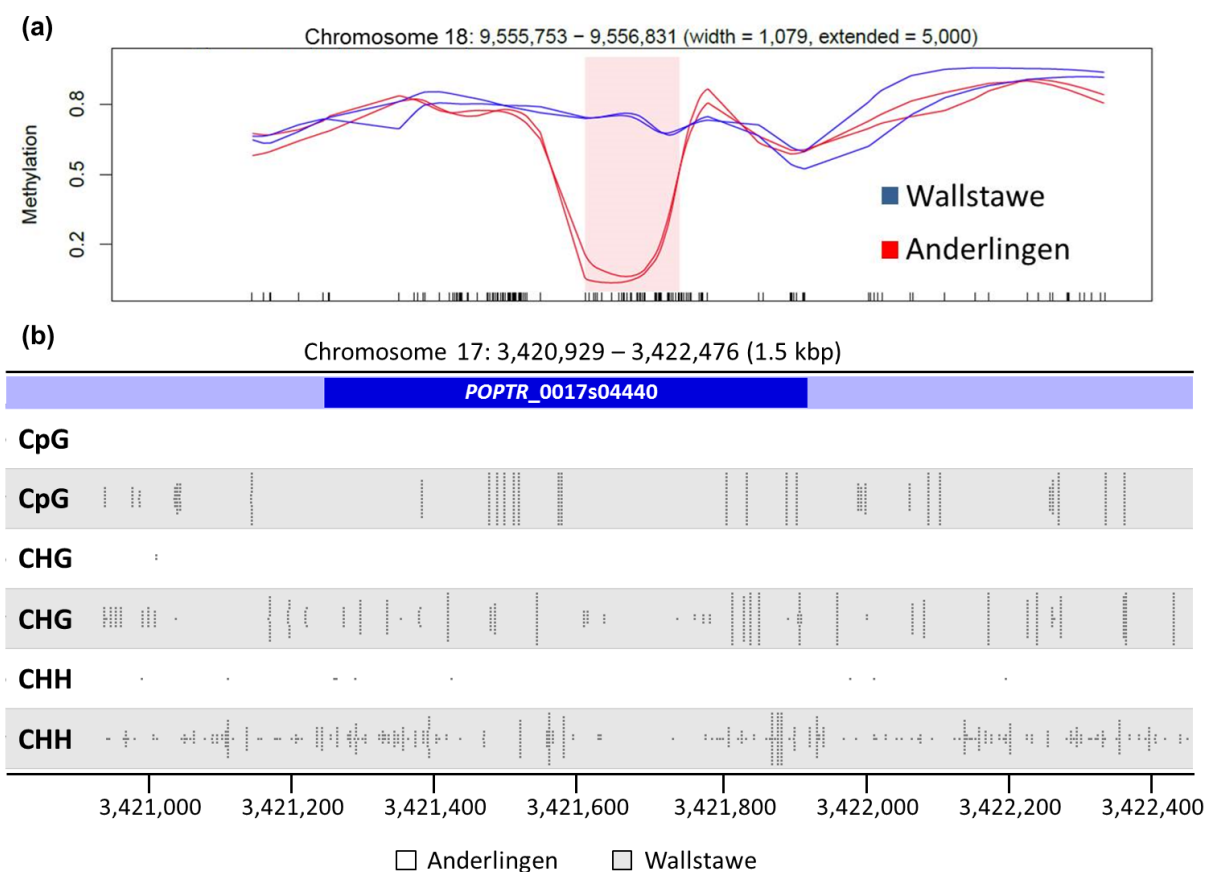
Figure 22: Differentially methylated regions (DMRs) between two bisulfite sequencing data sets.
Pink shade (a) shows one of the top 200 DMRs in a CpG context between clonal *Populus trichocarpa* (cv. Muhle Larson) leaf material derived from two different short rotation forestry sites (Anderlingen vs. Wallstawe). The x-axis represents CpG events (black bars) in the defined chromosome area (header) and the smoothed methylation level is shown on the y-axis (0 = no methylation; 1 = fully methylated sequence area). The base pair (bp) length of the shown DMR (width = 1,079 bp) is noted in the header as well as the extended chromosomal area (5,000 bp) surrounding the DMR. Methylation calls (b) of one of the top 200 DMRs, occurring in all cytosine contexts (CpG, CHG and CHH – where H represents the nucleotides A, T or C; single letter abbreviation; y-axis) and around the gene *POPTR*_0017s04440, are illustrated by using the SeqMonk software (Babraham bioinformatics). Grey spots indicate the methylation level. Besides, the sequence window (header) is stated in kilo base pairs (kbp) and the genomic coordinates are given in base pairs (x-axis).

About half (~ 50 %) of the top 200 DMRs in every context (CpG, CHG and CHH; in total 600 DMRs) were covering non-gene coding regions, potentially including many transposons or sequences transcribing miRNAs (Figure 23).
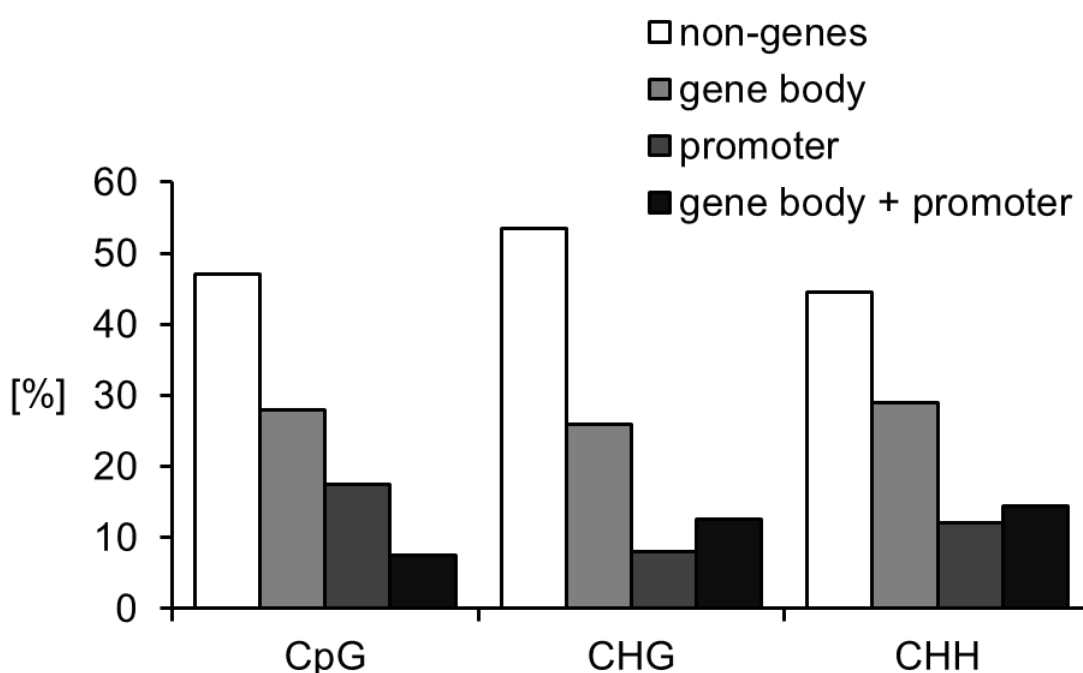
Figure 23: Proportion of differentially methylated regions (DMRs) in coding and non-coding regions in clonal *Populus trichocarpa*.

Bisulfite sequenced clonal *Populus trichocarpa* (cv. Muhle Larson) leaf material derived from two short rotation forestry sites in northern Germany (Anderlingen vs. Wallstawe) and their methylation proportions of the top 200 DMRs (y-axis) in coding and non-coding regions for every methylated cytosine context (CpG, CHG and CHH – where H represents the nucleotides A, T or C; x-axis) are shown.

However, from the top 200 differentially methylated regions in every context (CpG, CHG and CHH), annotated promoter or gene body methylations were quantified, partially overlapping and distributed differentially between Anderlingen and Wallstawe in gene body and promoter or in both coding regions (Figure 24). Interestingly, DMRs tended to appear in a higher proportion in promoter sequences in plant material derived from Anderlingen, suggesting a gene repression by methylation. Besides, a higher proportion of gene body methylation was obtained in plant material derived from Wallstawe, implying a positive correlation between DNA methylation and gene expression.

	Anderlingen	Wallstawe	
gene body	48	60	108
promoter	30	22	52
gene body + promoter	14	19	33
	92	101	193
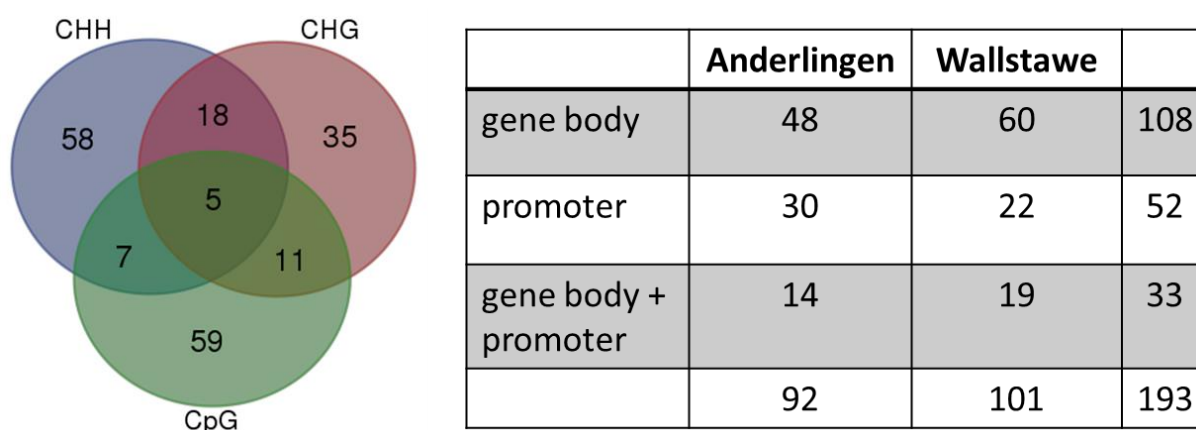
Figure 24: Numbers of differentially methylated regions in coding sequences.
Venn-Diagram of all annotated differentially methylated regions (DMRs) in coding regions shared within every cytosine context (CpG (green), CHG (pink) and CHH (violet) – where H represents the nucleotides A, T or C; single letter abbreviation) is shown. Additionally, tabular description of all DMRs distributed in gene body, promoter or both regions occurring in clonal *Populus trichocarpa* (cv. Muhle Larson) material from two different short rotation forestry sites (Anderlingen vs. Wallstawe) is illustrated. Total amount of DMRs is calculated for every row and column.

With the overall higher methylation in plantlets derived from the P-rich site Wallstawe, differential methylation was often due to higher methylation in the high P-site Wallstawe (Figure 17 and Figure 24), but the reverse pattern was also found (Figure 18 [absolute CHH amount] and Figure 20c). Asymmetric and "de-novo" methylations (CHH) in coding regions were dominating. Though, clear differences in the CHH context were only observed in the absolute methylation level and the chromosomal methylation distribution (Figure 18 and Figure 20), but not around TSS or in relative methylation proportions (Figure 17 and Figure 21).

Additionally, all DMRs in coding regions were used to potentially assign specific metabolic pathways, influenced by DNA methylation via MapMan (Thimm *et al.*, 2004). Thereby, a possible relation between differentially methylated genes and the lignin and lignan biosynthesis was revealed (Figure 25a). Thus, lignin proportions of plants from the two distinct sites were determined following the instructions of the acid detergent

lignin method (VDLUFA, 2012). Unfortunately, there was no significant difference between lignin fractions of wooden *Populus trichocarpa* material derived from Anderlingen or Wallstawe (Figure 25b), indicating no direct correlation of lignin biosynthesis and the expression of differentially methylated coding regions.

Hence, an enrichment analysis was performed using PopGenIE (Sjödin *et al.*, 2009) to assess overrepresented differentially methylated genes in functional gene classes. As expected due to the lignin analysis, no functional enrichments were detected.
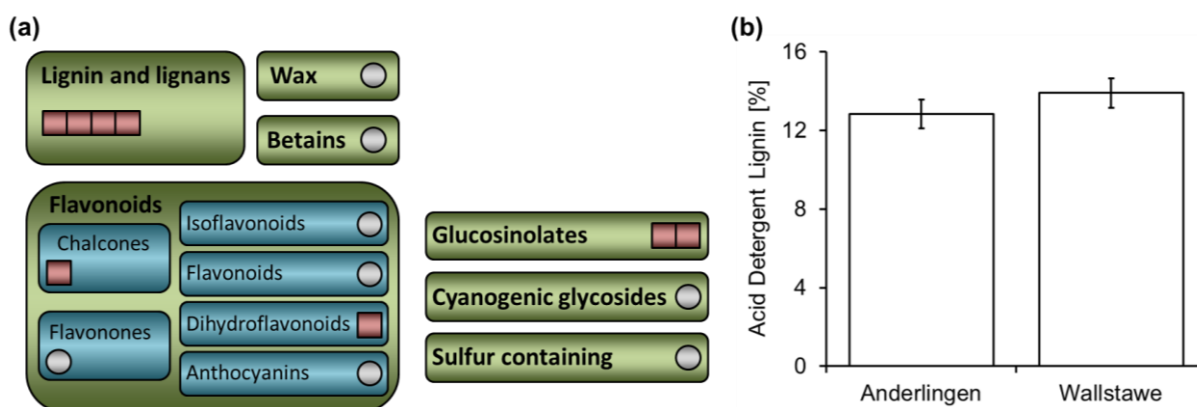
Figure 25: Lignin analysis of clonal *Populus trichocarpa* derived from two distinct sites.
Excerpt of MapMan analysis (Thimm *et al.*, 2004) showing all differentially methylated coding regions in clonal *Populus trichocarpa* (cv. Muhle Larson) distributed over functional gene classes (a). Red squares indicate DMRs involved in functional classes, whereas grey spots display functional classes unaffected by differentially methylated coding regions. Quantification of acid detergent lignin proportion (VDLUFA, 2012; y-axis) of wood material from clonal *Populus trichocarpa* cuttings derived from two short rotation forestry sites (Anderlingen vs. Wallstawe; x-axis) is shown in (b).

4.3. Gene expression in shoots and roots of differentially methylated genes

Differential gene expression was then studied for the selected top 40 differentially methylated genes in promoter and gene body regions (overlapping regions in Figure 26), whereas some cytosine contexts shared the same DMRs leading to an actual number of DMRs in promoter and gene body regions of 33 top DMR events (Figure 24 and Table 9).
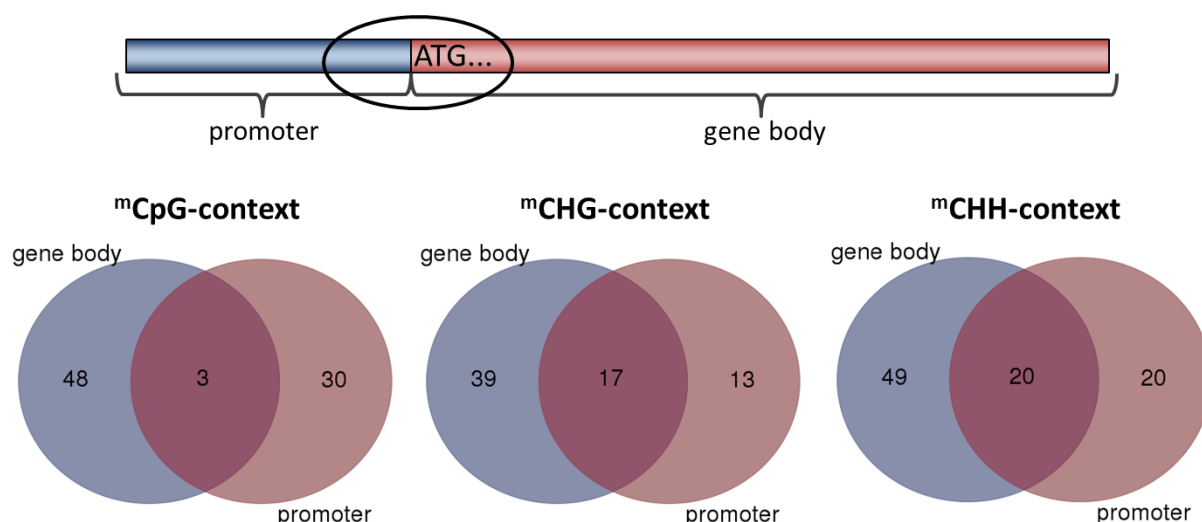
Figure 26: Selection of differentially methylated regions (DMRs) in coding sequences for gene expression analysis.

Schematic drawing of a promoter (blue) next to a gene body region (red), where ATG shows the start codon of a gene and the circuited area represents the selection of differentially methylated genes analyzed by qPCR. These selection is shown in the overlapping areas (pink) of the three Venn-diagrams in every methylated cytosine (ᵐC) context (CpG, CHG and CHH – where H represents the nucleotides A, T or C; blue = DMRs in gene body, red = DMRs in promoter, pink = DMRs in promoter and gene body region).

Table 9: Differentially methylated regions (DMRs) occurring in annotated promoter and gene body sequences of the *Populus trichocarpa* genome.

DMR gene IDs	annotation	higher methylation level site	cytosine context
*POPTR*_0001s01660	NBS-LRR resistance gene-like protein ARGH35	Wallstawe	CHG & CHH
*POPTR*_0001s06110	dirigent-like protein, regulates coupling of monolignol plant phenols to generate the cell wall polymers lignins and lignans that are involved in structural fortification and defense against pathogens	Wallstawe	CHH
*POPTR*_0001s17820	DNA polymerase III	Wallstawe	CHG
*POPTR*_0001s19460	zinc knuckle – zinc ion binding, nucleic acid binding	Anderlingen	CHG
*POPTR*_0001s42010	catalytic domain of protein kinases	Wallstawe	CHH
*POPTR*_0002s03260	horseradish peroxidase and related secretory plant peroxidases	Anderlingen	CHG & CHH
*POPTR*_0002s07850	encodes a component of the thylakoid-localized Sec system involved in the translocation of cytoplasmic proteins into plastid	Wallstawe	CHG
*POPTR*_0002s23200	aconitate hydratase, encodes a aconitase that can catalyze the conversion of citrate to isocitrate through a cis-aconitate intermediate, indicating a role in the response to oxidative stress	Wallstawe	CHG
*POPTR*_0003s12640	glycosyl hydrolase family 32, beta-fructosidases	Wallstawe	CHH
*POPTR*_0005s01450	PPR repeat family, DYW family of nucleic acid deaminases	Wallstawe	CHH
*POPTR*_0005s08440	NAC domain protein	Wallstawe	CHG
*POPTR*_0005s11730	AAA+ superfamily represents an ancient group of ATPases belonging to the ASCE division of the P-loop NTPase fold	Anderlingen	CHH
*POPTR*_0006s02510	glutathione S-transferases	Anderlingen	CHH

DMR gene IDs	annotation	higher methylation level site	cytosine context
*POPTR*_0006s09150	aldo-keto reductases, a superfamily of soluble NAD(P)(H) oxidoreductases whose chief purpose is to reduce aldehydes and ketones to primary and secondary alcohols	Anderlingen	CHG & CHH
*POPTR*_0006s18990	effector domain of the CAP family of transcription factors, members include CAP (or cAMP receptor protein (CRP)), which binds cAMP, FNR (fumarate and nitrate reduction)	Anderlingen	CHH
*POPTR*_0006s20500	elongation factor Tu family protein	Wallstawe	CHG
*POPTR*_0006s22680	NAD(P)-binding Rossmann-like domain	Anderlingen	CHG
*POPTR*_0008s18840	chromosome segregation protein	Wallstawe	CHG
*POPTR*_0009s09810	UDP-glucosyl transferase	Anderlingen	CHG
*POPTR*_0009s17130	lectin L-type, legume lectins	Wallstawe	CpG & CHH
*POPTR*_0010s05110	catalytic domain of protein kinases	Anderlingen	CHG
*POPTR*_0010s20390	peptidases S8 3	Wallstawe	CHH
*POPTR*_0011s15760	S-locus glycoprotein family	Wallstawe	CHH
*POPTR*_0011s15770	galactose mutarotase-like	Wallstawe	CHH
*POPTR*_0014s01810	peroxisomal membrane 22 kDa family protein	Anderlingen	CHG & CHH
*POPTR*_0014s18950	glycosyltransferase like family	Wallstawe	CpG
*POPTR*_0015s09330	galactinol-sucrose galactosyltransferase	Anderlingen	CHH
*POPTR*_0016s021501	glycosyltransferase family 28 C-terminal domain	Wallstawe	CHG
*POPTR*_0016s04630	cysteine/histidine-rich C1 domain family protein	Anderlingen	CHH
*POPTR*_0017s03570	transcription factor Tfb4, TFIIH (subunit of the general transcription factors for promoter recognition and initiation of transcription)	Anderlingen	CHG
*POPTR*_0017s04440	leucine-rich repeat receptor-like protein kinase	Wallstawe	CHG & CHH & CpG
*POPTR*_0017s06300	AAA+ superfamily represents an ancient group of ATPases belonging to the ASCE division of the P-loop NTPase fold	Wallstawe	CHH
*POPTR*_0019s00260	LRR 8, leucine rich repeat	Anderlingen	CHH
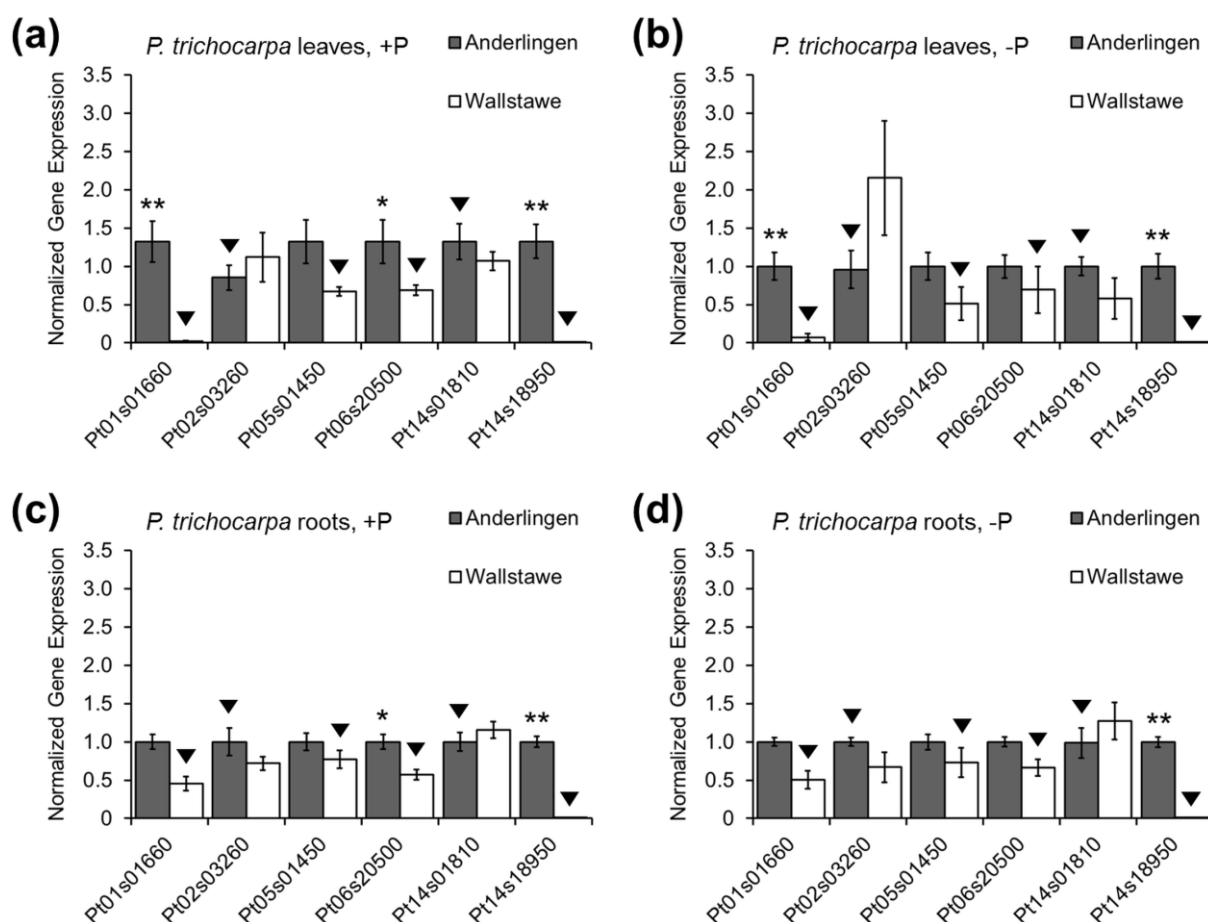
Figure 27: Gene expression differences of differentially methylated coding regions in clonal *Populus trichocarpa* material.

qPCR results from *Populus trichocarpa* (cv. Muhle Larson) leaf (a,b) and root (c,d) material derived from two different short rotation forestry sites (Anderlingen vs. Wallstawe), grown under controlled adequate (+P; (a,c)) and deficient (-P; (b,d)) phosphorus nutrition using 3 reference genes (*POPTR*_EF1α, *POPTR*_RP and *POPTR*_18s) for normalization. Normalized gene expression (y-axis) is shown for six differentially methylated genes (x-axis): *POPTR*_0001s01660 as Pt01s01660, *POPTR*_0002s03260 as Pt02s03260, *POPTR*_0005s01450 as Pt05s01450, *POPTR*_0006s20500 as Pt06s20500, *POPTR*_0014s01810 as Pt14s01810 and *POPTR*_0014s18950 as Pt14s18950. Black triangles indicate, which plant material had a higher methylation level. Data are presented as the mean ± SEM, $p* \leq 0.05$, $p** \leq 0.01$ and 95 % confidence intervals and were obtained from 3 independent experiments.

Only a small subset of the genes, which were differentially methylated in promoter and gene body region, showed a reliable expression in either shoot or root (Figure 27). Importantly, no gene with obvious relation or function in P acquisition or P metabolism was identified in this list of DMR-regulated coding regions (Table 9), explaining the missing alterations in gene expression in the –P treatments (Figure 27a,c vs. Figure

27b,d). Though mutational changes between plants derived from Anderlingen or Wallstawe could not be excluded as a potential reason for different expression profiles, there was overall little difference between root and shoot expression of the tested and selected top 33 genes (Figure 27a,b vs. Figure 27c,d) and little difference between +P and –P treatment (Figure 27a,c vs. Figure 27b,d). Only a few genes were differentially expressed or even knocked down (*POPTR*_0001s01660, *POPTR*_0006s20500 and *POPTR*_0014s18950) between plants that were grown in the same climate chamber, but that were derived from different sites, suggesting a site-dependent, but not necessarily P-related "memory" effect (Figure 27). This was mostly related to "de-novo" DNA methylations (CHH and CHG context), but in a single case also to a differential symmetric CpG methylation (Table 9). Differentially methylated genes that showed reliable but not always significantly different gene expression in leaves and roots, analyzed via qPCR, include:

> an nucleotide-binding site leucine-rich repeat (NBS-LRR)

  resistance gene-like gene (*POPTR*_0001s01660),

> a secretory peroxidase gene (*POPTR*_0002s03260),

> a pentatricopeptide repeat (PPR) family gene (*POPTR*_0005s01450),

> an elongation factor Tu family gene (*POPTR*_0006s20500),

> a peroxisomal membrane 22 kDa protein gene (*POPTR*_0014s01810) and

> a glycosyltransferase (*POPTR*_0014s18950).

Furthermore, to investigate DNA methylation effects just in promoter regions or just in gene body sequences, a small subset of reliable expressed genes, which showed DMRs just in their promoter or gene body sequences, were additionally quantified in leaves and roots via qPCR (Figure 28 and Table 10).
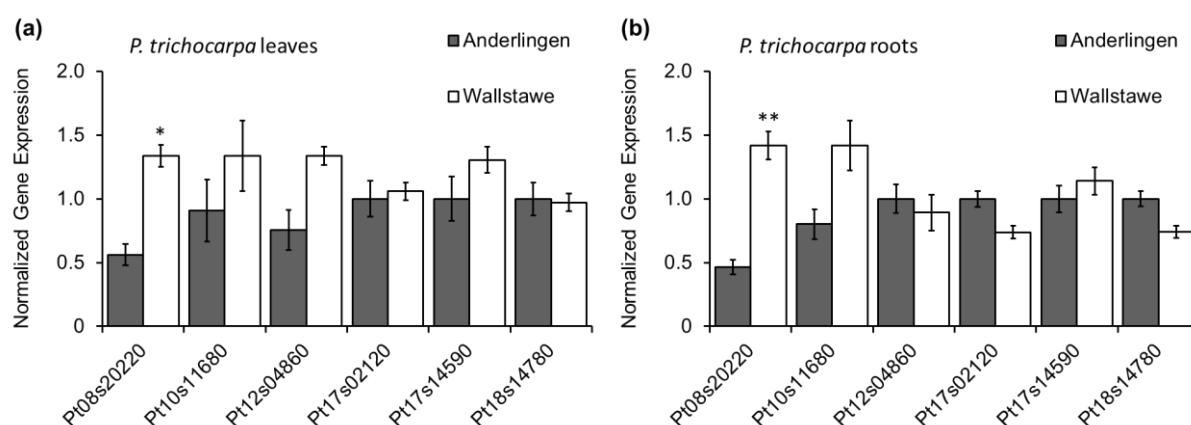
Figure 28: Gene expression differences of differentially methylated promoter or gene body sequences in clonal *Populus trichocarpa* material.

qPCR results from *Populus trichocarpa* (cv. Muhle Larson) leaf (a) and root (b) material derived from two different short rotation forestry sites (Anderlingen vs. Wallstawe), grown under optimal conditions, using 3 reference genes (*POPTR*_EF1α, *POPTR*_RP, and *POPTR*_18s) for normalization. Normalized gene expression (y-axis) is shown for six differentially methylated genes (x-axis): *POPTR*_0008s20220 as Pt08s20220, *POPTR*_0010s11680 as Pt10s11680, *POPTR*_0012s04860 as Pt12s04860, *POPTR*_0017s02120 as Pt17s02120, *POPTR*_0017s14590 as Pt17s14590 and *POPTR*_0018s14780 as Pt18s14780. In the differentially methylated genes, Anderlingen plants always showed a higher methylation level. Data are presented as the mean ± SEM, $p^* \leq 0.05$, $p^{**} \leq 0.01$ and 95 % confidence intervals and were obtained from 3 independent experiments.

Table 10: Loci of differential DNA methylation in coding regions of clonal *Populus trichocarpa* derived from two short rotation forestry sites.

differentially methylated gene ID	differentially methylated coding region	higher methylation level site	cytosine context
*POPTR*_0008s20220	promoter	Anderlingen	CpG
*POPTR*_0010s11680	gene body	Anderlingen	CHH
*POPTR*_0012s04860	gene body	Anderlingen	CpG
*POPTR*_0017s02120	promoter	Anderlingen	CHH
*POPTR*_0017s14590	gene body	Anderlingen	CHG & CHH
*POPTR*_0018s14780	promoter	Anderlingen	CHH

Based on the site- and not P-dependent gene expression differences between plants derived from Anderlingen or Wallstawe (Figure 27), gene expression analysis of differentially methylated promoter or gene body sequences was only performed in leaves and roots, grown under optimal nutrient supply. Thereby, no clear trend was observed due to the location of DNA methylation in the coding regions. These results were similar to the previous ones, where the gene expression for DMRs in both promoter and gene body regions were analyzed (Figure 27). Exceptionally, *POPTR*_08s20220 differed significantly in its expression in roots as well as in leaves due to a higher methylation level in the promoter sequence of Anderlingen plants, confirming gene repression by promoter methylation. Though, differences in gene expression by mutational changes cannot be excluded. Nevertheless, differentially methylated promoter or gene body sequences that showed reliable but almost no significantly different gene expression in leaves and roots, analyzed by qPCR, include:

> ➢ the putative histidine-containing phosphotransfer protein 2
> (*POPTR*_0008s20220),
> ➢ a non-repetitive nucleoporin family protein (*POPTR*_0010s11680),
> ➢ a chaperonin family protein (*POPTR*_0012s04680),
> ➢ a zinc finger family protein (*POPTR*_0017s02120),
> ➢ the DNA-directed RNA polymerase 2 (*POPTR*_0017s14590) and
> ➢ the vacuolar protein sorting-associated protein 26 (*POPTR*_0018s14780).

As a summary, although differential gene expression was partially observed, mostly by repression via methylation, it was rare in the analyzed top differentially methylated genes, and thus likely to be different on whole genome scale. However, direct differential gene expression via DMR was unlikely to be the main target of dynamic plant growth and site-dependent DNA methylation in *Populus trichocarpa*.

4.4. Methylation state in DMRs and transcript expression dynamics
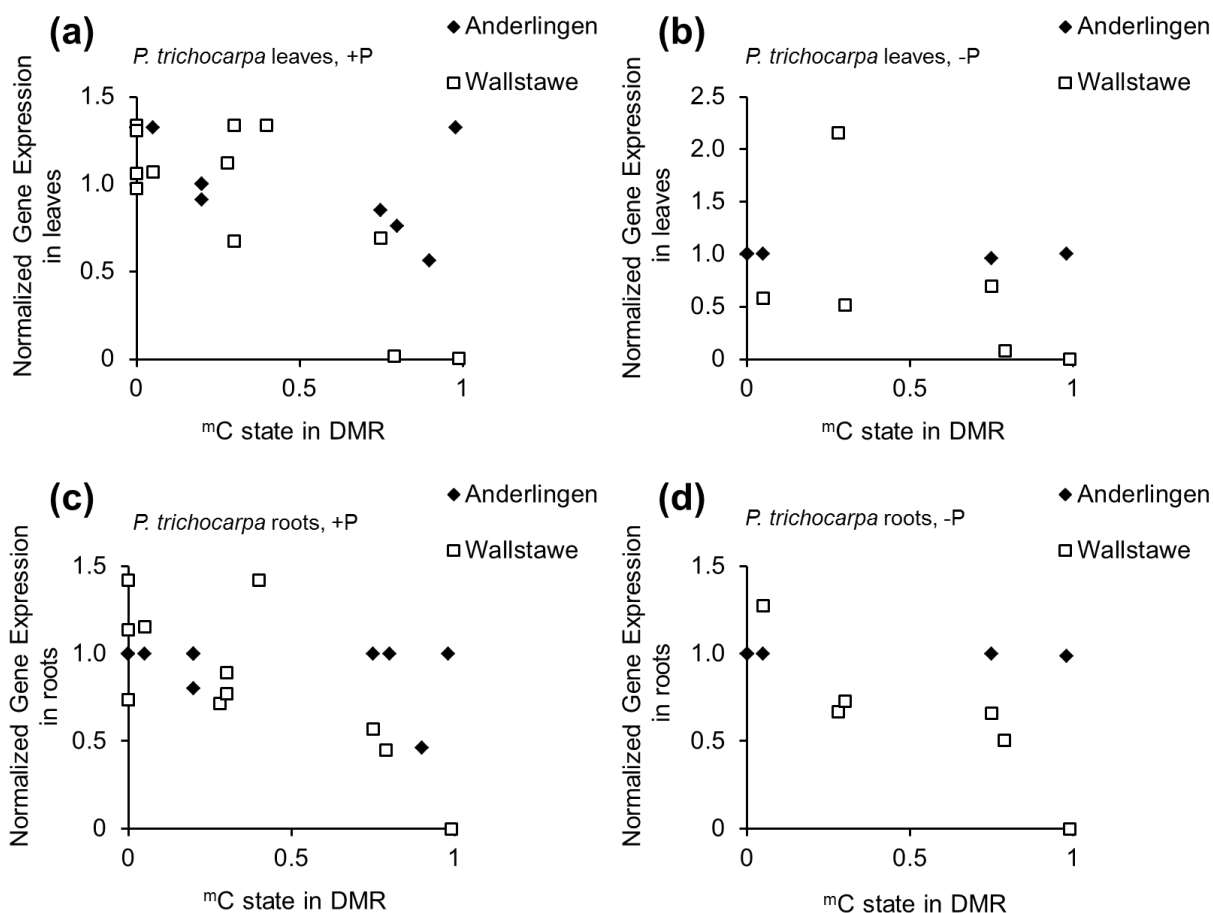
Figure 29: Gene expression vs. methylated cytosine state of differentially methylated regions (DMRs) in clonal *Populus trichocarpa* material.

Methylated cytosine (^{m}C) states (0 = no methylation; 1 = fully methylated sequence area; x-axis) in differentially methylated regions (DMRs) plotted against normalized gene expression (y-axis) of leaf (a,b) and root (c,d) material from clonal *Populus trichocarpa* (cv. Muhle Larson) cuttings derived from two different short rotation forestry sites (Anderlingen vs. Wallstawe), but grown under optimal (+P; a,c) and deficient (-P; b,d) phosphorus conditions - deficiency treatment with smaller data set.

Although relatively few genes (the top 33 differentially methylated) were investigated and quantified by qPCR, there was a trend that DMRs and their associated gene expression were somewhat different in poplar trees derived from the two different sites. The normalized gene expression in leaves or roots was more similar in plants derived from cuttings from the low P_i site Anderlingen, while normalized gene expression dynamics were larger for plants derived from cuttings of the better

P-supplied site Wallstawe. This was irrespective on the methylation state within a DMR, but similar when plants were cultivated in –P or +P (Figure 27 and Figure 29).

In accordance with a repression of transcription by methylation, fully methylated genes from plants derived from Wallstawe cuttings were not expressed, while high expression was observed for low or not-methylated genes (Figure 29). For this observation, Pearson's product-moment correlation coefficient (r) was calculated and amounted for leaves r = -0.80 (+P), r = -0.52 (-P) and for roots r = -0.71 (+P), r = -0.87 (-P) derived from Wallstawe cuttings, describing a negative, mainly significant, linear correlation between methylation levels in differentially methylated genes and gene expression (Table 11).

Table 11: Pearson's product-moment correlation of methylation states in differentially methylated genes and gene expression in plant material from clonal *Populus trichocarpa* (cv. Muhle Larson) derived from two different short rotation forestry sites (Anderlingen vs. Wallstawe).

sites	tissue	treatment	correlation coefficient (r)	p-value
Anderlingen		+P	-0.57	0.0522
	leaves	-P	-0.50	0.3156
		+P	-0.39	0.2150
	roots	-P	-0.75	0.0862
Wallstawe		+P	-0.80	0.0018
	leaves	-P	-0.52	0.2860
		+P	-0.71	0.0100
	roots	-P	-0.87	0.0227

However, irrespective of whether the ^{m}C state was high or low (fully or not methylated gene region) genes from plants derived from Anderlingen cuttings were similarly expressed. Thus, Pearson's product-moment correlation coefficient (r) was also determined for Anderlingen's data set with an output of r = -0.57 (+P), r = -0.5 (-P) in leaves and of r = -0.39 (+P), r = -0.75 (-P) in roots, showing a less negative and not significant linear correlation between methylation state in differentially methylated genes and gene expression (Figure 29 and Table 11). Thus, methylation level changes influencing gene expression alterations occurred stronger in plants derived from Wallstawe than in plants from Anderlingen.

4.5. miRNA quantification and expression differences in DMRs

In addition, short, non-coding RNAs were isolated to investigate whether miRNAs, besides DNA methylation, affect gene expression. Therefore, short RNAs were quantified via Agilent 2100 Bioanalyzer and differed significantly between plants derived from Anderlingen or Wallstawe cuttings, despite that these cutting-derived plants were grown under identical conditions (+P or –P) in the growth chamber.
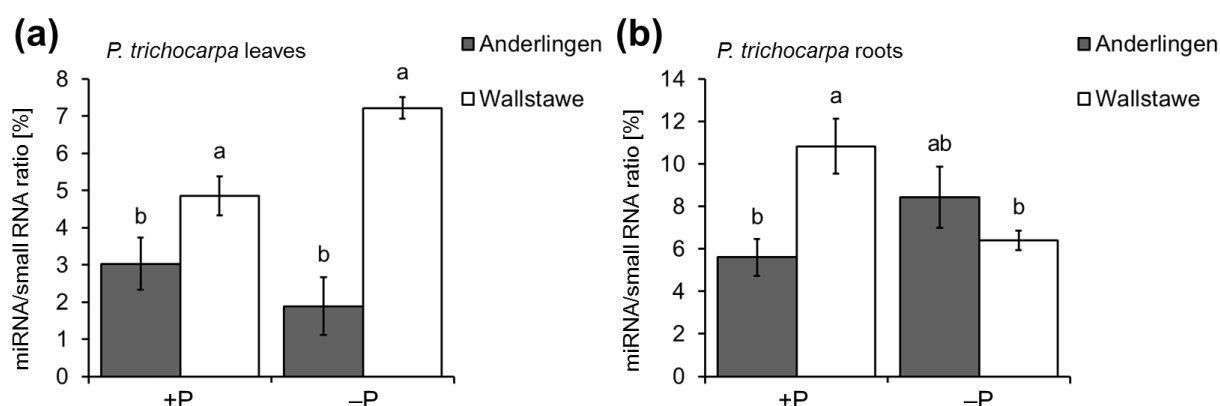
Figure 30: miRNA quantification of clonal *Populus trichocarpa* material.
Quantification of miRNA/small RNA ratio in total RNA samples (y-axis) of leaf (a) and root (b) material from clonal *Populus trichocarpa* (cv. Muhle Larson) cuttings derived from two different short rotation forestry sites (Anderlingen vs. Wallstawe), grown under adequate (+P) and deficient (-P) phosphorus supply (x-axis). Data are presented as the mean ± SE, p ≤ 0.05 and 95 % confidence intervals and were obtained from 3 independent experiments.

Abundance of miRNAs (~ 20 bp) in leaves were significantly down in material with "poor" Anderlingen site history (Figure 30a), showing site-specific adaptation. In roots, these were different only under +P conditions, but not under –P (Figure 30b), suggesting a P-related "memory" effect. As mentioned before, plants derived from the "poor" Anderlingen site showed overall, in the DMRs, smaller dynamics in their methylation states - probably repressing transposons or other short transcribed sequences, such as miRNAs. The overall abundance of miRNAs was also slightly affected (but not significantly) in leaves by changing the P supply (Figure 30a). Higher methylation status thus targeted miRNA repression in an organ-specific manner, similar to the repressing function of ^{m}C in other non-coding chromosome areas.

Interestingly, miRNA quantification showed significant differences between cutting-derived plant tissue material from Anderlingen and Wallstawe, indicating a different processing or synthesis of miRNA. Therefore, expression analysis of Dicer homologs in *Populus trichocarpa* was performed in accordance with the enzyme's function: the cleavage of double stranded RNA or pre-mature RNA producing siRNAs and miRNAs, respectively (Figure 3). However, qPCR results showed no significance in Dicer homolog expression between plant material derived from Anderlingen or Wallstawe (Figure 31), suggesting that processing or synthesis of miRNA between plants originating from the two distinct sites was not caused by differential Dicer expression. Additionally, Dicer homologs were not listed in differentially methylated coding regions and therefore shared a similar methylation pattern between plants derived from the two sites (Figure 32).

(a)

(b)

(c)

(d)

Figure 31: Endoribonuclease Dicer expression differences of clonal *Populus trichocarpa* material. qPCR results from *Populus trichocarpa* (cv. Muhle Larson) leaf (a,b) and root (c,d) material derived from two different short rotation forestry sites (Anderlingen vs. Wallstawe), grown under controlled adequate (+P; (a,c)) and deficient (-P; (b,d)) phosphorus nutrition using 3 reference genes (*POPTR*_EF1α, *POPTR*_RP and *POPTR*_18s) for normalization. Normalized gene expression (y-axis) is shown for endoribonuclease Dicer homologs (x-axis): *POPTR*_0018s30840 as DCL3 and *POPTR*_0002s182401 as Dicer. Data are presented as the mean ± SEM, 95 % confidence intervals and were obtained from 3 independent experiments.

Furthermore, it was investigated whether differences in total miRNA expression were also reflected by differential expression of individual miRNAs in DMRs. Therefore, five miRNAs (*Ptc*-miR1446a-e, *Ptc*-miR481ab, *Ptc*-miR481cd, *Ptc*-miR6432 and *Ptc*-miR827) encoded in the top 200 DMRs of every context (CpG, CHG and CHH) were identified by miRBase (Kozomara & Griffiths-Jones, 2014) and their expression in plant material from both sites (Anderlingen & Wallstawe) and treatments (+P & -P) was quantified, to verify the relationship between DNA methylation and miRNA expression (Figure 33 and Table 12).

(a)

Populus trichocarpa – chromosome 18: 9,286,579 – 9,301,400 (14.8 kbp)

(b)

Populus trichocarpa – chromosome 2: 14,170,000 – 14,182,000 (12 kbp)
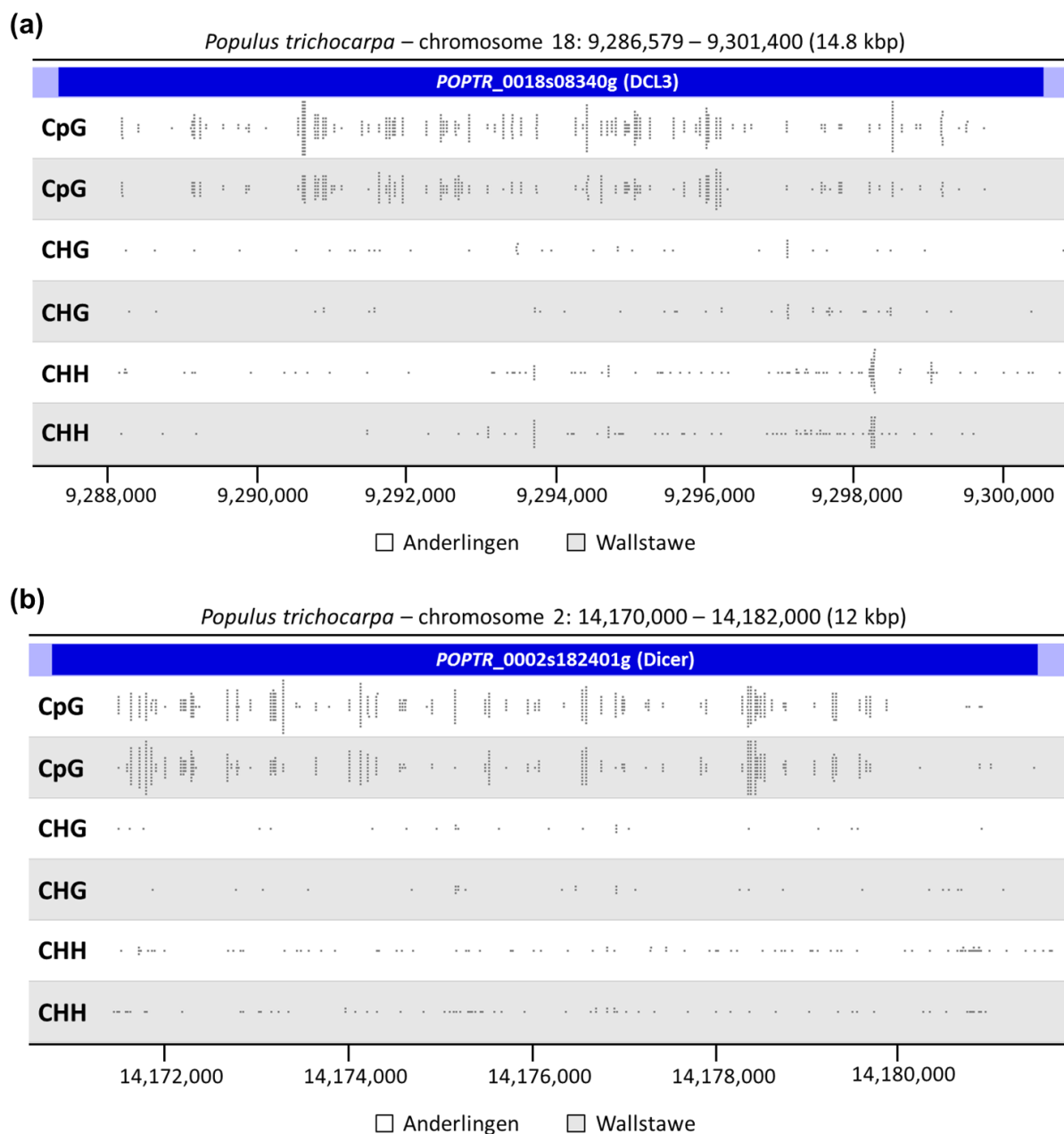
Figure 32: Methylation pattern of endoribonuclease Dicer homologs in clonal *Populus trichocarpa*.

Methylation calls of all cytosine contexts (CpG, CHG and CHH – where H represents the nucleotides A, T or C; single letter abbreviation; y-axis) are shown for Dicer gene homologs (a,b) in clonal *Populus trichocarpa* (cv. Muhle Larson) material derived from two different short rotation forestry sites (Anderlingen vs. Wallstawe) by using the SeqMonk software (Babraham bioinformatics). Grey spots indicate the methylation level. Besides, the sequence window (header) is stated in kilo base pairs (kbp) and the genomic coordinates are given in base pairs (x-axis).

Interestingly, miRNA expression was highly dependent on the methylation status in individual encoded regions. Once again, miRNAs derived from the P-rich site Wallstawe showed a higher adaptation in expression similar to the previously described expression of the differentially methylated genes (Figure 27, Figure 29 and Figure 33). Though, methylation levels tended to be higher in plants derived from Anderlingen than from Wallstawe (Table 12), no difference in miRNA expression was overall observed in the tested low P_i site tissues (Figure 33). However, some of these miRNAs were regulated significantly in a P-nutrition-dependent way, especially in roots (Figure 33a,c vs. Figure 33b,d).

Table 12: Differentially methylated miRNAs in clonal *Populus trichocarpa* material derived from two different short rotation forestry sites (Anderlingen vs. Wallstawe).

miRNA	methylation context	higher methylation level site	expression in roots and leaves
Ptc-miR1446a-e	CpG	Anderlingen	Yes
Ptc- miR481ab	CHH	Anderlingen	Yes
Ptc-miR481cd	CHH	Anderlingen	Yes
Ptc-miR6432	CHG	Wallstawe	Yes
Ptc-miR6470	CpG	Anderlingen	No
Ptc-miR827	CpG	Anderlingen	Yes

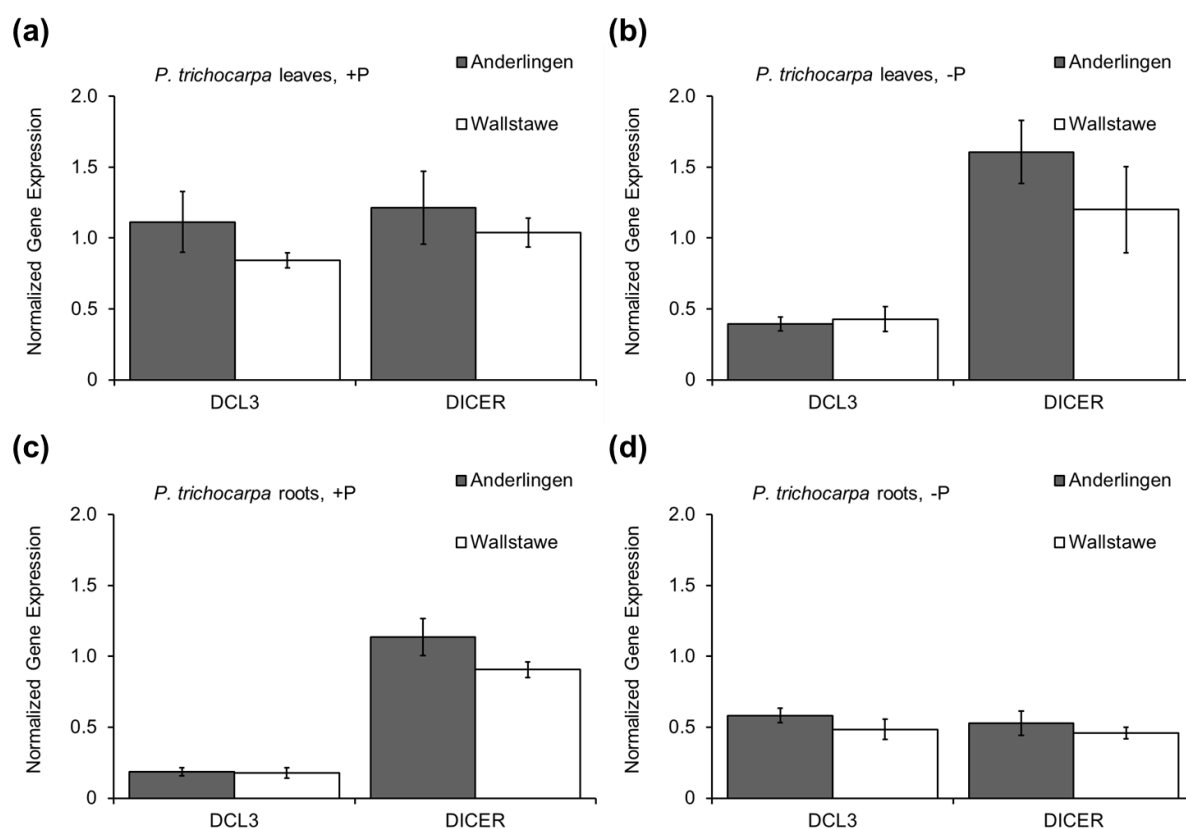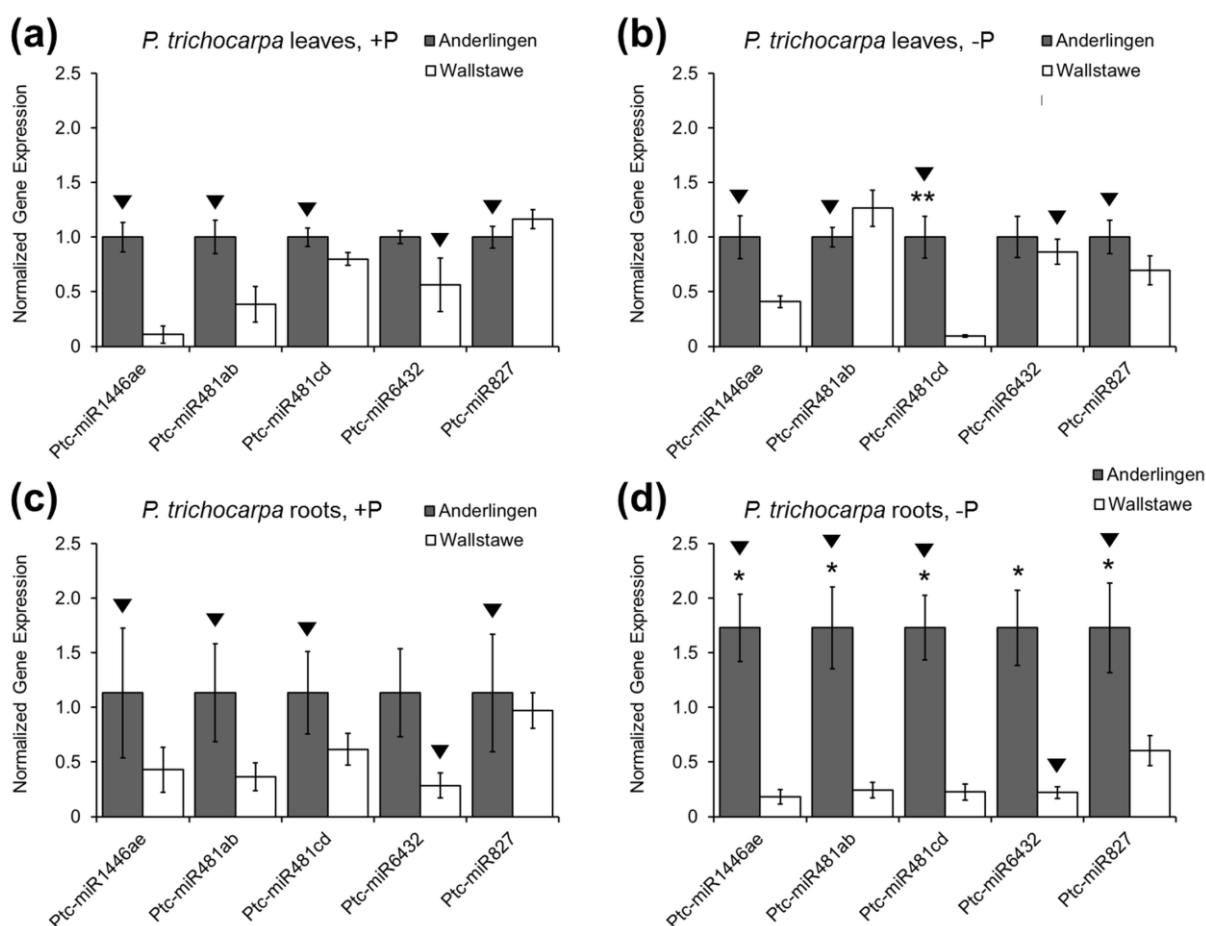**Figure 33: miRNA expression differences of clonal *Populus trichocarpa* material.**
qPCR results from *Populus trichocarpa* (cv. Muhle Larson) leaf (a,b) and root (c,d) material derived from two different short rotation forestry sites (Anderlingen vs. Wallstawe), grown under controlled adequate (+P; (a,c)) and deficient (-P; (b,d)) phosphorus nutrition using 3 reference genes (*POPTR*_EF1α, *POPTR*_RP and *POPTR*_18s) for normalization. Normalized gene expression (y-axis) is shown for five differentially methylated miRNAs (x-axis): *Ptc*-miR1446ae*, Ptc*-miR481ab*, Ptc*-miR4b1cd*, Ptc*-miR6432 and *Ptc*-miR827. Black triangles indicate, which plant material had a higher methylation level. Data are presented as the mean $\pm$ SEM, p* ≤ 0.05, p** ≤ 0.01 and 95 % confidence intervals and were obtained from 3 independent experiments.

In addition to the miRNA expression analysis according to their methylation, transcriptional levels were once again plotted against the DMR methylation states (Figure 34; see 4.4). Thereby, no significant, linear correlation was detected between methylation state of the DMR and miRNA expression due to correlation coefficients (r) near zero (Table 13). These observations were independent from phosphorus nutrition and from which forestry site the plant material was originating.

In conclusion, DNA methylation levels seemed to have some effects on the expression of miRNAs, but the methylation was not suppressive.
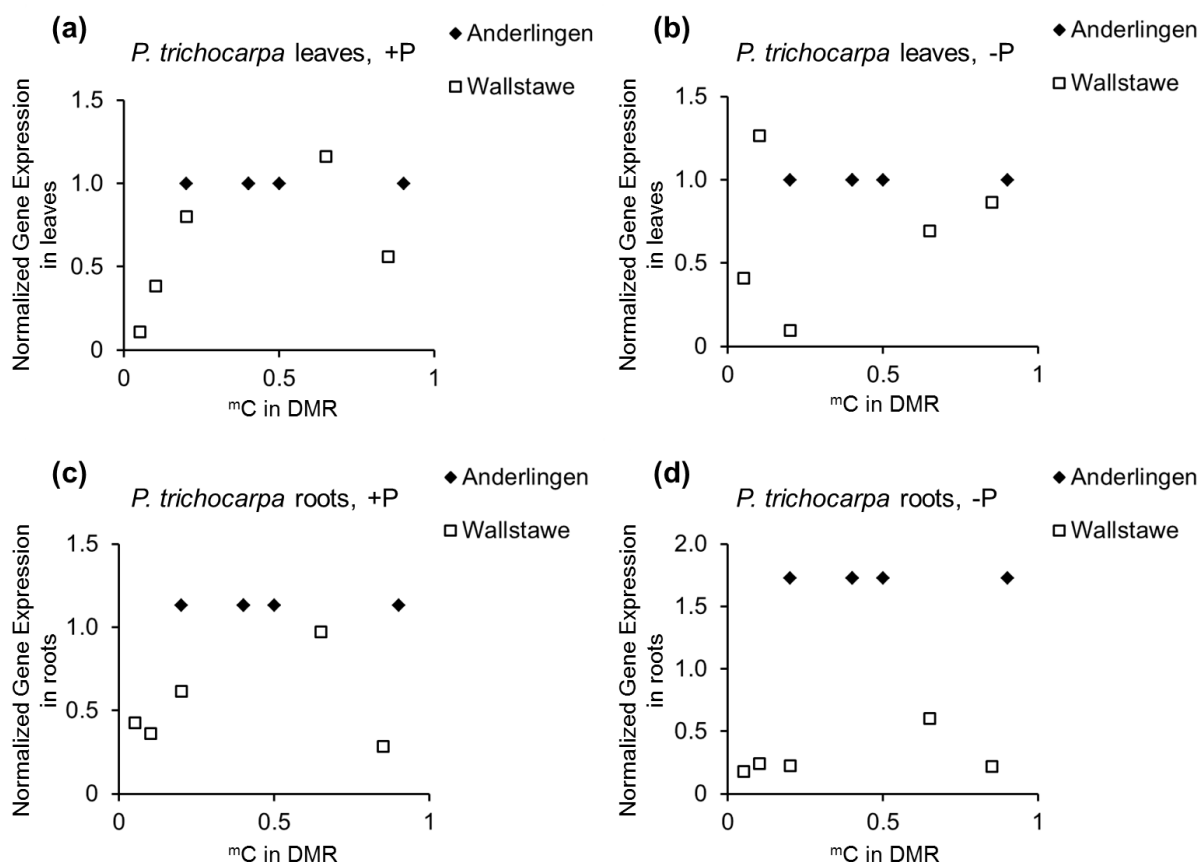
Figure 34: miRNA expression vs. methylated cytosine state of DMRs in clonal *Populus trichocarpa* material.

Differentially methylated miRNAs and their methylated cytosine (^{m}C) states (0 = no methylation; 1 = fully methylated sequence area; x-axis) plotted against their normalized miRNA expression (y-axis) of leaf (a,b) and root (c,d) material from clonal *Populus trichocarpa* (cv. Muhle Larson) cuttings derived from two different short rotation forestry sites (Anderlingen vs. Wallstawe), but grown under optimal (+P; a,c) and deficient (-P; b,d) phosphorus conditions.

Table 13: Pearson's product-moment correlation of methylation states in differentially methylated miRNAs and their expression in plant material from clonal *Populus trichocarpa* (cv. Muhle Larson) derived from two different short rotation forestry sites (Anderlingen vs. Wallstawe).

sites	tissue	treatment	correlation coefficient (r)	p-value
Anderlingen		+P	-0.19	0.7579
	leaves	-P	0.08	0.9003
		+P	-0.03	0.9646
	roots	-P	-0.08	0.8950
Wallstawe		+P	0.56	0.3285
	leaves	-P	0.19	0.7579
		+P	0.17	0.7795
	roots	-P	0.45	0.4443

4.6. Prediction of possible target genes and their expression

Depending on the chosen maximum expectation value to score the complementarity between small RNA and their target transcript (Zhang, 2005), prediction coverage proposed a large number of genes targeted by these differentially methylated miRNAs. An overrepresentation analysis of these target transcripts with a maximum expectation value of 3.0 was performed via PopGenIE (Sjödin *et al.*, 2009) to potentially assign specific metabolic pathways or functional gene classes, influenced by DMR-regulated miRNAs. Thereby, the analysis did not detect any functional enrichment, again concluding no overrepresented stress condition in the two different sites (see 4.3).

Additionally, the analysis of the most stringent chosen possible targets (maximum expectation value of 2.0) only revealed four possible target genes (*POPTR*_0004s02320, *POPTR*_0006s04360, *POPTR*_0006s09220 and *POPTR*_0013s14900), which showed reliable gene expression in leaves and roots from *Populus trichocarpa* (Figure 35 and Table 14).

Table 14: Possible genes targeted by differentially methylated miRNAs in *Populus trichocarpa.*

miRNA	target gene	expression in leaves and roots	maximum expectation[1]
Ptc-miR1446a-e	*POPTR*_0013s14900	Yes	1.5
Ptc-miR1446a-e	*POPTR*_0006s04360	Yes	2.0
Ptc-miR481ab	*POPTR*_0012s01480	No	1.5
Ptc-miR481cd	*POPTR*_0013s11260	No	1.5
Ptc-miR6432	*POPTR*_0004s02320	Yes	2.0
Ptc-miR827	*POPTR*_0006s09220	Yes	2.0

[1] maximum expectation value to score the complementarity between small RNA and their target transcript (Zhang, 2005) - with a lower maximum expectation value $(0 - 2.0)$, a more stringent cut-off threshold and thereby a lower false positive prediction is set

The annotations of these four primary target genes include:

➢ a serine/threonine kinase (*POPTR*_0004s02320),

➢ an acetyltransferase family protein (*POPTR*_0006s04360),

➢ a prenylated rab acceptor family protein (*POPTR*_0006s09220) and

➢ an N-acetyltransferase (*POPTR*_0013s14900).

Gene expression of these target transcripts was investigated via qPCR. Due to minor P effects in leaves, when quantifying the miRNA abundance and DMR-regulated miRNA expression (Figure 30 and Figure 33a,b), the P-dependent expression in roots of differentially methylated miRNAs and of their target genes was separately focused in the two different sites (Figure 35).

However, target expression in roots differed significantly in a P-related way (Figure 35c,d), which was partially consistent with the gene expression pattern of the associated differentially methylated miRNAs (Figure 35a,b): By comparing the miRNA expression in roots under P deficiency and optimal P supply, a trend of lower miRNA expression in Wallstawe under P deficient conditions was detected. This observation was consistent with the predicted target gene expression. In Wallstawe plants, higher miRNA expression led to partially significant lower target gene expression and vice versa, indicating gene silencing by miRNAs (Figure 35b,d).

Nevertheless, in Anderlingen plants, except *POPTR*_0004s02320, target gene expression showed almost no difference due to the expression level of the corresponding miRNA, suggesting a site-specific adaptation (Figure 35a,c).

Although it cannot be excluded that the real targets of the identified DMR-regulated miRNAs were not yet identified, it appeared that differential methylation of miRNAs was only affecting plants derived from the P-rich site Wallstawe, in an organ-specific and P-related way.
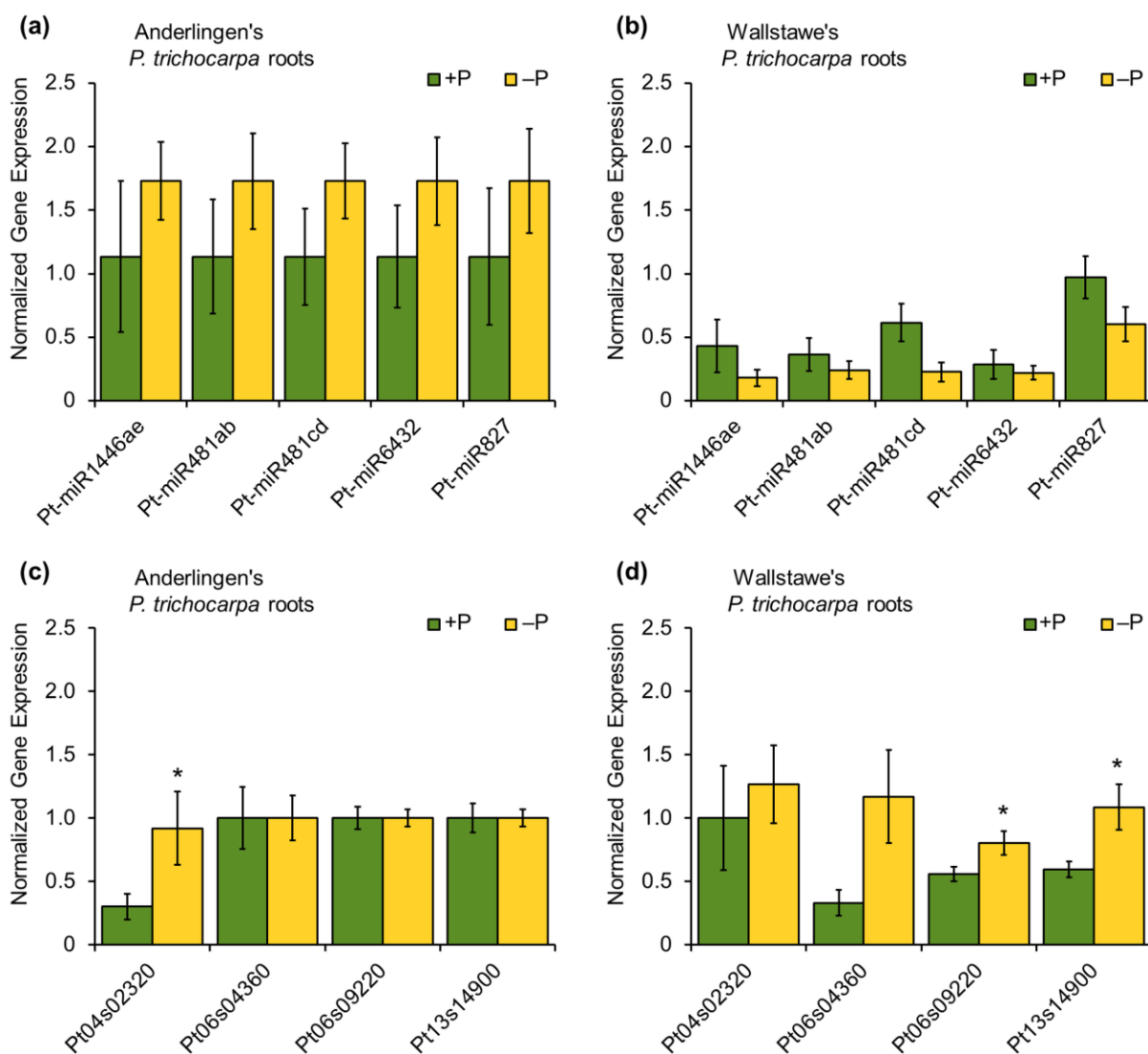
Figure 35: Target gene expression differences of clonal *Populus trichocarpa* material.

qPCR results from *Populus trichocarpa* (cv. Muhle Larson) root material derived from two different short rotation forestry sites (Anderlingen (a,c) and Wallstawe (b,d)), grown under controlled adequate (+P) vs. deficient (-P) phosphorus nutrition using 3 reference genes (*POPTR*_EF1α, *POPTR*_RP and *POPTR*_18s) for normalization. Normalized gene expression (y-axis) is shown for differentially methylated miRNAs (a,b) and their possible target genes (c,d): *Ptc*-miR1446ae, *Ptc*-miR481ab, *Ptc*-miR4b1cd, *Ptc*-miR6432, *Ptc*-miR827, *POPTR*_0004s02320 as Pt04s02320, *POPTR*_0006s04360 as Pt04s04360, *POPTR*_0006s09220 as Pt06s09220 and *POPTR*_0013s14900 as Pt13s14900 (x-axis). Data are presented as the mean ± SEM, p* ≤ 0.05 and 95 % confidence intervals and were obtained from 3 independent experiments.

5. Discussion

5.1. Growth performance and P in material from two different sites

In general, it was shown that higher P supply increases the growth performance in different poplar varieties (Van Den Driessche, 2000). The maximum P_i uptake is typically specified within a pH range of 5-6 (Schachtman, 1998). This range was also detected in the analyzed sites. Additionally, standard values for sufficient P supply and non-limiting growth were defined as 0.18-0.30 % in mature poplar leaves (Bergmann, 1993). Although Anderlingen was considered as the low P_i site, its P concentration in mature leaves only bordered on the lower standard values (Figure 11a). In fact, the wood P concentration showed the same trend than in leaves, but was not significantly different between the distinct sites (Figure 11b). Furthermore, the categorization of a low (Anderlingen) and sufficient (Wallstawe) P available soil is based on a fertilizing classification used for agricultural soils (Figure 11c and Table 6), which might not be valid for forest soils. Besides, soil classification, according to VDLUFA, 2000, just indicated minor differences between soil features of the two short rotation forestry sites (Figure 11d). These assertions could explain the minor P-related, but higher site-dependent "memory" effect via DNA methylation.

Nevertheless, P starvation reversibly affected DNA methylation differently in *Arabidopsis thaliana* and rice (Secco *et al.*, 2015). In P-starved rice and after resupply, transient phosphate starvation-induced methylation changes were identified, preferentially in transposable elements close to highly induced genes. Methylation changes occurred after nearby gene transcription and could be partially propagated through mitosis, but no transgenerational inheritance was observed. Only a minor effect of P starvation on the methylome of *Arabidopsis* was found, similar to the

methylome of the analyzed clonal *Populus trichocarpa*, suggesting species-specific mechanisms (Secco *et al.*, 2015).

Besides P availability, water and temperature stress were also previously correlated to DNA methylation and gene expression changes in poplar (Liang *et al.*, 2014; Ci *et al.*, 2015). However, these additional stress conditions were not analyzed further in this study due to no enrichment of differential methylated genes in functional classes of biological processes, indicating no overrepresented stress at the two sites.

5.2. Site-dependent methylome and context-specific methylation differences

However, a site-specific plant establishment, growth performance and root morphology of clonal *Populus trichocarpa* cuttings derived from two distinct sites were observed, independent from P nutrition (Figure 12, Figure 13 and Figure 14). Interestingly, plantlets derived from Anderlingen showed a higher sensitivity towards P deficiency than plantlets derived from Wallstawe (Figure 12). In flax and wild tobacco, similar environmental conditioning experiments were performed, showing that over years remarkably large differences in growth performance might be produced as a result of environmental conditions, like nutrient deficiencies, on previous generations (Sharman, 1958; Hill, 1965). Though, epigenetic modifications were not investigated at this time due to missing advanced sequencing techniques, this might explain the differences in growth performance and the higher visible sensitivity towards P deficiency of poplar trees derived from Anderlingen, where P deficiency might be a more common environmental stress, leading to a continuously vegetatively propagated, smaller growth performance and therefore to a higher sensitivity towards P deficiency (Figure 11).

Nevertheless, these observations were attended by different, site-specific methylation patterns in plant material derived from the two different short rotation forestry sites (Figure 22). In addition, a site-dependent adaptation in plant establishment of clonal white poplar, has been also related to DNA methylation, suggesting an inclusion not only of genetic but also of epigenetic aspects in plant biodiversity studies of vegetatively propagated plant species (Guarino *et al.*, 2015).

Besides, considering cutting-derived poplar clones, a deeper impact on growth performance via "de novo" methylations (^{m}CHG and ^{m}CHH) than via conserved methylations (^{m}CpG) was expected, due to a missing transgenerational methylome inheritance (Vining *et al.*, 2012). These expectations were confirmed by a more variable absolute number and chromosomal distribution of asymmetric CHH methylations between the plant material derived from Anderlingen or Wallstawe (Figure 18 and Figure 20c), although the relative and absolute amount of methylation was higher in the CpG context than in the CHG or CHH context (Figure 17 and Figure 18). Similar results in ^{m}C context proportions were obtained in *Arabidopsis* (Cokus *et al.*, 2008), but not in poplar under different water stress treatments (Liang *et al.*, 2014). Nevertheless, "de-novo" methylations upon P starvation were reversible in *Arabidopsis*, when the stress was abolished (Secco *et al.*, 2015), showing the flexibility of "de novo" methylations in short-term stress conditions and explaining different data about methylated CHG and CHH levels.

However, genome-wide analyses of DNA methylation in every cytosine context revealed enrichments in hypervariable chromosome regions and in transposable elements (TE) leading to their silencing (Zhang *et al.*, 2006; Zilberman *et al.*, 2007; Lister *et al.*, 2008; Becker *et al.*, 2011; Saze & Kakutani, 2011; Liang *et al.*, 2013). This statement was partially confirmed by the highest proportion of DMRs occurring in non-gene regions (Figure 23) and by a higher centromeric chromosomal ^{m}CpG

distribution (Figure 20a). Though, the annotation of the heterochromatin and TEs in poplar is still not sufficiently advanced to capture all TEs (Zhou & Xu, 2009). Therefore, the analysis of DNA methylations in TEs and their silencing effect were not focused in this study. Although, advanced annotations and transposon analyses might reveal a direct relation between DNA methylation and phosphorus nutrition, like it was described in rice (Secco *et al.*, 2015).

5.3. Differentially methylated gene expression and their expression dynamics

Still largely unknown, however, is the function of DNA methylation within coding regions in plants: they could prevent aberrant expression from intragenic promoters (Zilberman *et al.*, 2007; Maunakea *et al.*, 2010) or increase the splicing accuracy (Luco *et al.*, 2010; Takuno & Gaut, 2012). In general, it was described that DNA methylation in promoter sequences tend to silence genes, whereas a positive correlation was observed in gene expression and gene body methylation (Yang *et al.*, 2014). These assumptions are partially confirmed in *Populus trichocarpa* under water stress, where the most significant gene expression changes occurred 100 bp upstream of the TSS (Liang *et al.*, 2014). Therefore, to improve the chances of significant alterations in gene expression due to DNA methylation differences, DMRs occurring simultaneously in gene body and promoter sequences were analyzed (Figure 26). Thereby, the selected genes and their relationship to abiotic stress and potential biotic interactions could be overrepresented (Table 9), but the significance of this observation was questionable, due to relatively little information or missing annotations on individual genes.

However, DMRs occurred in a higher level in promoter sequences in Anderlingen plants and to a higher number in gene body regions in Wallstawe plants (Figure 24), indicating different functions of DNA methylation within coding regions. Similar

observations have been described in poplar under water stress, where gene body methylation is positively correlated with gene expression (Liang *et al.*, 2014).

Although differentially methylated coding regions with reliable expression in leaves and roots indicated no direct link to gene up- or down-regulation due to a differential methylation in coding regions (Figure 27 and Figure 28). In addition, gene expression analysis just detected minor effects under different P supply (Figure 27). Though mutational changes seemed to be limited in vegetatively propagated perennials (Guarino *et al.*, 2015), they could not be excluded as a possible reason for the few observed significant gene expression differences. Nevertheless, the so far described correlation between DNA methylation in coding regions and gene expression profiles in *Arabidopsis* (Aceituno *et al.*, 2008), rice (Secco *et al.*, 2015) and poplar (Liang *et al.*, 2014) under different stress conditions was not confirmed, when considering individual cases of differential methylated genes and their expression (Figure 28). Although analyzing the total data set, a negative correlation between methylation level in coding regions and gene expression was detected (Figure 29), similar to the study of Vining *et al.*, 2012, where gene body methylation has been associated with transcriptional repression in poplar. Nevertheless, this observation depended from which site the plant material derived, suggesting not only an indirect correlation between DNA methylation in coding regions and gene expression, but also a site-specific "memory" effect. Though, a causal relationship between DNA methylation in coding regions and transcriptional changes still remains unclear.

These assertions were also confirmed by a higher proportion of differentially methylated coding regions in the lignin biosynthesis, detected via the MapMan tool. Subsequently, lignin quantification also showed no significance between wooden cuttings derived from Anderlingen and Wallstawe, suggesting no direct effect of differential DNA methylation on gene expression (Figure 25).

Hence, the importance of differential DNA methylation in actively regulating gene expression has been questioned more recently (Seymour *et al.*, 2014). In addition, previous studies on poplar described a more repressive effect on transcription by gene body methylation than by promoter methylation, which is again in contrast to *Arabidopsis*, supporting diverse, species-specific gene regulation patterns by methylation (Vining *et al.*, 2012).

5.4. Expression of differentially methylated miRNAs

Clearly, the detection of a negative correlation between gene expression and methylation state in coding regions of clonal poplar material from Wallstawe, but not from Anderlingen, was an important observation (Figure 29). Thus, there must be different regulatory levels of gene expression and their dependence on DNA methylation, e.g. by post-transcriptional gene silencing mechanisms via pre-microRNAs from transposon sites or mature miRNAs (Piriyapongsa & Jordan, 2008; Roberts *et al.*, 2014). A close correlation of DMR and individual gene expression was not observed and questions a causal relationship, which is in agreement with recent studies (Seymour *et al.*, 2014).

This novel link to P-nutrition, of DMR-derived miRNAs that respond to P nutrition, is especially interesting, as plant P signaling involves a mechanistic network of protein coding genes targeted by microRNAs, such as the miR399-PHR1-PHO2 regulon, which was identified in many plant species, including poplar (Bari *et al.*, 2006). PHO2 is a ubiquitin-conjugating E2 enzyme for post-translational protein degradation (Calderón-Vázquez *et al.*, 2011) and controls P starvation response genes, such as PHT1;8 and PHT1;9. The phloem-mobile shoot to root signal for low shoot P include sucrose, hormones and miR399, which targets the major PHR1 transcription factor gene. Overexpression of miR399 phenocopies the response to low P_i in roots (Chiou &

Lin, 2011). In addition, miR156-SPL3-PHT1;5 pathways also constitute a component of the P deficiency-induced regulatory mechanism in *Arabidopsis*. During P starvation miR156 is induced and therefore its target SPL3 is repressed. This influences the anthocyanin accumulation as well as the expression of high affinity PHTs, increasing the P_i uptake (Lei *et al.*, 2016). However, miR399 and miR156 were not among the differentially methylated miRNAs, excluding that these regulons are directly targeted by DNA methylation.

Furthermore, the low P-induced miR827, targeting the NLA, is also described to be involved in the repression of P_i uptake, demonstrating that miR827 and its target NLA have a crucial role in regulating P_i homeostasis (Kant *et al.*, 2011). Remarkably, the significantly different expressed *Ptc*-miR827 was a direct target of DNA methylation, confirming a site-specific and P-dependent adaptation via differentially methylated miRNAs. Although, the miR827 family is conserved between rice, *Populus trichocarpa* and *Arabidopsis* (Lu *et al.*, 2008), the predicted targets in all three species occur to have different functions, indicating a species-specific function of miR827 (Lu *et al.*, 2008; Kant *et al.*, 2011).

Nevertheless, most of the novel identified DMR-regulated miRNAs appear to have no direct analog in *Arabidopsis* and to be involved in stress responses (Lu *et al.*, 2005, 2008; Puzey *et al.*, 2012). Additionally, previous expression analyses also suggested that the methylation pattern of identified miRNAs probably influences their expression (Ci *et al.*, 2015; Song *et al.*, 2015). Thus, the normalized miRNA expression level stayed similar in poplar clones derived from Anderlingen, independent from treatment or analyzed tissue, but not from Wallstawe (Figure 33). This observation was consistent with the gene expression levels of differentially methylated genes (Figure 27 and Figure 35), suggesting a site-specific adaptation in miRNA and gene expression and therefore in plant establishment (Guarino *et al.*, 2015).

5.5. miRNA target genes and their expression

Although minor effects of DNA methylation depending on P nutrition were previously described, the quantification of miRNA differed significantly between +P and –P treatments in root material from the two distinct sites (Figure 30), indicating a direct P-related "memory" effect. Additionally, these results were consistent with the expression of differentially methylated miRNAs and their target genes, showing P-related expression differences in roots derived from the two short rotation forestry sites, especially from Wallstawe. Thereby, mRNA cleavage, mRNA degradation or transcriptional repression by miRNA would explain the down- or up-regulated expression of the target genes under different P nutrition states correlated with the expression pattern of the associated miRNAs and miRNA quantification (Figure 30, Figure 33 and Figure 35).

In addition, including more potential target genes in the expression analysis by increasing the maximum expectation value to score the complementarity between small RNA and their target transcript could also reveal a direct link between epigenetic modifications and P-related genes and acquisition strategies, due to multiple targeting of miRNA (Lam *et al.*, 2015). Although, further annotations as well as high throughput gene expression analysis techniques, like microarray or RNA sequencing, would be necessary to investigate a higher number of targets and potentially detect a direct impact between epigenetic modifications and P nutrition.

Furthermore, in rice, P deficiency induced changes in DNA methylation (Secco *et al.*, 2015) and in the *Arabidopsis* phosphate starvation response, genes were regulated by chromatin remodeling, an epigenetic mechanism, suggesting a direct, but species-specific link between P nutrition and epigenetic adaptation (Smith *et al.*, 2010). In poplar, this P-related species-and site-specific epigenetic modification might be the RNA interference by differentially methylated miRNAs.

5.6. Summary

In the end, it was observed that clonal *Populus trichocarpa* material derived from two distinct short rotation forestry sites (Anderlingen vs. Wallstawe) with diverse environmental conditions differed in their plant establishment, growth performance, P deficiency sensitivity and root morphology. These physiological and morphological measured parameters were actually attended by differences in the DNA methylation pattern between the clonal perennial plant material derived from the two different sites, suggesting a site-specific impact by epigenetic modifications. Hence, DMRs occurring in coding regions and miRNAs revealed a site-dependent effect on gene, miRNA and their target expression (Figure 36). Remarkably, in perennials derived from Anderlingen, DNA methylation in coding regions and miRNAs seemed to have almost no or just an indirect effect on gene, miRNA and their target expression, independent from phosphorus nutrition. On the other hand, in clonal plants originating from Wallstawe, DNA methylation was negatively correlated with gene expression and thereby tended to differ from the gene expression in Anderlingen, even though a direct link between differential methylation in coding regions and their corresponding gene expression changes was not found and questions a causal relationship (Figure 27, Figure 29 and Figure 36).

Consequently, miRNA quantification as well as DMR-regulated miRNAs and their target expression analysis showed a site-specific as well as P-dependent difference, especially in plants derived from Wallstawe (Figure 30, Figure 33 and Figure 35). More explicitly, in roots derived from Wallstawe cuttings, general and DMR-regulated miRNA synthesis was increased under optimal and decreased under deficient phosphorus conditions, leading to a more or less distinctive target gene silencing by miRNA, depending on the P supply (Figure 36). In addition, this phenomenon was

mainly observed in roots, confirming an organ-specific RNA interference and DNA methylation impact.

In conclusion, clonal *Populus trichocarpa* material derived from Anderlingen showed no or little effect towards DNA methylation and RNA interference, independent from P nutrition. Thus, in the metabolism pathway of Anderlingen plants, a processing step from DNA methylation and gene silencing by DMR-regulated miRNAs to gene expression might be missing, though Dicer homolog expression analysis showed no significant difference between plant material derived from Anderlingen or Wallstawe (Figure 31), suggesting another regulon of miRNA expression in the analyzed plants (Chan *et al.*, 2005). Besides, clonal plant material derived from Wallstawe appeared to be more sensitive towards DMR-based RNA interference and DNA methylation effects on gene expression. Therefore, Wallstawe plants seemed to be more flexible and adaptive towards environmental stresses, like phosphorus deficiency, explaining an increased growth performance, plant establishment and lower sensitivity towards P deficiency.

Thus, epigenetic modifications act to be responsible for the adaptation potential of perennials towards abiotic stress conditions and potentially biotic interactions. Additional analyses, especially of "de novo" methylations (CHG and CHH) in transposable elements in combination with high throughput gene expression analysis techniques, like RNA sequencing or microarray, might reveal and confirm these assertions, but further genomic annotations of *Populus trichocarpa* are necessary to investigate these research questions. Besides, the analysis of histone modification, an epigenetic mechanism not investigated in this study, could also reveal further links between nutrient supply and epigenetic adaptation.
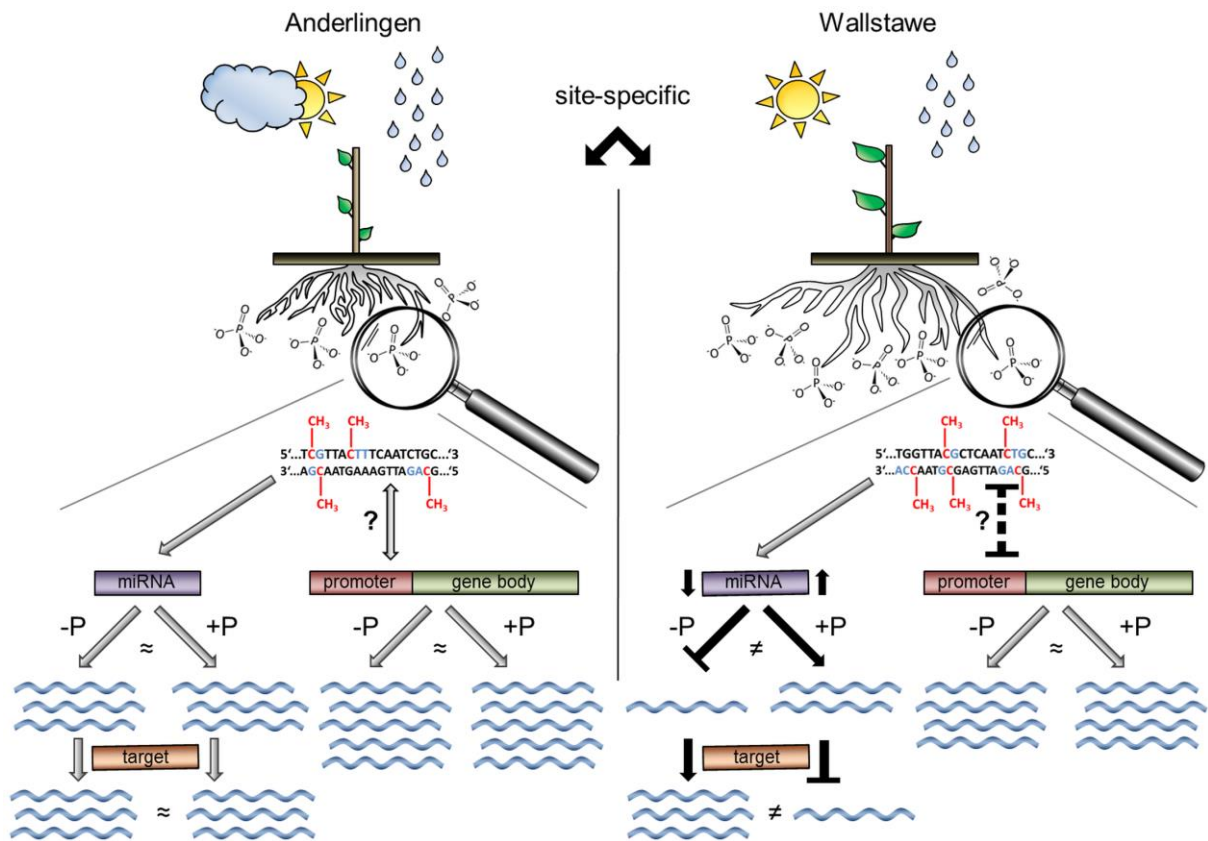
Figure 36: Schema of site-dependent differences in DNA methylation and their impact on plant establishment in clonal *Populus trichocarpa*.

Two different short rotation forestry sites (Anderlingen vs. Wallstawe) are shown; where the same *Populus trichocarpa* clone (cv. Muhle Larson) is grown. Growth conditions differ on the two sites, e.g. phosphate availability. DNA nucleotides are presented as T (thymine), G (guanine), A (adenine) and C (cytosine). Analysis of the DNA methylation pattern (red in DNA sequence) has revealed differentially methylated regions (DMRs) in all C contexts (blue in DNA sequence) between plants derived from Anderlingen or Wallstawe. A causal relationship between DNA methylation in coding regions (promoter and gene body) and gene expression changes still remains unclear: In Anderlingen plants, the methylation rate in coding regions has no effect on gene expression (blue waves), independent from optimal (+P) or deficient (-P) phosphorus nutrition. In Wallstawe plants, methylation level in coding regions is negatively correlated with the gene expression (indicated by black dashed T-shaped bar). This observation is independent from phosphorus nutrition (indicated by neutral grey arrows). Though, DNA methylation has a different impact on DMR-regulated miRNAs and their targets: In Anderlingen plants, miRNA expression is not related to phosphorus supply or DNA methylation. Therefore, gene expression of their targets in both conditions is not different. In Wallstawe plants, miRNA expression depends on the phosphorus nutrition. -P leads to lower DMR-regulated miRNA expression (indicated by black arrows) and thereby to higher target gene expression. +P leads to a higher DMR-regulated miRNA expression and thereby to a lower target gene expression (indicated by a black arrow and T-shaped bar).

6. Conclusions

Up to date, studies in epigenetics have been applied to just a few annual plant species, leaving perennials relatively uninvestigated. Hence, in this research project, clonal *Populus trichocarpa* (cv. Muhle Larson) material derived from two different short rotation forestry sites in northern Germany with different P status was analyzed to investigate site-dependent and potentially species-specific epigenetic adaptations, following these major hypotheses (see 1.7):

➢ Clonal *Populus trichocarpa* material grown at different sites with contrasting P availability shows differences in yield and phenotype

➢ The genome of these clonal trees grown at different sites reveals site-specific epigenetic modifications (context-dependent methylations in CpG, CHG and CHH)

➢ DNA methylation differences in coding regions and miRNAs are related to their expression and thereby to previous host site adaptations

➢ Species-specific epigenetic mechanisms are responsible for the P starvation adaptation and/or P acquisition strategies

The established hypotheses could be partially confirmed. To be more precisely, the establishment, phenotype and yield of plantlets derived from the two distinct sites in full nutrition depended on their background history, confirming a site-dependent adaptation and suggesting that epigenetic mechanisms might be involved.

Indeed, site-specific epigenetic modifications were identified. More explicitly, context-dependent genome-wide DNA methylation differences (in symmetric CpG as well as in "de novo" methylations in CHG and in asymmetric CHH) were revealed, inter alia, in coding regions and in DMRs regulating miRNAs. Expression analyses of differentially methylated genes showed just a few significant expression profiles, not confirming a direct relation between DNA methylation in coding regions and their alterations in gene expression and therefore questioning a causal relationship. However, a general repression of transcription by higher methylation levels was detected, but only in plants derived from Wallstawe, suggesting a site-specific adaptation and growth performance to environmental stress, but with overall little relation to the P supply. Though, recent studies have linked P starvation to different epigenetic modifications, species-specific mechanisms might be responsible for different epigenetic adaptations. Hence, differentially methylated miRNAs and their predicted targets indicated not only an organ-specific and site-dependent, but also P-related expression in poplar. Thereby, plants derived from Wallstawe seemed to be more adaptive to environmental stresses, including P starvation, than Anderlingen, indicating not only site-specific, but also species-specific epigenetic modifications.

Besides the genetic basis, such epigenetic aspects might be of importance in plant breeding, conservation biology and biodiversity studies, especially of vegetatively propagated perennials, like poplar.

7. Acknowledgements

Brigitte Schönberger

8. References

Aceituno FF, Moseyko N, Rhee SY, Gutiérrez RA. **2008**. The rules of gene expression in plants: organ identity and gene body methylation are key factors for regulation of gene expression in Arabidopsis thaliana. *BMC Genomics* **9**: 438–452.

Bari R, Datt Pant B, Stitt M, Scheible W-R. **2006**. PHO2, microRNA399, and PHR1 define a phosphate-signaling pathway in plants. *Plant Physiology* **141**: 988–999.

Becker C, Hagmann J, Müller J, Koenig D, Stegle O, Borgwardt K, Weigel D. **2011**. Spontaneous epigenetic variation in the Arabidopsis thaliana methylome. *Nature* **480**: 245–249.

Bergmann W. **1993**. *Ernährungsstörungen bei Kulturpflanzen: Entstehung, visuelle und analytische Diagnose*. Heidelberg, Germany: Springer Spektrum Akademischer Verlag.

Björkman E. **1970**. Forest tree mycorrhiza — The conditions for its formation and the significance for tree growth and afforestation. *Plant and Soil* **32**: 589–610.

Bolger AM, Lohse M, Usadel B. **2014**. Trimmomatic: A flexible trimmer for Illumina sequence data. *Bioinformatics* **30**: 2114–2120.

Calderón-Vázquez C, Sawers RJH, Herrera-Estrella L. **2011**. Phosphate deprivation in maize: genetics and genomics. *Plant Physiology* **156**: 1067–1077.

Cao X, Aufsatz W, Zilberman D, Mette MF, Huang MS, Matzke M, Jacobsen SE. **2003**. Role of the DRM and CMT3 Methyltransferases in RNA-Directed DNA Methylation. *Current Biology* **13**: 2212–2217.

Cao X, Jacobsen SE. **2002a**. Locus-specific control of asymmetric and CpNpG methylation by the DRM and CMT3 methyltransferase genes. *Proceedings of the National Academy of Sciences of the United States of America* **99**: 16491–16498.

Cao X, Jacobsen SE. **2002b**. Role of the Arabidopsis DRM Methyltransferases in De Novo DNA Methylation and Gene Silencing. *Current Biology* **12**: 1138–1144.

Castel SE, Martienssen R a. **2013**. RNA interference in the nucleus: roles for small RNAs in transcription, epigenetics and beyond. *Nature Reviews Genetics* **14**: 100–112.

Chan SW-L, Henderson IR, Jacobsen SE. **2005**. Gardening the genome: DNA methylation in Arabidopsis thaliana. *Nature Reviews Genetics* **6**: 351–360.

Chiou T-J, Lin S-I. **2011**. Signaling network in sensing phosphate availability in plants. *Annual Review of Plant Biology* **62**: 185–206.

Ci D, Song Y, Tian M, Zhang D. **2015**. Methylation of miRNA genes in the response to temperature stress in Populus simonii. *Frontiers in Plant Science* **6:921**: doi:10.3389/fpls.2015.00921.

Cokus SJ, Feng S, Zhang X, Chen Z, Merriman B, Haudenschild CD, Pradhan S, Nelson SF, Pellegrini M, Jacobsen SE. **2008**. Shotgun bisulphite sequencing of the Arabidopsis genome reveals DNA methylation patterning. *Nature* **452**: 215–219.

Cosgrove MS, Wolberger C. **2005**. How does the histone code work? *Biochemistry and cell biology* **83**: 468–476.

Dai X, Zhao PX. **2011**. PsRNATarget: A plant small RNA target analysis server. *Nucleic Acids Research* **39**: doi:10.1093/nar/gkr319.

Van Den Driessche R. **2000**. Phosphorus, copper and zinc supply levels influence growth and nutrition of a young Populus trichocarpa (Torr. and Gray) x P. deltoides (Bartr. ex Marsh) hybrid. *New Forests* **19**: 143–157.

Feng S, Jacobsen SE. **2011**. Epigenetic modifications in plants: An evolutionary perspective. *Current Opinion in Plant Biology* **14**: 179–186.

Finnegan EJ, Peacock WJ, Dennis ES. **2000**. DNA methylation, a key regulator of plant development and other processes. *Current Opinion in Genetics & Development*

10: 217–223.

Fujii H, Chiou T-J, Lin S-I, Aung K, Zhu J-K. **2005**. A miRNA involved in phosphate-starvation response in Arabidopsis. *Current Biology* **15**: 2038–2043.

Guarino F, Cicatelli A, Brundu G, Heinze B, Castiglione S. **2015**. Epigenetic Diversity of Clonal White Poplar (Populus alba L.) Populations: Could Methylation Support the Success of Vegetative Reproduction Strategy? *PLoS ONE* **10(7)**: doi:10.1371/journal.pone.0131480.

Gutzat R, Mittelsten Scheid O. **2012**. Epigenetic responses to stress: triple defense? *Current Opinion in Plant Biology* **15**: 568–573.

Hansen KD, Langmead B, Irizarry RA. **2012**. BSmooth: from whole genome bisulfite sequencing reads to differentially methylated regions. *Genome Biology* **13**: R83.

Heard E, Martienssen R a. 2014. Transgenerational epigenetic inheritance: Myths and mechanisms. *Cell* **157**: 95–109.

Henderson IR, Chan SR, Cao X, Johnson L, Jacobsen SE. **2010**. Accurate sodium bisulfite sequencing in plants. *Epigenetics: Official Journal of the DNA Methylation Society* **5**: 47–49.

Hill J. **1965**. Environmental Induction of heritable Changes in Nicotiana rustica. *Nature* **207**: 732–734.

Holliday R. **2006**. Epigenetics: A Historical Overview. *Epigenetics* **1:2**: 76–80.

Janßen A, Fehrenz S, Fey-Wagner C, Hüller W. **2012**. *Züchtung und Ertragsleistung schnellwachsender Baumarten im Kurzumtrieb*. Göttingen, Germany: Universitätsverlag Göttingen.

Jones-Rhoades MW, Bartel DP. **2004**. Computational identification of plant microRNAs and their targets, including a stress-induced miRNA. *Molecular Cell* **14**: 787–799.

Kankel MW, Ramsey DE, Stokes TL, Flowers SK, Haag JR, Jeddeloh JA, Riddle

NC, Verbsky ML, Richards EJ. **2003**. Arabidopsis MET1 Cytosine Methyltransferase Mutants. *Genetics* **163**: 1109–1122.

Kant S, Peng M, Rothstein SJ. **2011**. Genetic regulation by NLA and microRNA827 for maintaining nitrate-dependent phosphate homeostasis in arabidopsis. *PLoS genetics* **7**: e1002021.

Karandashov V, Bucher M. **2005**. Symbiotic phosphate transport in arbuscular mycorrhizas. *TRENDS in Plant Science* **10**: 22–29.

Khanna A, Czyz A, Syed F. **2013**. EpiGnome^TM Methyl-Seq Kit: a novel post–bisulfite conversion library prep method for methylation analysis. *Nature methods* **10**: iii–iv.

Kozomara A, Griffiths-Jones S. **2014**. miRBase: annotating high confidence microRNAs using deep sequencing data. *Nucleic Acids Research* **42**: 68–73.

Krueger F, Andrews SR. **2011**. Bismark: a flexible aligner and methylation caller for Bisulfite-Seq applications. *Bioinformatics* **27**: 1571–1572.

Lam JK, Chow MY, Zhang Y, Leung SW. **2015**. siRNA Versus miRNA as Therapeutics for Gene Silencing. *Molecular Therapy - Nucleic Acids* **4**: e252; doi: 10.1038/mtna.2015.23.

Lei K-J, Lin Y-M, Ren J, Bai L, Miao Y-C, An G-Y, Song C-P. **2016**. Modulation of the Phosphate-Deficient Responses by MicroRNA156 and its Targeted SQUAMOSA PROMOTER BINDING PROTEIN-LIKE 3 in Arabidopsis. *Plant & Cell Physiology* **57**: 192–203.

Lewis JD, Ward JK, Tissue DT. **2010**. Phosphorus supply drives nonlinear responses of cottonwood (Populus deltoides) to increases in CO2 concentration from glacial to future concentrations. *The New Phytologist* **187**: 438–448.

Liang C, Piñeros MA, Tian J, Yao Z, Sun L, Liu J, Shaff J, Coluccio A, Kochian L V, Liao H. **2013**. Low pH, aluminum, and phosphorus coordinately regulate malate exudation through GmALMT1 to improve soybean adaptation to acid soils. *Plant*

Physiology **161**: 1347–1361.

Liang D, Zhang Z, Wu H, Huang C, Shuai P, Ye C-Y, Tang S, Wang Y, Yang L, Wang J, *et al.* **2014**. Single-base-resolution methylomes of Populus trichocarpa reveal the association between DNA methylation and drought stress. *BMC Genetics* **15**: doi:10.1186/1471–2156–15–S1–S9.

Lister R, O'Malley RC, Tonti-Filippini J, Gregory BD, Berry CC, Millar AH, Ecker JR. **2008**. Highly integrated single-base resolution maps of the epigenome in Arabidopsis. *Cell* **133**: 523–536.

Lister R, Pelizzola M, Dowen RH, Hawkins RD, Hon G, Tonti-Filippini J, Nery JR, Lee L, Ye Z, Ngo Q-M, *et al.* **2009**. Human DNA methylomes at base resolution show widespread epigenomic differences. *Nature* **462**: 315–322.

Loth-Pereda V, Orsini E, Courty P-E, Lota F, Kohler A, Diss L, Blaudez D, Chalot M, Nehls U, Bucher M, *et al.* **2011**. Structure and expression profile of the phosphate Pht1 transporter gene family in mycorrhizal Populus trichocarpa. *Plant Physiology* **156**: 2141–2154.

Lu S, Sun YH, Chiang VL. **2008**. Stress-responsive microRNAs in Populus. *The Plant Journal* **55**: 131–151.

Lu S, Sun Y-H, Shi R, Clark C, Li L, Chiang VL. **2005**. Novel and mechanical stress-responsive MicroRNAs in Populus trichocarpa that are absent from Arabidopsis. *The Plant Cell* **17**: 2186–2203.

Luco RF, Pan Q, Tominaga K, Blencowe BJ, Pereira-Smith OM, Misteli T. **2010**. Regulation of alternative splicing by histone modifications. *Science* **327**: 996–1000.

Martienssen R a, Colot V. **2001**. DNA Methylation and Epigenetic Inheritance in Plants and Filamentous Fungi. *Science* **293**: 1070–1074.

Maunakea AK, Nagarajan RP, Bilenky M, Ballinger TJ, D'Souza C, Fouse SD, Johnson BE, Hong C, Nielsen C, Zhao Y, *et al.* **2010**. Conserved role of intragenic

DNA methylation in regulating alternative promoters. *Nature* **466**: 253–257.

Mirouze M, Reinders J, Bucher E, Nishimura T, Schneeberger K, Ossowski S, Cao J, Weigel D, Paszkowski J, Mathieu O. **2009**. Selective epigenetic control of retrotransposition in Arabidopsis. *Nature* **461**: 427–430.

Ong-Abdullah M, Ordway JM, Jiang N, Ooi S-E, Kok S-Y, Sarpan N, Azimi N, Hashim AT, Ishak Z, Rosli SK, *et al.* 2015. Loss of Karma transposon methylation underlies the mantled somaclonal variant of oil palm. *Nature* **525**: 533–537.

Piriyapongsa J, Jordan IK. **2008**. Dual coding of siRNAs and miRNAs by plant transposable elements. *RNA* **14**: 814–821.

Puzey JR, Karger A, Axtell M, Kramer EM. **2012**. Deep Annotation of Populus trichocarpa microRNAs from Diverse Tissue Sets. *PLoS ONE* **7(3)**: doi:10.1371/journal.pone.0033034.

Radersma S, Grierson PF. **2004**. Phosphorus mobilization in agroforestry: Organic anions, phosphatase activity and phosphorus fractions in the rhizosphere. *Plant and Soil* **259**: 209–219.

Roberts JT, Cardin SE, Borchert GM. **2014**. Burgeoning evidence indicates that microRNAs were initially formed from transposable element sequences. *Mobile Genetic Elements* **4**: doi.org/10.4161/mge.29255.

Sato A, Miura K. **2011**. Root architecture remodeling induced by phosphate starvation. *Plant Signaling & Behavior* **6:8**: 1122–1126.

Saze H, Kakutani T. **2011**. Differentiation of epigenetic modifications between transposons and genes. *Current Opinion in Plant Biology* **14**: 81–87.

Saze H, Mittelsten Scheid O, Paszkowski J. **2003**. Maintenance of CpG methylation is essential for epigenetic inheritance during plant gametogenesis. *Nature Genetics* **34**: 65–69.

Schachtman DP. **1998**. Phosphorus Uptake by Plants: From Soil to Cell. *Plant*

Physiology **116**: 447–453.

Schmitz RJ, Schultz MD, Lewsey MG, O'Malley RC, Urich MA, Libiger O, Schork NJ, Ecker JR. **2011**. Transgenerational epigenetic instability is a source of novel methylation variants. *Science* **334**: 369–373.

Secco D, Wang C, Shou H, Schultz MD, Chiarenza S, Ecker JR, Whelan J, Lister R. **2015**. Stress induced gene expression drives transient DNA methylation changes at adjacent repetitive elements. *eLife*: doi.org/10.7554/eLife.09343.

Seymour DK, Koenig D, Hagmann J, Becker C, Weigel D. **2014**. Evolution of DNA Methylation Patterns in the Brassicaceae is Driven by Differences in Genome Organization. *PLoS Genetics* **10(11)**: doi:10.1371/journal.pgen.1004785.

Sharman BC. **1958**. Environmental Conditioning of Flax. *Nature* **181**: 928–929.

Sjödin A, Street NR, Sandberg G, Gustafsson P, Jansson S. **2009**. The Populus Genome Integrative Explorer (PopGenIE): a new resource for exploring the Populus genome. *The New Phytologist* **182**: 1013–1025.

Smith AP, Jain A, Deal RB, Nagarajan VK, Poling MD, Raghothama KG, Meagher RB. **2010**. Histone H2A.Z Regulates the Expression of Several Classes of Phosphate Starvation Response Genes But Not as a Transcriptional Activator. *Plant Physiology* **152**: 217–225.

Song Y, Tian M, Ci D, Zhang D. **2015**. Methylation of microRNA genes regulates gene expression in bisexual flower development in andromonoecious poplar. *Journal of Experimental Botany* **66**: 1891–1905.

Sterck L, Rombauts S, Vandepoele K, Rouze P, Van de Peer Y. **2007**. How many genes are there in plants (... and why are they there)? *Current Opinion in Plant Biology* **10**: 199–203.

Sunkar R, Zhu J-K. **2004**. Novel and stress-regulated microRNAs and other small RNAs from Arabidopsis. *The Plant Cell* **16**: 2001–2019.

Taghavi S, Barac T, Greenberg B, Borremans B, Vangronsveld J, Lelie D Van Der. **2005**. Horizontal Gene Transfer to Endogenous Endophytic Bacteria from Poplar Improves Phytoremediation of Toluene. *Applied and Environmental Microbiology* **71**: 8500–8505.

Takuno S, Gaut BS. **2012**. Body-methylated genes in Arabidopsis thaliana are functionally important and evolve slowly. *Molecular Biology and Evolution* **29**: 219–227.

Theodorou ME, Plaxton WC. **1993**. Metabolic Adaptations of Plant Respiration to Nutritional Phosphate Deprivation. *Plant Physiology* **101**: 339–344.

Thimm O, Bläsing O, Gibon Y, Nagel A, Meyer S, Krüger P, Selbig J, Müller LA, Rhee SY, Stitt M. **2004**. MAPMAN: a user-driven tool to display genomics data sets onto diagrams of metabolic pathways and other biological processes. *The Plant Journal* **37**: 914–939.

Ticconi CA, Abel S. **2004**. Short on phosphate: plant surveillance and countermeasures. *TRENDS in Plant Science* **9**: 548–555.

Tomizawa S, Kobayashi H, Watanabe T, Andrews S, Hata K, Kelsey G, Sasaki H. **2011**. Dynamic stage-specific changes in imprinted differentially methylated regions during early mammalian development and prevalence of non-CpG methylation in oocytes. *Development and Stem Cells* **138**: 811–820.

Tuskan G a, Difazio S, Jansson S, Bohlmann J, Grigoriev I, Hellsten U, Putnam N, Ralph S, Rombauts S, Salamov A, *et al.* 2006. The Genome of Black Cottonwood, Populus trichocarpa (Torr. & Gray). *Science* **313**: 1596–1604.

Vance CP, Uhde-Stone C, Allan DL. **2003**. Phosphorus acquisition and use: critical adaptations by plants for securing a nonrenewable resource. *New Phytologist* **157**: 423–447.

VDLUFA. **1997a**. *VDLUFA-Methodenbuch. Handbuch der landwirtschaftlichen*

Versuchs- und Untersuchungsmethodik. Speyer, Germany: VDLUFA-Verlag.

VDLUFA. **1997b**. *Phosphordüngung nach Bodenuntersuchung und Pflanzenbedarf*. Darmstadt, Germany: VDLUFA-Verlag.

VDLUFA. **2000**. *Standpunkt. Bestimmung des Kalkbedarfs von Acker- und Grünlandböden*. Darmstadt, Germany: VDLUFA-Verlag.

VDLUFA. **2012**. *VDLUFA - Methodenbuch. Die chemische Untersuchung von Futtermitteln.* Speyer, Germany: VDLUFA-Verlag.

Vining KJ, Pomraning KR, Wilhelm LJ, Priest HD, Pellegrini M, Mockler TC, Freitag M, Strauss SH. **2012**. Dynamic DNA cytosine methylation in the Populus trichocarpa genome: tissue-level variation and relationship to gene expression. *BMC Genomics* **13:27**: doi:10.1186/1471–2164–13–27.

Wolffe AP. **1999**. Epigenetics: Regulation Through Repression. *Science* **286**: 481–486.

Wright SJ, Yavitt JB, Wurzburger N, Turner BL, Tanner EVJ, Sayer EJ, Santiago LS, Kaspari M, Hedin LO, Harms KE, *et al.* **2011**. Potassium, phosphorus, or nitrogen limit root allocation, tree growth, or litter production in a lowland tropical forest. *Ecology* **92**: 1616–1625.

Xu M, Zhang B, Su X, Zhang S, Huang M. **2011**. Reference gene selection for quantitative real-time polymerase chain reaction in Populus. *Analytical Biochemistry* **408**: 337–339.

Yang X, Han H, De Carvalho DD, Lay FD, Jones PA, Liang G. **2014**. Gene Body Methylation Can Alter Gene Expression and Is a Therapeutic Target in Cancer. *Cancer Cell* **26**: 577–590.

Ye J, Coulouris G, Zaretskaya I, Cutcutache I, Rozen S, Madden TL. **2012**. Primer-BLAST: a tool to design target-specific primers for polymerase chain reaction. *BMC Bioinformatics* **13:134**: doi:10.1186/1471–2105–13–134.

Zaidi SK, Young DW, Montecino M, Lian B, Stein JL, Wijnen AJ Van, Gary S, Lian JB, Stein GS. **2010**. Architectural Epigenetics: Mitotic Retention of Mammalian Transcriptional Regulatory Information. *Molecular and Cellular Biology* **30**: 4758–4766.

Zhang Y. **2005**. miRU: an automated plant miRNA target prediction server. *Nucleic Acids Research* **33**: W701–704.

Zhang X, Yazaki J, Sundaresan A, Cokus S, Chan SW-L, Chen H, Henderson IR, Shinn P, Pellegrini M, Jacobsen SE, *et al.* **2006**. Genome-wide high-resolution mapping and functional analysis of DNA methylation in arabidopsis. *Cell* **126**: 1189–1201.

Zhou F, Xu Y. **2009**. RepPop: a database for repetitive elements in Populus trichocarpa. *BMC Genomics* **10:14**: doi:10.1186/1471–2164–10–14.

Zilberman D, Gehring M, Tran RK, Ballinger T, Henikoff S. **2007**. Genome-wide analysis of Arabidopsis thaliana DNA methylation uncovers an interdependence between methylation and transcription. *Nature Genetics* **39**: 61–69.

Curriculum vitae

Brigitte Schönberger

Personal information

Address	Senefelderstr. 93 in 70176 Stuttgart, Germany
E-Mail	Brigitte_Schoenberger@uni-hohenheim.de
Date of birth	May 10th, 1988 – Isfara (Tajikistan)
Family status	unmarried, no children
Nationality	German

Education

06/2013 – 12/2016	**PhD Program,** Institute of Crop Sciences, Department of Nutritional Crop Physiology, University of Hohenheim PhD Thesis: „Site-dependent differences in DNA methylation and their impact on plant establishment in *Populus trichocarpa*"

10/2010 – 04/2013	**Master of Science**
	University of Hohenheim (Grade: A⁻)
	   ➤ major subject: agricultural biotechnology
	   ➤ specialization: plant biotechnology
	
	Master Thesis:
	„Identification, cloning and functional characterization of plant-derived constitutive promoters in *Petunia x hybrida*" (Grade: A)

10/2007 - 09/2010	**Bachelor of Science**
	University of Hohenheim (Grade: B⁻)
	   ➤ major subject: agricultural biology
	   ➤ specialization: plant protection
	
	Bachelor Thesis:
	„Gene expression analysis and functional characterization of the subtilase gene *At*4g34980 in *Arabidopsis thaliana*" (Grade: B)

07/2007	**Abitur** - German university entrance qualification by the secondary school "Allgemeines Gymnasium, Albstadt" (Grade: B)

Work experience

03/2012 – 03/2013	**Internship**, including Master Thesis, in the Biotechnology Department of Klemm + Sohn GmbH & Co. KG, Stuttgart
	   ➤ *in vitro* and anther cultures
	   ➤ stable and transient plant transformations
	   ➤ pot tests with transgenic plants
	   ➤ evaluation and data management of drought stress tests
	   ➤ PCR, Primer Design and Gateway® Cloning
	   ➤ Particle Bombardment

10/ – 12/2011	**Student assistant** in the Institute of Crop Sciences, Department of Nutritional Crop Physiology, University of Hohenheim

  ➢ nitrogen uptake analyses in *Arabidopsis thaliana*
  ➢ PCR, DNA extraction

04/ – 07/2011 **Student assistant** in the Institute of Zoology, University of Hohenheim

  ➢ supervision of students during practical courses
  ➢ dissection of insects, fledglings, fishes and mice
  ➢ identification of *Arthropoda species*

11/2009 – 02/2010 **Tutor** in the field of molecular biology, University of Hohenheim

  ➢ teaching basic knowledge of molecular biology
  ➢ supervision of students

08/ – 09/2009 **Internship** in the Governmental Institute of Viniculture, Freiburg

  ➢ detection of *Bois noir* and ripeness degree in grapes
  ➢ hardware maintenance
  ➢ field grown ratings of *Botrytis cinerea*
  ➢ pheromone experiments in the field
  ➢ supervision of the trade fair
    "Prädikat Wine Estates (VDP)", Berlin

04/ – 09/2009 **Tutor** in the field of organic chemistry, University Hohenheim

  ➢ teaching basic knowledge of organic chemistry
  ➢ supervision of students

Foreign languages

German	native
English	fluent
French	basic knowledge (capable of improvement in short term)
Russian	basic knowledge (capable of improvement in short term)

Electronic data processing

MS Office	very good knowledge
SAS	basic knowledge (capable of improvement in short term)
R	very good basic knowledge
Unix/Linux	very good basic knowledge

Stuttgart, July 05th, 2016

Brigitte Schönberger